CRREL Report 87-14

August 1987

17247628

Physical and structural characteristics of Weddell Sea pack ice

Anthony J. Gow, Stephen F. Ackley, Kurt R. Buck and Kenneth M. Golden

REPORT DOCUMENTATION PAGE

Form Approved
OMB No 0704-0188
Exp. Date: Jun 30, 1986

1a. REPORT SECURITY CLASSIFICATION	1b. RESTRICTIVE MARKINGS
Unclassified	

2a. SECURITY CLASSIFICATION AUTHORITY	3. DISTRIBUTION/AVAILABILITY OF REPORT
2b. DECLASSIFICATION/DOWNGRADING SCHEDULE	Approved for public release; distribution is unlimited.

4. PERFORMING ORGANIZATION REPORT NUMBER(S)	5. MONITORING ORGANIZATION REPORT NUMBER(S)
CRREL Report 87-14	

6a. NAME OF PERFORMING ORGANIZATION	6b. OFFICE SYMBOL (If applicable)	7a. NAME OF MONITORING ORGANIZATION
U.S. Army Cold Regions Research and Engineering Laboratory	CECRL	Division of Polar Programs National Science Foundation

6c. ADDRESS (City, State, and ZIP Code)	7b. ADDRESS (City, State, and ZIP Code)
Hanover, New Hampshire 03755-1290	Washington, D.C. 20550

8a. NAME OF FUNDING/SPONSORING ORGANIZATION	8b. OFFICE SYMBOL (If applicable)	9. PROCUREMENT INSTRUMENT IDENTIFICATION NUMBER
		Grant No. DP77-24528

8c. ADDRESS (City, State, and ZIP Code)	10. SOURCE OF FUNDING NUMBERS			
	PROGRAM ELEMENT NO.	PROJECT NO.	TASK NO.	WORK UNIT ACCESSION NO.

11. TITLE (Include Security Classification)

Physical and Structural Characteristics of Weddell Sea Pack Ice

12. PERSONAL AUTHOR(S)
Gow, Anthony J.; Ackley, Stephen F.; Buck, Kurt R.; and Golden, Kenneth M.

13a. TYPE OF REPORT	13b. TIME COVERED FROM _____ TO _____	14. DATE OF REPORT (Year, Month, Day) August 1987	15. PAGE COUNT 80

16. SUPPLEMENTARY NOTATION

17. COSATI CODES			18. SUBJECT TERMS (Continue on reverse if necessary and identify by block number)
FIELD	GROUP	SUB-GROUP	Ice Weddell Sea
			Ice characteristics
			Sea ice

19. ABSTRACT (Continue on reverse if necessary and identify by block number)

During February and March 1980 the physical properties of Weddell Sea pack ice were investigated via core drilling of 66 floes located along a transect of 600 nautical miles from 64°S to 74°S latitude at roughly 40°W longitude. These studies revealed widespread frazil ice in amounts not known to exist in Arctic sea ice of comparable age and thickness. It is estimated from structure studies of 62 of the 66 floes that 54% of the total ice production in the Weddell Sea is generated as frazil. The disposition and exceptional thicknesses of the frazil show that mechanisms other than surface turbulence effects are involved and imply that the circulation and structure of water in the upper levels of the Weddell Sea are significantly different from those in the Arctic basin. Salinities of both first-year and multi-year floes are notably higher than those of their Arctic counterparts because summer surface melting is rare or absent in the Weddell Sea; in the Arctic, downward percolating meltwater flushes through the ice and lowers its salinity. Fluorescence was evaluated as a means of revealing biological activity in Weddell Sea pack ice. It proved useful as an index of combined living and dead material in the ice, but measurements failed to establish any consistent relationship between fluorescence and salinity as suggested by earlier work in the Weddell Sea.

20. DISTRIBUTION/AVAILABILITY OF ABSTRACT	21. ABSTRACT SECURITY CLASSIFICATION
☒ UNCLASSIFIED/UNLIMITED ☐ SAME AS RPT. ☐ DTIC USERS	Unclassified

22a. NAME OF RESPONSIBLE INDIVIDUAL	22b. TELEPHONE (Include Area Code)	22c. OFFICE SYMBOL
Anthony J. Gow	603-646-4256	CECRL-RS

DD FORM 1473, 84 MAR   83 APR edition may be used until exhausted.   SECURITY CLASSIFICATION OF THIS PAGE
All other editions are obsolete.   Unclassified

PREFACE

This report was prepared by Dr. Anthony J. Gow, Research Geologist, Stephen Ackley, Chief, Snow and Ice Branch, Research Division, U.S. Army Cold Regions Research and Engineering Laboratory; Kurt R. Buck, Research Associate, Department of Marine Sciences, University of California at Santa Cruz; and Kenneth M. Golden, Post-doctoral Fellow, Department of Mathematics, Rutgers University.

The contents of this report are not to be used for advertising or promotional purposes. Citation of brand names does not constitute an official endorsement or approval of the use of such commerical products.

CONTENTS

ILLUSTRATIONS

Figure | Page

TABLES

Table

Physical and Structural Characteristics of Weddell Sea Pack Ice

ANTHONY J. GOW, STEPHEN F. ACKLEY, KURT R. BUCK AND KENNETH M. GOLDEN

INTRODUCTION

Recent studies by CRREL researchers of the dynamics and thermodynamics of sea ice in the Antarctic have included investigations of the physical and structural properties of pack ice in the Weddell Sea. The formation of pack ice and its subsequent movement from source areas in the Weddell Sea is particularly important in modifying ocean-atmosphere and water mass development both in and beyond the Weddell Sea embayment. The pack ice area affected by Weddell Sea processes is 8-10 million square kilometers (Ackley 1979a), thus representing about one-third of the total area os sea ice encircling Antarctica at its maximum extent.

The current studies, conducted during February and March 1980, the latter part of the austral summer, represent the most comprehensive investigations yet made of Antarctic pack ice. The overall scope of this research, including some results of earlier work, is reported in Ackley (1979a, b, 1981), Ackley et al. (1978, 1980) and Gow et al. (1981, 1982). In this report we describe, in greater detail, the physical properties and structural characteristics of 66 individual ice floes in the Weddell Sea. Our observations have produced some surprising results that show that, in both its structure and its salinity characteristics, Weddell Sea ice differs appreciably from sea ice of comparable age and thickness in the Arctic.

SEA ICE STRUCTURE AND CLASSIFICATION

The general belief has been that most sea ice is congelation ice; that is, it is formed by direct freezing of seawater to the underside of the ice sheet. Such growth typically yields ice with columnar-shaped crystals that exhibit a characteristic substructure of ice plates and brine lamellae (Fig. 1). This substructure, the trademark of congelation sea ice, results from the dendritic ice growth interface that forms in response to the needs of the constitutional supercooling of sea water, caused by the build-up of brine at the ice/water interface. Since the ice lattice can tolerate only minimal inclusions of salt, the structure of the ice/water interface is forced to change from a planar to a dendritic morphology. In this way excess brine at the interface becomes systematically incorporated in the spaces between the pure ice dendrites. Continued growth of the ice leads to the formation of vertically elongated columnar crystals composed of packets of dendrites (ice plates) with layers of brine inclusions (brine lamellae) sandwiched between the plates. This arrangement of brine layers in the vertical direction, which also corresponds to the dominant direction of heat flow in the ice, is the structual feature that controls the migration of brine and hence the changing salinity distribution in sea ice as it ages. Initial salinity values depend mainly on the freezing velocity of the seawater. Salinity and freezing velocity are related: the faster the growth, the higher the salinity.

Granular sea ice, which includes frazil as well as snow ice, is commonly assumed to be of very restricted occurrence in undeformed ice sheets and floes. Frazil results from the free nucleation of crystals in the water column. The crystals then freeze together to form frazil ice, which is relatively easy to distinguish from congelation ice on the basis of its generally fine-grained, equidimensional texture, together with the absence of a brine lamella and ice plate substructure (Fig. 2). Since frazil is generally believed to be produced by turbulence in the water column, it should be restricted to ice edges, leads and polynyas (large open areas in the pack ice). In the Arctic, frazil ice typically occurs in the top 20 cm or so of the ice sheet, so it is generally associated with the earliest stages of ice sheet growth. According to Martin (1979) frazil ice accounts for only 5-10% of the ice sheet thickness in the Arctic, and the studies of Weeks and Gow (1978, 1980) confirm this, at least for fast ice and near-shore ice in the Beaufort and Chukchi seas.
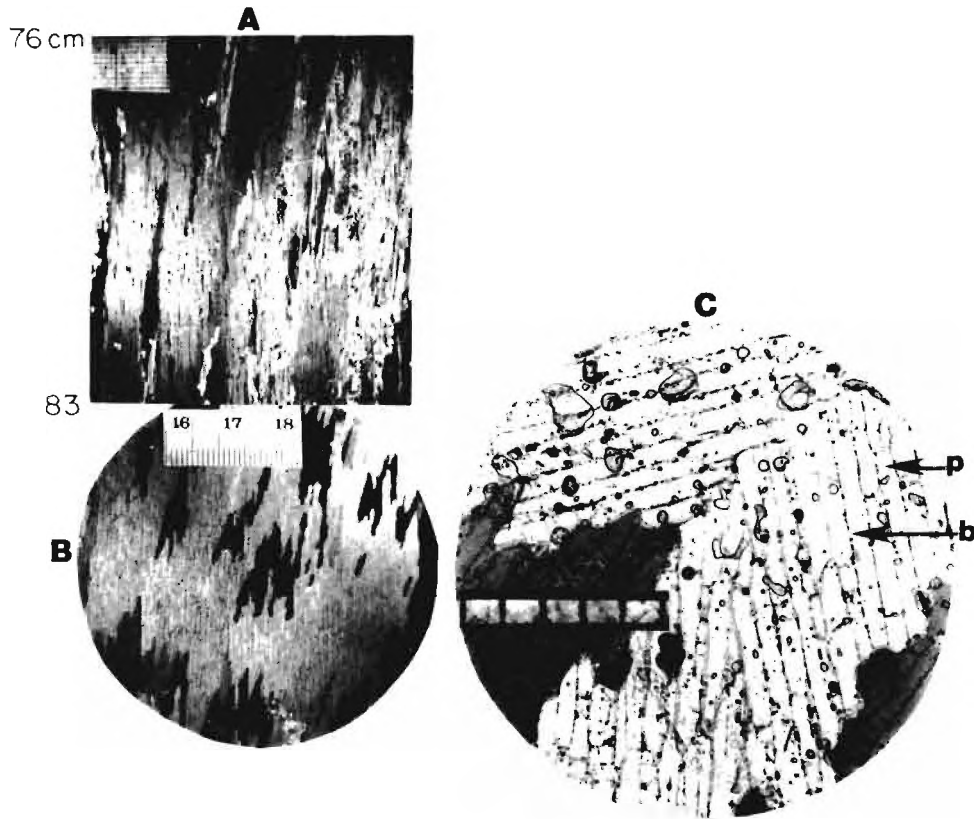
Figure 1. Examples of vertical (A) and horizontal (B and C) thin sections of congelation sea ice photographed between crossed polaroids. Section A demonstrates the columnar texture of crystals and the tubular nature of brine inclusions in warm sea ice. Section B illustrates the brine layer and ice plate substructure of sea ice crystals. In the magnified Section C, b and p denote a brine layer and an ice plate, respectively. The scale subdivisions measure 1 mm.
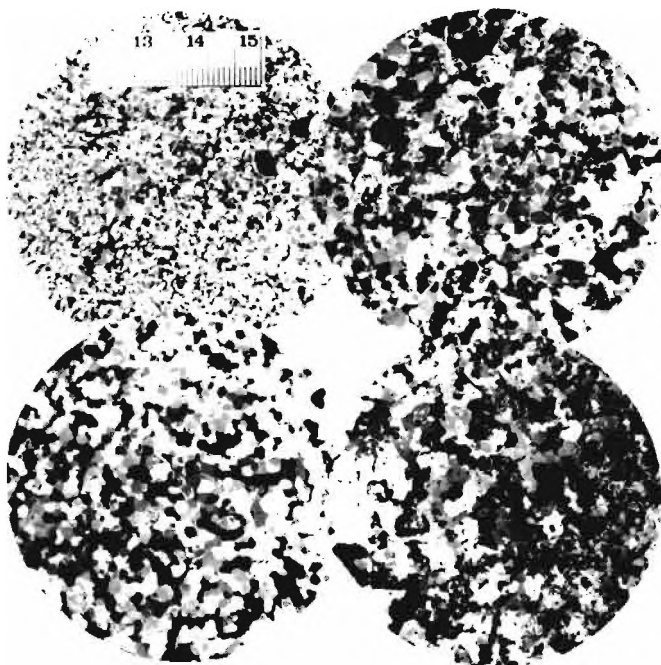
Figure 2. Examples of variable grain size and texture in frazil ice in Weddell Sea pack ice.

Figure 3. Examples of variable nature of grain size and texture in snow ice in Weddell Sea pack ice.

Figure 4. Locations of the primary sea ice sampling sites (circles). Data buoys used for satellite monitoring of drift and deformation of the pack ice in the Weddell Sea are indicated by triangles.

Another component of granular ice is snow ice, formed when snow containing interstitial water (derived from meltwater, rain or seawater) freezes. Such ice is necessarily restricted to the top of the ice sheet and it can usually be distinguished from frazil ice by its texture; snow ice tends to be more bubbly and coarser grained than frazil ice (Fig. 3).

Ice floes are generally classified as first-year, second-year or multi-year ice. For this report we define multi-year ice as all ice that has survived at least one melt season. This conforms to the broader usage of the term as it is applied by most of today's specialists,* though it differs from the WMO definition (WMO 1956), which would restrict the term multi-year to ice that has survived two or more melt seasons. Ice that has survived one melt season is called second-year ice. First-year ice is ice that has survived just a single winter's growth.

---

* This usage is justified because it is generally difficult to distinguish second-year ice from older ice using just surface observations. However, salinity and structure analyses of cores usually permit such distinctions to be made.

LOGISTICS AND FIELD OPERATIONS

Weddell Sea pack ice was investigated in February and March 1980, using helicopters aboard USCGC *Polar Sea* to collect core samples from drifting floes located along a north-south transect that covered approximately 600 nautical miles from 64°S to 74°S latitude at roughly 40°W longitude (Fig. 4). Two teams, the one lead by S. Ackley and the other by A. Gow, were deployed to obtain samples from as large and representative a selection of ice floes as possible. This selection included both first-year and multi-year ice floes, with the higher freeboards of the latter usually serving to distinguish them from first-year floes. This proved to be the only reliable method of identifying multi-year floes, since multi-year floes in the Weddell Sea lacked the summer surface melt features that characterize multi-year floes in the Arctic. Sampling sites were identified by Julian day and a site number keyed to the name of the two team leaders. For example, the designation 60-G-2 means this particular core was collected by Gow's team from the second site visited by the team on Julian day 60.
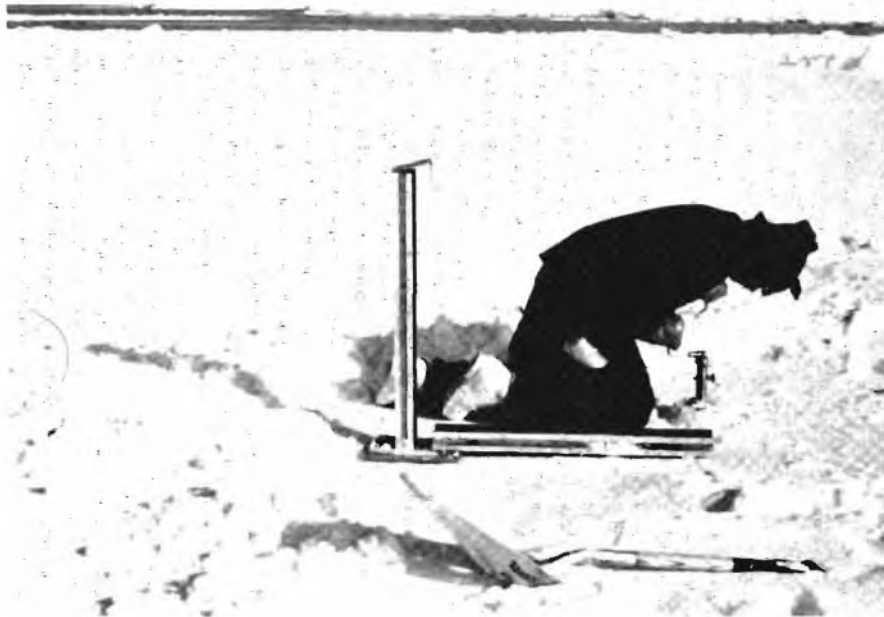
Figure 5. Coring a multi-year floe. Also shown is the insulated split-tube core sampler used for measuring ice temperatures and for cutting cores for salinity measurements.

A total of 66 ice floes, including 14 multi-year floes, were successfully penetrated by drilling with a 7.5-cm-diameter CRREL coring auger (Fig. 5). At several sites two or more cores were drilled to examine variations in the salinity, fluorescence and structure profiles at closely spaced locations (such cores were generally located within a few meters of one another). This brought the number of cores to 77, from which 76 salinity profiles, 68 fluorescence profiles and 75 structure profiles were obtained. A total of 142.16 m of core was retrieved. The precise locations of sites were established by fixes between the ship and the helicopters as they hovered over the ice floes.

Of the 66 floes we sampled, 52 (79%) consisted of first-year ice, and the remaining 14 (21%) were identified as multi-year ice. However, the size of the floes was so variable that it would be incorrect to conclude that these percentages are representative of first-year and multi-year ice concentrations in the Weddell Sea pack.

On-site investigations included estimates of the floe size, photographic documentation of the size, shape and surface characteristics of the floe, measurements of the snow thickness, and a cursory examination of the cores. The cores were in-spected for layering related to structural banding and algae incorporation, brine drainage features such as channeling and cavities, and other distinguishing features. Where duplicate cores were taken, one was usually sectioned on site at 10-cm intervals for salinity measurements. Most of the remaining cores were split lengthwise onboard the *Polar Sea*, where salinity measurements and preliminary examination of the ice structure were also made. The remaining half cores, together with several whole cores, were returned to CRREL for further analysis.

About 80% of the floes we drilled were small- to medium-sized floes (30–500 m in diameter). The remaining 20% were up to 3 km in diameter but also included two giant floes that exceeded 20 km in their longest dimensions.

The thickness of snow on top of the floes ranged from 2 to 56 cm at drilling sites. The snow cover tended to be heaviest on floes thicker than 4 m. The snow was generally dry, though evidence of metamorphism and recrystallization, leading to substantial increases in grain size, was widespread. Occasional wet snow could usually be attributed to infiltration of seawater. We observed little or no evidence of surface melting.

4

ANALYTICAL TECHNIQUES

Salinity

Salinity was determined by measuring the ionic conductivity of melted samples of sectioned cores. Measurements were made with a temperature-compensating Beckman Solubridge that was periodically calibrated against solutions prepared from Copenhagen Standard Seawater (chlorinity of 19.373‰). Individual determinations are considered accurate to within 0.2‰.

Crystalline structure

The crystalline structure (including texture and c-axis fabric) was investigated on both vertically and horizontally sectioned core. Because the floes in the Weddell Sea ice pack drift freely, cores from any particular floe can be oriented only in the relative sense. However, the orientations of horizontal sections were maintained along the length of the whole core in order to evaluate the persistence of azimuthal c-axis orientations in an ice floe.

Preliminary studies aboard the *Polar Sea* were restricted to examinations of horizontal thin sections prepared on a microtome using techniques previously applied to arctic sea ice by Weeks and Gow (1978, 1980). These preliminary studies, performed on cores from 16 floes ranging in thickness from 0.2 to 5 m, utilized thin sections that for convenience were cut at or close to natural breaks in an ice core before the core was split lengthwise on the bandsaw. The suspicion that the core breaks might coincide with structural discontinuities, for example, the transition from columnar crystal to granular ice, was subsequently confirmed when thin vertical slices were cut from the core and examined between crossed polaroid sheets on a light table. With this technique the outlines of individual crystals are revealed by the interference colors they produce. Following this discovery, thin vertical slices for optical examination were always taken from the side of the core, in conjunction with horizontal thin section samples, before splitting the cores in half on the bandsaw.

All thin sections were photographed at full scale on a 10-cm × 12.5-cm press-type camera that yields high-quality negatives that can be contact-printed at natural scale or can be enlarged to allow examination of the finer details of ice structure, such as the cellular substructure of columnar crystals and the nature of the boundaries between crystals of fine-grained frazil.

Fluorescence

Based on some preliminary work on Antarctic cores (Ackley et al. 1978), in vivo fluorescence was measured on half-core-sized samples as an indicator of biological material in the ice. The fluorescence was measured with a Turner Designs Fluorometer, which unfortunately gave erratic values on low-sensitivity settings, that is, when sizeable concentrations of material were being measured. To overcome this problem, samples were diluted with distilled water to a known dilution, and the fluorescence was then measured at a higher sensitivity. This scale showed good repeatability. The measurement was then converted linearly to the concentration appropriate for the undiluted sample.

We have since discovered that converting fluorescence values to separate chlorophyll a and phaeopigment values is not easy. Clarke and Ackley (1984), for example, found that the correlation coefficient of either chlorophyll a or phaeopigments with in vivo fluorescence was in the 0.5 range for both materials found in relatively fresh sea ice samples. The correlation of fluorescence with the sum of chlorophyll a and phaeopigments was, however, very high (> 0.9). The in vivo fluorescence must give some index value of biological material contained within the ice.

In the worst case two peaks in fluorescence in an ice core could represent several competing mechanisms and so could not be unequivocally interpreted as living or dead material. Here we furnish fluorescence measurements simply as an index of where biological material resides within the ice. Because of these difficulties we can only use this information in the broader context in comparing the relative importance of surface, interior or bottom communities in the Weddell Sea pack ice. Also, we do not know whether the long storage times of samples at –20°C at CRREL and the high osmotic stress associated with melting the samples would affect the data. Garrison and Buck (1984) discussed some of these aspects in greater detail and showed differences in the numbers of full and empty diatom cells for one of our Weddell Sea cores (51-G-4).

RESULTS

Table 1 lists the pertinent data we obtained on the 66 individual floes of Weddell Sea pack ice. These data include average (bulk) salinity for each

Table 1. Ice core data from Weddell Sea floes, February–March 1980.

Core number	Lat. (south)	Long. (west)	Thickness (m)	Average salinity (°/₀₀)	Structural composition (%)			Ice type
					Congelation	Frazil	Other	
41-A-1	64°07.2′	48°25.2′	1.25	2.0 ±1.1	66	21	13	First-year
41-G-1	64°07.6′	48°19.6′	3.82	2.5 ±1.5	25	70	5	Multi-year
42-A-1	66°39.7′	44°14.1′	4.52	3.4 ±1.6	35	61	4	Multi-year
⌈42-A-2A*	67°24′	43°56′	0.60	1.9 ±1.0	—	100	—	First-year
⌊42-A-2B	67°24′	43°56′	0.76	4.0 ±2.1	53	35	12	First-year
42-A-3	67°24′	43°34′	1.80	3.2 ±1.4	6	92	2	First-year
42-G-1	66°22′	44°28′	4.55	2.5 ±0.7	8	79	13	Multi-year
42-G-2	67°21′	43°49′	1.57	3.4 ±1.4	28	66	6	First-year
42-G-3	67°20′	43°40′	0.94	nd	nd	nd	nd	First-year
⌈43-A-1	69°21′	41°44′	0.98	3.4 ±0.9	69	22	9	First-year
⌊43-A-2	69°21′	41°44′	2.40	3.2 ±1.1	6	91	3	Multi-year
⌈43-A-3	69°29.8′	41°15.5′	0.41	3.6 ±0.5	82	18	—	First-year
⎸43-A-4	69°29.8′	41°15.5′	0.74	4.3 ±0.6	82	—	18	First-year
⌊43-A-5	69°29.8′	41°15.5′	0.48	3.6 ±1.0	79	21	—	First-year
43-A-6	69°30.5′	41°25.5′	1.11	4.2 ±0.8	85	15	—	First-year
43-G-1	69°14′	42°39′	1.67	3.9 ±1.1	61	32	7	First-year
⌈43-G-2	69°29.8′	41°15.5′	1.30	4.0 ±0.7	69	28	3	First-year
⌊43-G-3	69°29.8′	41°15.5′	1.91	4.2 ±1.2	60	33	7	First-year
43-G-4	69°30.5′	41°25.5′	1.45	4.2 ±2.0	46	54	—	First-year
44-A-1	71°18′	38°13′	1.98	4.7 ±1.4	57	39	4	First-year
44-A-2	71°22′	38°07′	4.86	3.4 ±1.8	15	75	10	Multi-year
44-G-1	71°18′	38°05′	1.79	3.5 ±1.5	48	45	7	First-year
44-G-2	71°20′	38°08′	3.40	4.7 ±1.2	36	56	8	Multi-year
44-G-3	72°10′	38°54′	1.92	5.1 ±0.9	94	3	3	First-year
48-A-1	73°52.8′	44°40.5′	1.47	5.0 ±1.6	83	11	6	First-year
48-A-2	73°52.8′	44°40′	1.28	4.3 ±0.7	80	17	3	First-year
48-A-3	73°53.1′	44°44′	1.18	5.0 ±1.0	92	—	8	First-year
⌈48-G-1	73°54′	44°40.5′	1.51	5.3 ±0.7	81	11	8	First-year
⌊48-G-2	73°54′	44°40.5′	1.44	5.7 ±1.0	nd	nd	nd	First-year
48-G-3	73°50.7′	44°36.5′	1.83	4.5 ±1.6	62	27	11	First-year
49-A-1	73°37′	43°40′	1.26	4.5 ±0.7	66	20	14	First-year
49-A-2	73°38.5′	43°32′	1.37	5.2 ±1.2	55	36	9	First-year
49-A-3	73°37.7′	43°32′	0.56	4.3 ±0.6	77	—	23	First-year
⌈49-G-1	73°32.5′	43°31′	1.43	4.7 ±1.8	nd	nd	nd	First-year
⌊49-G-2	73°32.5′	43°31′	1.53	4.7 ±1.0	72	23	5	First-year
49-G-3	73°33.8′	43°35′	1.43	4.8 ±1.1	80	9	11	First-year
51-A-1	73°22.7′	41°50.5′	1.29	4.4 ±0.8	61	36	3	First-year
51-A-2	73°27.2′	41°36.5′	1.32	5.2 ±1.4	14	83	3	First-year
51-A-3	73°23′	43°32.5′	1.45	4.6 ±1.2	79	14	7	First-year
51-A-4	73°22.7′	43°41.5′	1.28	4.8 ±1.1	87	—	13	First-year
51-G-1	73°29.2′	41°53′	1.33	5.3 ±1.0	28	72	—	First-year
51-G-2	73°31.8′	41°59.5′	1.30	5.3 ±1.3	41	41	18	First-year
51-G-3	73°24.5′	43°35′	2.55	5.7 ±2.0	59	33	8	First-year
51-G-4	73°24.3′	43°43′	2.00	4.5 ±1.4	25	65	10	First-year
51-G-5	73°23.5′	43°35′	1.10	4.8 ±0.8	94	—	6	First-year

* Brackets indicate cores from the same floe.

Table 1 (cont'd). Ice core data from Weddell Sea floes, February–March 1980.

Core number	Lat. (south)	Long. (west)	Thickness (m)	Average salinity (‰)	Structural composition (%)			Ice type
					Congelation	Frazil	Other	
52-A-1	74°01.6′	43°13′	1.51	5.0 ±1.2	69	22	9	First-year
52-A-2	73°48.5′	43°24.5′	1.30	5.3 ±0.9	74	20	6	First-year
⌈52-G-1*	73°56′	42°46.5′	1.47	5.5 ±1.4	nd	nd	nd	First-year
∣52-G-2	73°56′	42°46.5′	1.49	5.3 ±1.0	62	30	8	First-year
⌊52-G-3	73°56′	42°46.5′	1.52	4.9 ±1.3	nd	nd	nd	First-year
54-A-1	72°38.2′	40°43′	>5.0	3.5 ±1.6	27	73	—	Multi-year
54-G-1	72°51.5′	40°08′	2.30	4.8 ±1.7	45	29	26	First-year
54-G-2	72°41.5′	40°38′	>5.0	3.8 ±1.7	nd	nd	nd	Multi-year
60-A-1	70°16.3′	39°22.1′	1.24	4.6 ±0.8	69	31	—	First-year
60-A-2	70°13.7′	39°21.5′	2.14	4.1 ±1.0	4	96	—	First-year
60-A-3	70°13.7′	39°26′	1.19	3.6 ±1.3	86	14	—	First-year
60-A-4	70°19.3′	39°19′	1.01	4.7 ±0.5	90	—	10	First-year
60-A-5	70°13.6′	38°33′	2.43	4.1 ±1.5	43	49	8	First-year
60-G-1	70°16.9′	39°26.2′	1.02	5.7 ±1.4	50	50	—	First-year
⌈60-G-2	70°16.5′	39°29′	1.59	4.8 ±1.5	42	49	9	First-year
⌊60-G-3	70°16.5′	39°29′	1.55	4.1 ±1.3	37	63	—	First-year
60-G-4	70°14.5′	39°21′	1.20	4.0 ±1.7	64	31	5	First-year
60-G-5	70°18.5′	39°16.5′	1.52	4.6 ±0.9	60	40	—	First-year
60-G-6	70°13′	38°34′	1.35	4.9 ±0.5	51	40	9	First-year
61-A-1	69°50.7′	38°29′	1.32	4.8 ±1.3	45	50	5	First-year
61-A-2	69°49.7′	38°31′	4.82	3.2 ±1.8	27	69	4	Multi-year
61-A-3	69°28′	38°29′	1.80	2.6 ±1.0	64	18	18	First-year
61-A-4	69°32′	38°10.5′	1.61	3.7 ±1.3	25	68	7	First-year
61-G-1	69°53.3′	38°33′	3.01	3.7 ±1.7	—	74	26	Multi-year
61-G-2	69°53.8′	38°33.5′	4.18	3.5 ±1.9	25	75	—	Multi-year
61-G-3	69°32.8′	37°53′	2.52	3.5 ±1.2	18	82	—	Multi-year
61-G-4	69°30.2′	37°57′	0.81	5.2 ±1.3	85	15	—	First-year
61-G-5	69°25.6′	37°56′	1.22	6.4 ±2.0	79	21	—	First-year
62-A-1	67°50.5′	39°04.5′	2.92	3.1 ±1.2	—	86	14	Multi-year
62-A-2	67°43.7′	39°05′	0.70	4.3 ±1.3	21	79	—	First-year
62-G-1	67°49.6′	38°58′	2.14	2.9 ±1.1	—	100	—	First-year
62-G-2	67°41.8′	38°59.2′	3.06	3.3 ±1.2	—	100	—	Multi-year

* Brackets indicate cores from the same floe.

floe and the percentages of congelation ice, frazil ice and undifferentiated ice (principally snow ice), estimated on the basis of a vertical section analysis of the crystalline structure along the entire length of a core. We will first discuss the general results of the salinity, structural and fluorescence studies and then describe in greater detail the physical properties of each core from the 66 ice floes. The detailed descriptions will compare salinity and fluorescence profiles with vertical structure profiles. We have also included horizontal thin-section photographs to illustrate variations in the crystalline texture of the ice.

Salinity

Figure 6 shows typical salinity distribution in first-year ice that has survived a summer in the Weddell Sea. Except for one sample from the middle of the floe, salinities all exceeded 4‰. A maximum salinity of 7.4‰ was measured directly below the lowest salinity value; the mean floe salinity measured 5.1‰. This floe consisted almost entirely of congelation ice.

In floe 61-G-2 (Fig. 7) the ice was composed dominantly of congelation crystals to a depth of 1.2 m, followed by an abrupt transition to a layer of frazil ice nearly 3 m thick. This floe was identi-
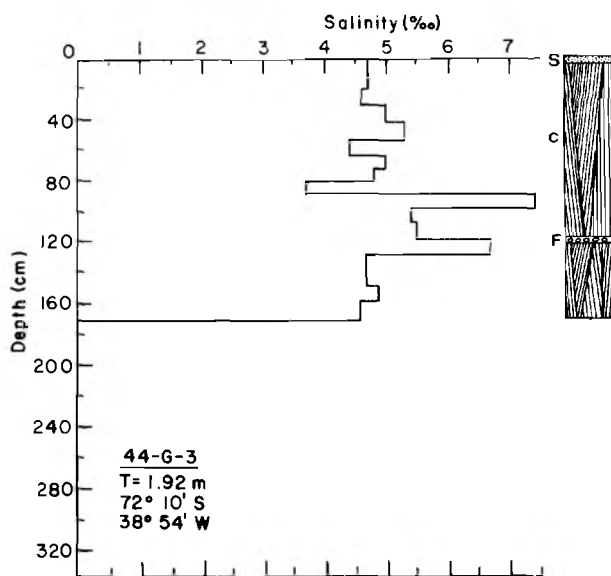
Figure 6. Salinity and vertical structure profiles of a first-year ice floe (44-G-3). The symbols S, C and F denote undifferentiated granular snow or frazil ice, congelation ice and frazil ice, respectively.

Figure 7. Salinity and vertical structure profiles of a multi-year ice floe (61-G-2).

fied as multi-year ice. Its salinity was low in the top 30 cm or so; salinities in deeper ice varied from 2 to 6‰, and the floe's average salinity was 3.5‰.

Ice from site 42-A-1 (Fig. 8) consisted of a mixture of congelation and frazil ice. The floe was also identified as multi-year, mainly on the basis of its thickness. In both 61-G-2 and 42-A-1 the tops of the floes appear much less desalinated than their Arctic counterparts, for example, multi-year floes recently examined in the Fram Strait (Tucker et al. 1985, Gow and Tucker 1987). In floe 42-A-1 the salinity exceeds 4‰ at many levels in the ice; the salinity averaged 3.4‰. The salinities were characterized by dramatic swings that did not appear to be related to changes in ice crystal type. This was also true for floe 61-G-2.

In Figure 9 we have plotted bulk salinity as a function of floe thickness. This was done to allow comparison with the data of Cox and Weeks (1973), who used the same kind of plot to extract salinity trend lines from their Arctic cold ice and Arctic warm ice data. The dominant features of the Cox and Weeks analysis are the strong negative correlation between bulk salinity and increasing ice sheet thickness in winter ice and the very weak positive correlation with summer ice. It is
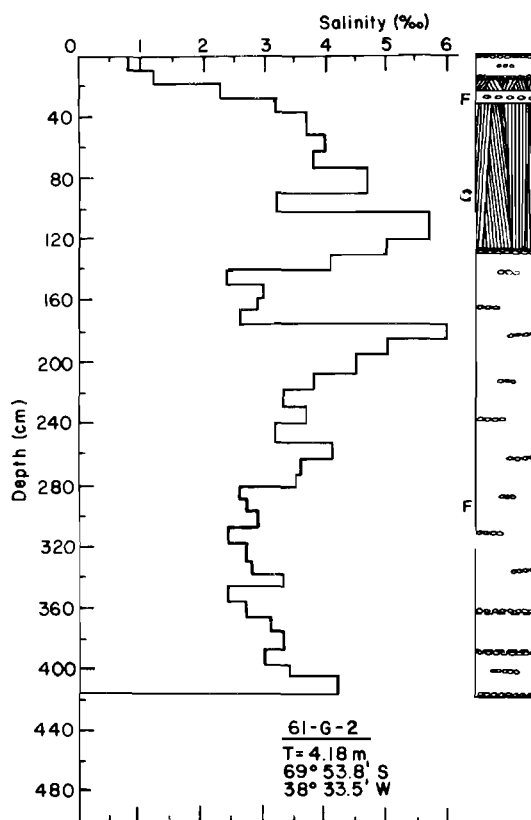
clear from the large number of samples measured during late summer in the Weddell Sea that sea ice in this region is appreciably more saline than ice of comparable age and thickness in the Arctic. In fact, floe salinities in late summer in the Weddell Sea are more comparable with Arctic winter ice than they are with Arctic summer ice. This applies particularly to multi-year ice floes, which in most cases yielded bulk salinities higher than those expected for Arctic cold multi-year ice. For example, the average salinity of 61 first-year ice profiles from the Weddell Sea measured 4.5‰ compared to values of around 3‰ that Cox and Weeks (1973) reported for warm Arctic ice of comparable thickness. Similarly, measurements of 14 warm multi-year ice profiles from the Weddell Sea yielded a mean salinity of 3.5‰, which is appreciably higher than the 2–2.5‰ value that Cox and Weeks reported for Arctic multi-year floes of comparable thickness (3–5 m).

For first-year Weddell Sea ice the best-fit linear regression line of salinity, S_i, to thickness, h, is

Figure 8. Salinity and vertical structure profiles of a multi-year ice floe (42-A-1).

Figure 9. Bulk salinities of Weddell Sea ice floes plotted as a function of thickness. Trend lines for Arctic cold ice (ACIT) and Arctic warm ice (AWIT), taken from Cox and Weeks (1973), illustrate the enhanced salinity of warm Antarctic sea ice over its Arctic counterpart.

$$S_i = 4.06 + 0.26h.$$

For multi-year ice the relationship is

$$S_i = 3.83 - 0.11h.$$

The higher salinity of Weddell Sea summer ice must reflect the small amount of top surface melting in Weddell Sea pack ice (Ackley 1979b, Andreas and Ackley 1982). This lack of summer melt, which we also observed in 1980, allows floes to retain brine that otherwise would be flushed out by downward percolating meltwater, considered an important if not the dominant mechanism controlling the loss of brine in Arctic sea ice (Untersteiner 1968). Ackley et al. (1980) also suggested that the higher average salinities in Weddell Sea pack ice might be caused by the formation of frazil ice, which, because of its sponge-like structure, might entrap more brine and retain it more effectively than congelation ice, thereby increasing overall salinities in floes containing large amounts of frazil ice. However, a more thorough analysis of the relationship between salinity and ice structure in all the Weddell Sea profiles now shows that frazil ice is not systematically more saline than congelation ice. This implies that the volume of interstices between frazil particles available for entrapment of seawater when the frazil particles freeze together is somewhat smaller than might have been expected from particle-packing considerations—probably less than 15% in freshly formed frazil ice. This is clearly related to particle shape. We saw several cases of frazil ice in the Weddell Sea pack that possessed a platy texture, which should favor tighter (less porous) packing of particles than equi-axed grains. The differences in particle shape probably originate via differences in the mechanisms of frazil crystallization discussed later in this report.

Crystalline structure

A major finding of our examination of 66 floes in the Weddell Sea was the discovery of granular ice, principally frazil, in amounts not previously observed in the Arctic or Antarctic. Prior to this study, and based largely on observations in the Arctic, frazil was considered a minor component of sea ice, confined to the top 20 cm or so of sea ice sheets and representing less than 10% of the total ice thickness (Martin 1979). Conventional wisdom (or ignorance) held that frazil growth was
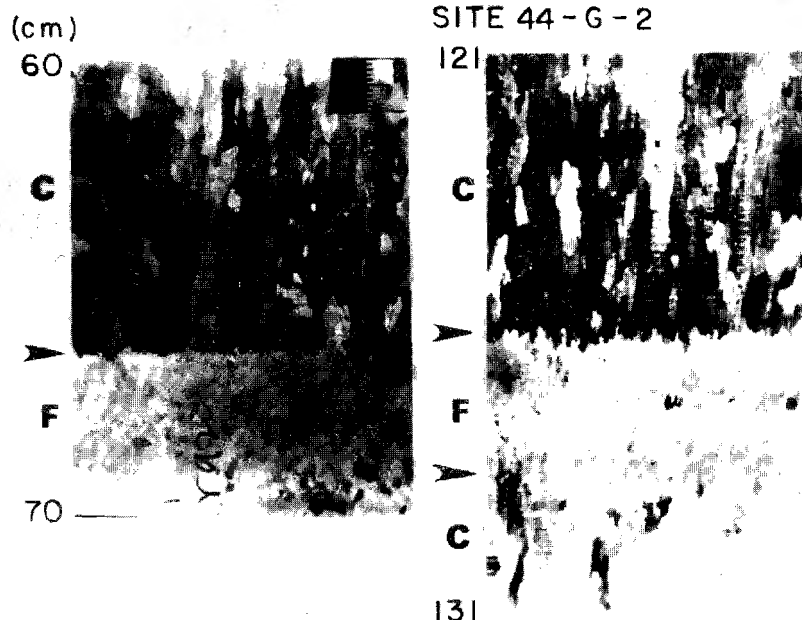

Figure 10. Vertical thick sections of ice from floe 44-G-2 showing the transition from congelation (C) to frazil (F) ice growth. Note how fine-grained frazil particles have become lodged within the interdendrite grooves of the congelation ice crystals. In the section from 121–131 cm, congelation ice growth returns at around 128 cm.

10

limited to leads and areas of open water, its formation mainly associated with wind- and wave-induced turbulence.

In many Weddell Sea floes, especially multi-year floes, frazil was the dominant component of the ice crystal structure. The frequent sandwiching of frazil between layers of congelation ice also shows that frazil production is episodic. Furthermore, frazil ice occurred in a variety of shapes and sizes (Fig. 4) and in relationships with congelation ice that indicate other mechanisms, in addition to surface turbulence effects, are involved in frazil ice production in the Weddell Sea. Frazil ice generally consisted of shapeless particles varying from 0.2 to 5 mm in cross-sectional diameter. Frazil particles lack the ice platelet and brine lamella substructure of congelation ice crystals. This difference is especially helpful in distinguishing between coarse-grained frazil and fine-grained congelation ice.

In conjunction with regular congelation ice growth, the formation of frazil can lead to a variety of transitions between the two crystal types. When congelation ice growth was interrupted by incursions of frazil, the frazil crystals can be packed into the interdendrite grooves of the congelation ice crystals (Fig. 10). The transition is not as sharp when frazil ice is replaced by congelation ice (Fig. 11). Because frazil ice forms by accretion, the interface would not be expected to be horizontal, as typifies the growth of congelation ice. Another structural transition is between tilted blocks
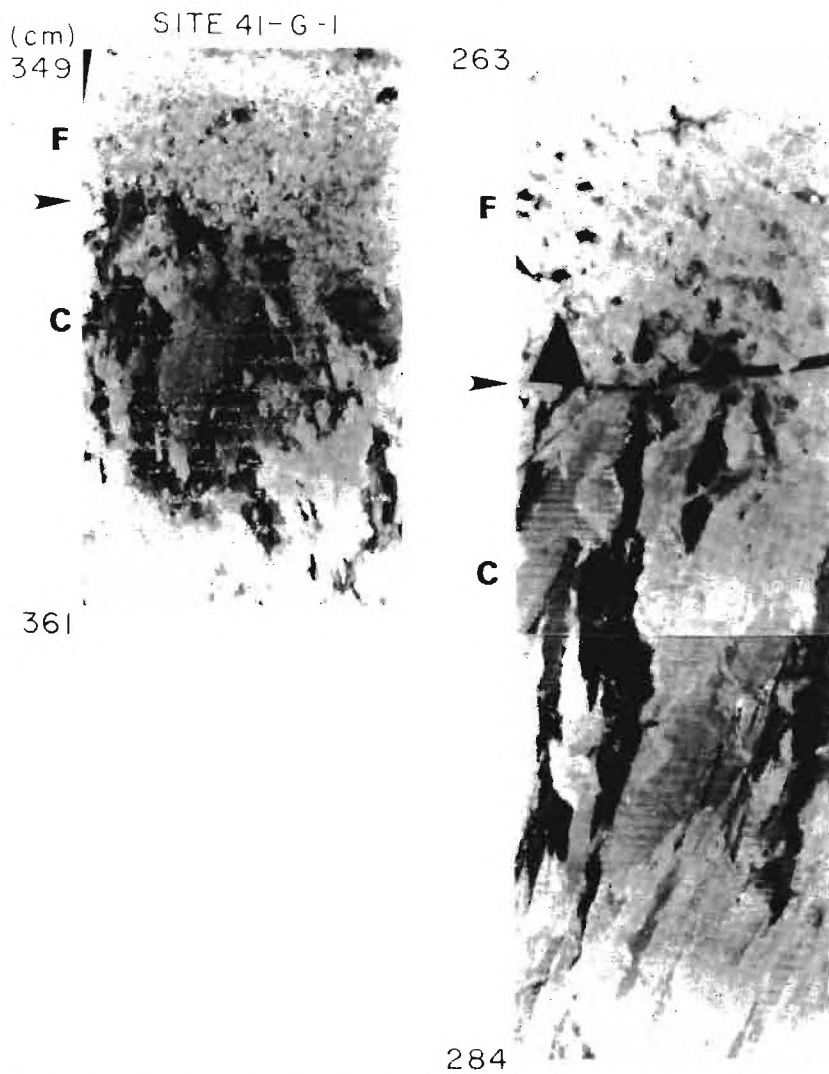
Figure 11. Vertical thick sections of ice from floe 41-G-1 showing the transition from frazil to congelation ice growth.

11
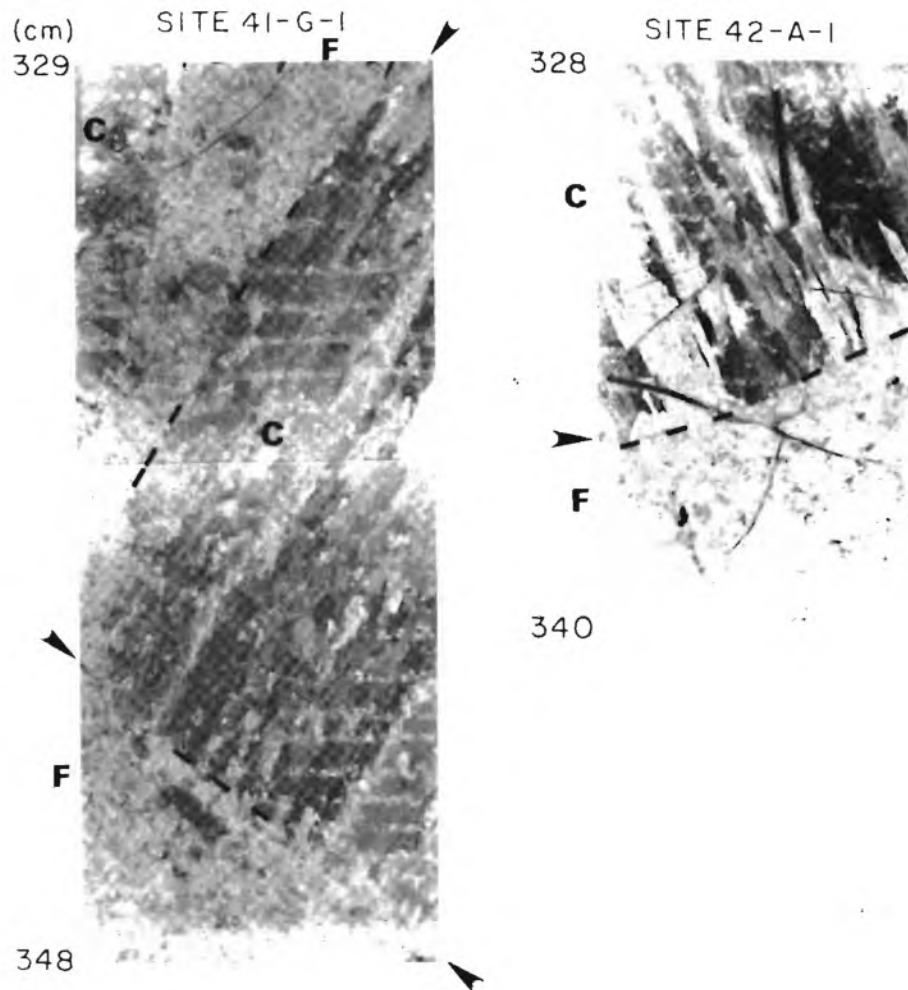
Figure 12. Vertical thick sections illustrating contact relations between tilted blocks of congelation ice and frazil in floes 42-A-1 and 41-G-1.

of congelation ice and granular ice, originating either as frazil or by actual crushing of ice during ridged or pressured ice (Fig. 12). "Banded" frazil (Fig. 13), another structural transition, is only apparent in thick or thin sections of ice examined between crossed polaroids. Banded frazil probably derives from the formation of horizontal plates with vertical c-axes in the water column beneath an existing ice sheet. On floating up to the underside of the ice, the plates tend to stay horizontal, a process leading to "bands" or layers exhibiting aggregate vertical c-axis orientation when vertical thin sections are viewed between crossed polaroids.

Large plate-like crystals measuring a centimeter or more across and even larger wafer-like crystals were also observed in the bottom ice of several multi-year floes (Fig. 14). These crystals appear

structurally equivalent to so-called underwater ice described by Serikov (1963) in East Antarctic sea ice, and the sub-ice platelet layer reported by Paige (1966) and Gow et al. (1982) in McMurdo Sound. Crystals may be so loosely bonded that it was often difficult to obtain competent core when drilling floes containing this kind of ice. Such loose, platy and wafer-like ice is perhaps best defined as transitional between frazil and congelation ice.

Most of the existing information on the crystalline characteristics of congelation ice stems from studies of shorefast ice. Very little is known of the structural properties of congelation ice in pack ice or the relative distributions of congelation and frazil ice in pack ice floes. In the Weddell Sea, congelation ice was found to be structurally identical to that observed by Gow and Weeks (1977) and
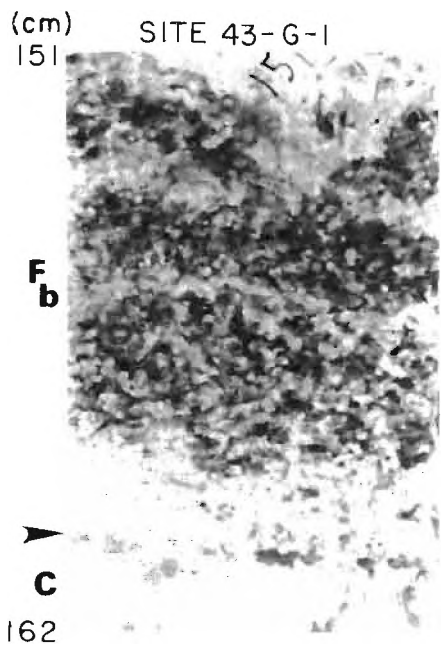
12

Figure 13. Vertical thick section of "banded" frazil (F_b) overlying congelation ice in floe 43-G-1.

Weeks and Gow (1978, 1980) in shorefast ice in the Arctic. This applied equally to first-year and multi-year ice, most of which must have formed far from the shore or shelf edge but within the confines of the winter pack. The typically columnar, vertically elongated crystals of congelation ice can reach lengths of several tens of centimeters. In cross sections, however, they do not generally exceed 3–4 cm in their longest dimension.

Congelation ice in the Weddell Sea included ice with both random and strongly aligned c-axis orientations. Weeks and Gow (1978, 1980) demonstrated that c-axis alignments in fast ice along the Alaska Coast generally parallel the measured or inferred direction of the ocean current directly beneath the ice. Recent laboratory experiments by Langhorne (1983) and Langhorne and Robinson (1986) on crystal alignments due to fluid motion confirm that large-scale preferred orientations of c-axes in Arctic sea ice (observed by several researchers to extend over areas of tens or even hundreds of square kilometers) are directly related to the action of ocean currents at the growing ice interface. We noted numerous occurrences of aligned
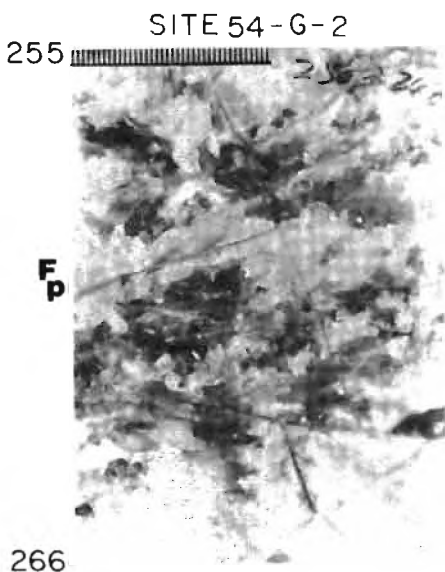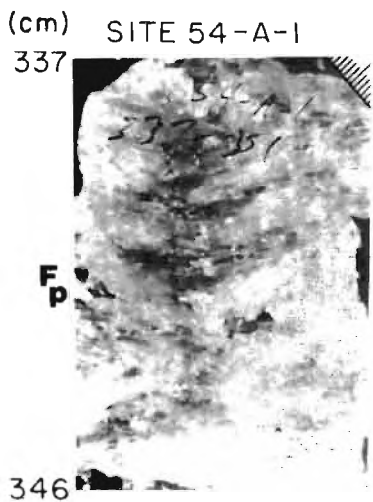
Figure 14. Vertical thick sections showing wafer-like and plate-like crystals of ice in deeper parts of floes 54-A-1 and 54-G-2, respectively.

13

c-axes in Weddell Sea ice floes. These alignments originate either under fast ice conditions (for example, in sea ice attached to shelf ice), or during the winter when tightly packed ice in the growth mode either remains stationary or maintains a constant direction with respect to the prevailing currents. Any significant or continued rotation of the floe would curtail formation of aligned c-axes. Examples of aligned c-axis structure are included in the petrographic descriptions of the 66 ice floes presented later in this report.

In addition to banded frazil, only recognizable in thin sections examined between crossed polaroids, cores from many of the floes also exhibited a visibly banded structure caused by optically clear layers in otherwise normally opaque sea ice. (Sea ice is normally opaque because of the large number of brine pockets scattering the light.) Bennington (1963) noted that banding is characteristic of Arctic Sea ice. He described three types of banding that are generally associated with changes in c-axis orientation. This, however, is not the case with the optically clear bands in the Weddell Sea ice. Here the bands are horizontal and are crystallographically identical with ice on either side. They appear to be related to fluctuations in the growth rate of the ice, most likely forming during periods of very slow growth when fewer brine pockets and air bubbles are trapped in the ice. Bands can vary in thickness from 1 to 3 mm and may occur in concentrations of up to 30 bands per meter. Vertical sectioning of cores confirms that optically transparent horizontal bands are only observed in congelation ice, never in frazil. Accordingly, the occurrence of such banding in sea ice is proof of the presence of congelation ice.

Figure 15 summarizes our observations of the abundances of congelation ice and granular ice (principally frazil) plotted as a function of ice floe thickness. These data indicate a generally higher percentage of congelation ice in floes up to 2 m thick. However, every thicker floe except one contained more frazil than congelation ice.

The total length of core analyzed for structural composition was 130.36 m. This consisted of 81.3 m of first-year ice (58 profiles from 49 floes) and 49.06 m of multi-year ice (13 profiles from 13 floes) for a total of 71 profiles.* Of the total length of first-year ice examined, 58% consisted of congelation ice and 37% of frazil ice, with the remaining 5% composed of snow ice and mixtures of frazil ice, snow ice and congelation ice. Of the multi-year ice, 72% was frazil ice, 22% was congelation ice and 6% was other forms of granular ice.

Much of the frazil ice in Weddell Sea floes is generated during the second year of growth, but there were instances where the entire floe was composed of frazil ice. This rate of frazil production has led to exceptional thicknesses of ice—up to 5 m and more—in ice less than two years old, according to drift measurements from data buoys (Ackley 1981).

In the Weddell Sea the percentage of frazil ice increases rapidly as the thickness of the floe exceeds 1.5–2.0 m. As shown in Figure 15 five of the six first-year floes 2 m thick or thicker and all the multi-year floes contained more frazil ice than
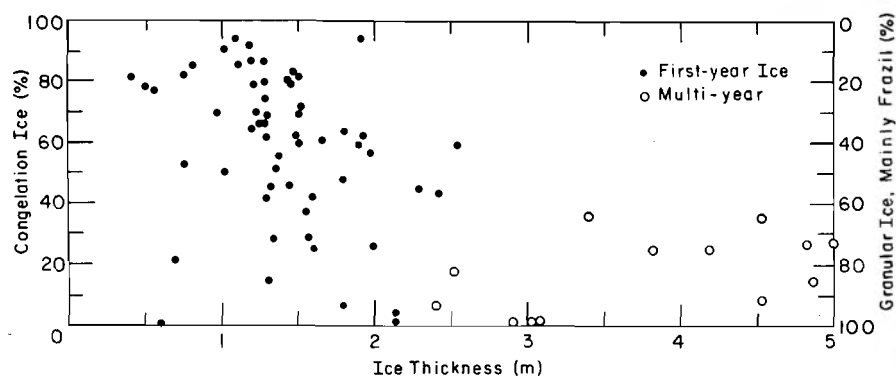
---

* A total of 75 cores were actually sectioned for structure examination but quantitative data on composition of the ice were only obtained on 71 cores.

Figure 15. Abundances of congelation ice and granular ice vs ice thickness in Weddell Sea floes.

14

congelation ice. This is the reverse of what is commonly observed in the Arctic, where the thinnest ice (< 1 m) usually contains the highest percentage of frazil. This situation not only applies to first-year ice in the Arctic but holds also for undeformed multi-year floes, based on recent studies by Tucker et al. (1985) of floes exiting the Arctic basin via Fram Strait. Generally frazil growth in the Arctic appears to be limited to the top 20 cm or so of the ice sheet, a situation consistent with turbulent crystallization of frazil in leads and areas of open water. Occasionally layers of frazil up to a meter thick have been observed in shallow, nearshore, storm-agitated waters off the coast of Alaska, often in combination with bottom-stirred sediments (Osterkamp and Gosink 1984). However, the Weddell Sea frazil ice, because of its texture, depth characteristics and exceptional thickness, must have been formed at least partly by mechanisms other than surface turbulence. For example, because of its buoyancy, surface-derived frazil is not likely to be transported downward to depths of 3 m or more, as is common in Weddell Sea floes. Similarly it is difficult to conceive of frazil growth in the open sea fronting the Weddell Sea ice pack contributing significantly to the growth in remoter areas of the pack. The rafting, one upon the other, of layers of surface frazil tens of centimeters thick could lead to aggregate thickness of a meter or more. Indeed, the top meter or so of a number of floes we examined possessed structures consistent with such a process. However, any plausible explanation of frazil occurrence in the deeper parts of ice floes must consider mechanisms that permit both episodic production of frazil between layers of congelation ice and in situ crystallization of frazil beneath ice sheets already several meters thick.

Weeks and Ackley (1982) described four processes by which frazil may form in polar oceans:

• Wind- and wave-induced turbulence. This well-known mechanism can only account for frazil growth in leads, polynyas and marginal ice zones. As noted above, rafting events may lead to enhanced thickness of frazil formed under turbulent conditions at the sea surface. However, rafting is likely to be further limited in the western Weddell Sea because of the generally heavy concentrations of ice.

• Adiabatic expansion of seawater as it ascends from beneath thick ice shelves. The Weddell Sea is backed by large ice shelves, including the Filchner and Ronne. Higher frazil percentages might be expected close to these ice shelves, but no such correlation has been established.

• Contact between two water masses of significantly different salinities. One such case would involve the interaction of seawater with freshwater. This occurs in limited situations in Antarctica, for example, beneath the floating Koettlitz ice tongue, where a layer of freshwater derived from surface ablation interacts with the underlying seawater, causing frazil crystals to form at the freezing interface between the two layers (Gow et al. 1965, Gow and Epstein 1972). A similar process was advocated by Untersteiner and Badgley (1958) to explain the freezing of freshwater frazil to the underside of Arctic ice floes. However, this mechanism is not likely to be an important source of frazil in the Weddell Sea because of the lack of surface melting.

• Thermohaline convection related to surface freezing. Such freezing results in the formation of cold brine plumes, which, as they descend, could cause frazil to crystallize in the water column underlying the growing ice sheet. This process, involving frazil production in deeper parts of the water column, is attractive because it is not constrained by the problem of crystals having to overcome the buoyancy forces encountered during downward advection of surface-derived crystals.

A fifth mechanism, not specifically mentioned by Weeks and Ackley, is associated with pressure ridging; the frazil forms in the voids between ice blocks thrust down several meters into the water during the ridging process. This is most likely to occur in very cold ice sheets. The few ridges preserved in vertical profiles of the Weddell Sea floes that we examined indicate that the filling of interblock voids with frazil could be an important source of granular ice* in areas of widespread pressuring and ridging of the ice. A similar mechanism is favored by Tucker et al. (1985) for the origin of granular ice in deformed, ridged ice in the Arctic.

If the formation of frazil in the Weddell Sea is influenced by the mixing of freshwater with seawater, then such a situation should be reflected in

---

* It is possible that void-filling granular ice identified here as frazil may include fine-grained ice with frazil-like texture derived from the actual crushing of blocks during the ridging process. However, crushing of ice should lead to breccia-like textures. Such textures were not observed in granular ice linked to ridging events in the Weddell Sea.

Table 2. Oxygen isotope variation in frazil ice in Weddell Sea ice floes.

Floe no.	Sample depth (cm)	δ¹⁸O (‰)	Floe no.	Sample depth (cm)	δ¹⁸O (‰)
41-G-1 (multi-year)	76–81	+1.76	60-A-2 (first-year)	30–35	+1.62
	196–206	+1.44			
	300–305	+1.71	60-A-5 (first-year)	8–12	+1.27
42-G-1 (multi-year)	110–116	−2.67		39–43	+2.08
	278–287	+1.58		175–179	+1.32
	430–436	+2.30		235–239	+1.73
43-A-2 (multi-year)	17–20	+1.72	60-G-1 (first-year)	11–17	+0.51
	194–198	+1.92		34–39	+1.01
	236–240	+2.09			
43-G-4 (first-year)	56–60	+1.03	60-G-5 (first-year)	8–12	+0.21
	85–90	+1.24		69–75	+0.06
44-A-1 (first-year)	67–72	+1.49	61-G-1 (multi-year)	28–36	−0.97
	143–148	+0.80		114–120	+1.65
				168–175	+1.54
49-A-2 (first-year)	107–114	+1.86		251–258	+1.89
			62-A-1 (multi-year)	14–18	+1.57
54-A-1 (multi-year)	12–16	+1.82		40–45	+1.80
	233–238	+1.70		129–133	+2.05
	360–365	+2.08		185–191	+1.94
				289–293	+1.84

the isotopic composition (either hydrogen or oxygen) of the ice itself. Isotope variations are usually expressed as a deviation (δD or $\Delta^{18}O$) from standard mean ocean water (SMOW), a positive value indicating enrichment and a negative value indicating depletion with respect to SMOW. Polar snow and glacial ice are highly depleted with respect to SMOW, so small inputs of meltwater of either to seawater should yield a diagnostic isotopic signal. Friedman et al. (1961), used δD measurements to show that the freezing of seawater yields ice that is aproximately 2‰ enriched in deuterium. This 2‰ enrichment was confirmed for Antarctic sea ice by Gow and Epstein (1972), who also found a corresponding enrichment with respect to $\delta^{18}O$ measurements. Data from the latter work proved critical in identifying the origins of different ice samples, principally sea ice growing onto the bottom and ultimately replacing the glacial ice of the floating shelf-like tongue of the Koettlitz Glacier in McMurdo Sound. Lyons et al. (1971) applied essentially the same technique to resolve the internal structure (which included glacial, seawater and brackish water ice components) of the Ward Hunt ice shelf, Ellsemere Island, Canada.

We sampled 13 floes exhibiting a variety of frazil textures; the results of the $\delta^{18}O$ analyses are listed in Table 2. The analytical precision is approximately 0.03‰. Of 35 samples from the 13 floes (seven first-year and six multi-year), all but three had positive $\delta^{18}O$ values, compositions that are essentially compatible with freezing from ordinary seawater. Excluding the three samples showing negative deviations, $\delta^{18}O$ values of the remaining 32 samples ranged from +2.30 to +0.21‰ and averaged +1.58‰. These data compare very closely with those obtained by Gow and Epstein (1972) on sea ice in McMurdo Sound, in which $\delta^{18}O$ ranged from +2.51 to +1.37‰ and averaged +1.75‰. The most negative value of −2.67‰ was measured at 110–116 cm in floe 42-G-1 and is probably linked to a small input of freshwater, possibly snow ice associated with the tilted block of thin congelation ice located close to the isotope sample. Similarly the $\delta^{18}O$ value of −0.97‰ for frazil at 28–36 cm in floe 61-G-1 is probably linked to mixing of snow and frazil during the early stages of the growth of the ice. Values of +0.21 and −0.06‰ at depths of 8–12 and 69–75 cm in floe 60-G-5 also likely reflect the addition of small amounts of snow to the seawater.

We observed no systematic difference in $\delta^{18}O$ with respect to differences in the texture of the frazil, for example, fine-grained frazil as opposed to coarse-grained frazil, large wafer-like plates or banded frazil. Our $\delta^{18}O$ measurements suggest that the bulk of the frazil in the Weddell Sea ice floes originates by crystallization from seawater containing very little or no freshwater component. This is consistent with the lack of surface snow melt and suggests that the frazil in the deeper parts of Weddell Sea ice floes forms by either adiabatic expansion of seawater as it ascends from beneath ice shelves or thermohaline convection related to surface freezing and the formation of descending plumes of brine. Weeks and Ackley (1982) considered the latter mechanism the more likely, given the depth characteristics, the exceptional thickness and the widespread occurrence of frazil in the Weddell Sea pack ice (Ackley et al. 1980, Gow et al. 1982). However, thermohaline convection should apply equally well under Arctic conditions. Yet frazil is a relatively minor component of Arctic sea ice, clearly indicating that other mechanisms, including adiabatic expansion of ascending seawater, are contributing to frazil production in the Weddell Sea. Deeper convection of water related to the greater thickness of the mixed layer—100 m in the Weddell Sea compared to only 30 m or so in the Arctic—may also contribute to greater frazil production in the Weddell Sea.

Fluorescence

Problems in the fluorescence measurement technique precluded the determination of any "universal" relationship between the biological and physical properties of ice cores from Weddell Sea floes. This is apparently partly linked to the highly general nature of the fluorescence, which is a combined index of both living and dead biological material.

In a study based on relatively few ice samples, Ackley et al. (1979) suggested that salinity may vary systematically with the level of biological material in the ice as measured by the fluorescence. Although this relationship can be found in some of the profiles we measured, it was not generally true for our 66 Weddell Sea floes. However, there is some evidence that brine drainage can potentially trigger an "elevated biology" near the surface of the sea ice (Ackley, unpub. data). Similarly we observed no conclusive or simple relationship between ice structure and substantial biological activity. Examples of both high and low levels of biological activity were found in all three principal

ice crystal types. Although ice structure may influence significantly how and where organisms develop in sea ice, our measurements do not permit us to differentiate between structural effects and other effects such as initial entrapment, in situ growth, brine drainage events, warming of the ice, snow cover, temperature, total ice thickness, and light levels.

Our fluorescence measurements do demonstrate, however, the tremendous variety of habitats or repositories that occur in Weddell Sea pack ice. Our fluorescence data also show that surface, near surface, interior and bottom populations all occur in the Weddell Sea floes, with no particular bias toward any one of these populations. Examples of highly elevated biological activity in any one of these population levels can be observed in a number of profiles presented here. This situation contrasts, for example, with the ice communities in the fast ice near McMurdo Sound, where the biology is dominated by late-season, ice-bottom communities with little activity at other locations within the sea ice cover.

Description of selected floes

Seventeen floes were selected for detailed descriptions of their major physical properties. They can be considered representative of the variations in salinity, fluorescence and petrographic structure observed in the 66 floes we examined in the Weddell Sea. Profiles of the remaining 49 floes, together with descriptions of their physical characteristics, are included in Appendix A.

Site 42-A-1 (Fig. 16)

Described briefly by Gow et al. (1982), this floe was of thick (4.52 m) multi-year ice with a maximum salinity of 9‰ and an average salinity of 3.4‰. It was composed of 4% snow ice at the top of the floe, 61% frazil ice located in layers throughout the floe and 35% congelation ice concentrated in the middle third of the floe. The physical disposition of the congelation ice is interesting because the vertical sectioning revealed evidence of a tilted structure, related possibly to rafting or ridging of ice blocks (Fig. 12). If this is the case, then the associated granular ice could have originated as frazil, by freezing of seawater in voids between the blocks, or by crushing of ice during ridging. Dramatic swings in salinity appear to be independent of changes in the structural composition of the ice. The same situation also seems to hold true for fluorescence, which attained a maximum of 602 in ice from the frazil/congelation transition at
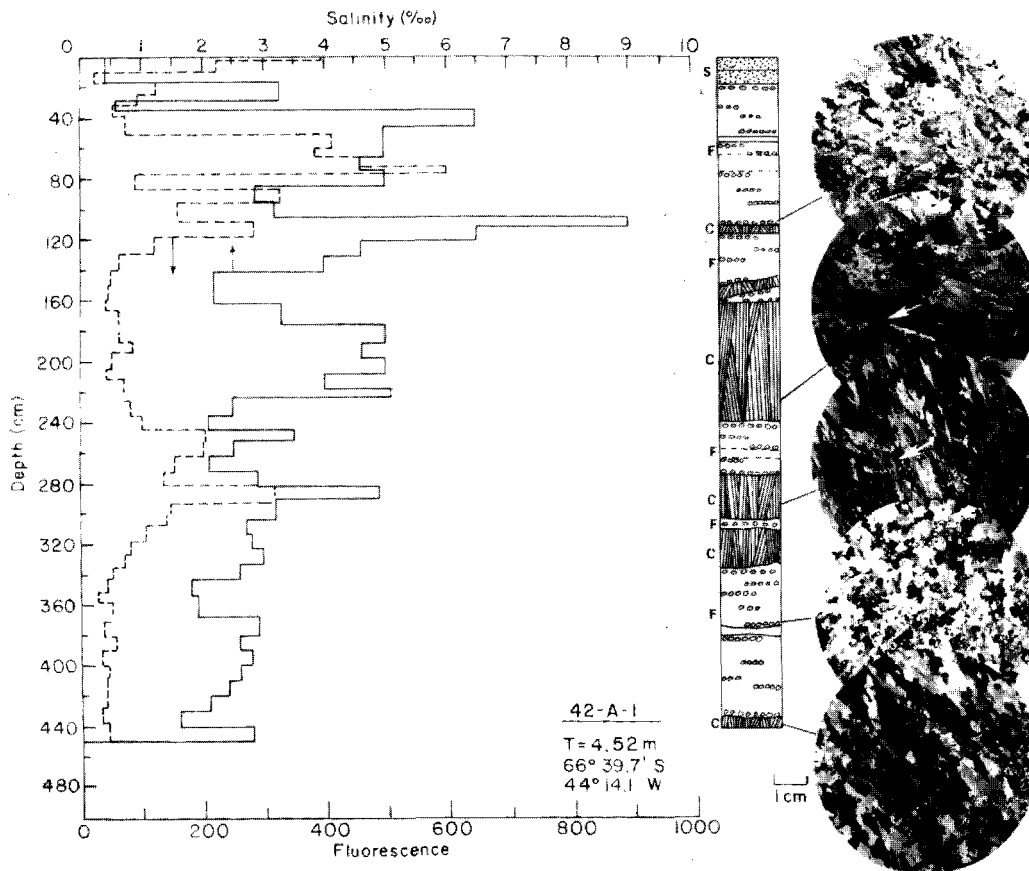
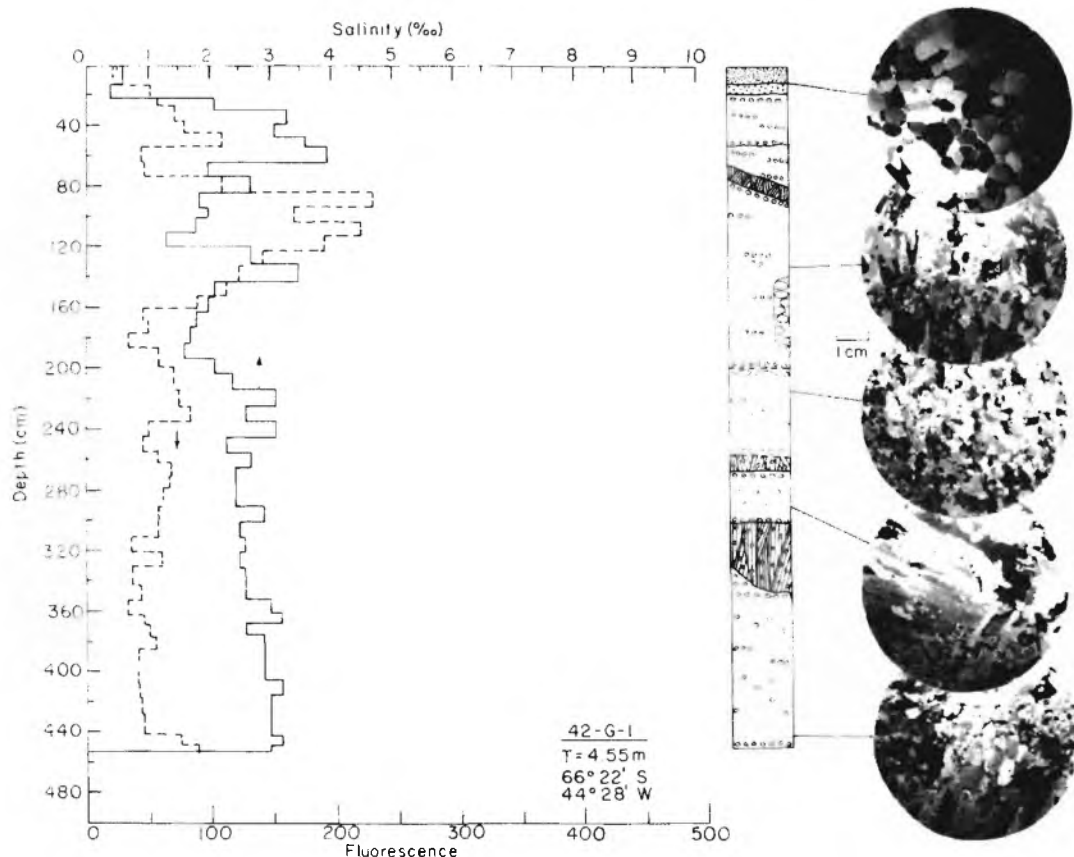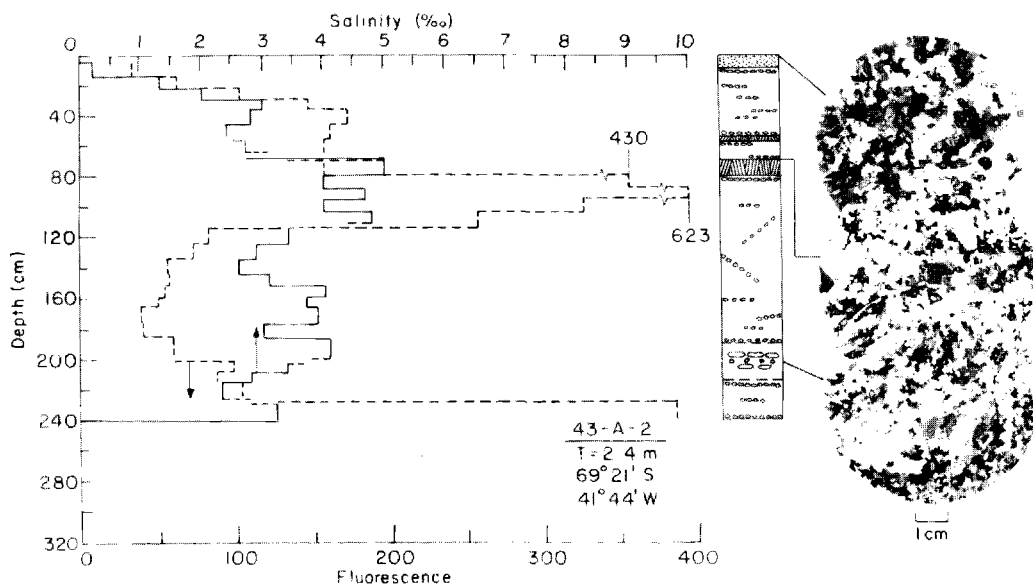*Figure 16. Salinity and fluorescence profiles, vertical structure section and horizontal thin sections of ice floe 42-A-1. The symbols S, F and C on the left side of the structure section denote undifferentiated granular ice (principally snow ice), frazil ice and congelation ice, respectively. The arrows indicate directions of strongly aligned c-axes.*

a depth of 72–76 cm. Much of the congelation ice was characterized by very strong alignment of the crystallographic c-axis, indicated by the arrows in the photomicrographs of thin sections from 2.24 m and 2.93 m. This kind of alignment is consistent with the concept of current-controlled growth of the congelation ice either under shorefast or shelf-fast conditions or when the floe was tightly held in the winter pack.

Site 42-G-1 (Fig. 17)

This 4.55-m-thick multi-year floe was overlain by 30–50 cm of snow and was composed principally of frazil ice (79%) of highly variable grain size but tending toward coarser grains, especially in the middle third of the floe. The top of the floe was riddled with brine channels. There was evidence of a tilted block of congelation ice at 70–95 cm. Petrographic examinations of several horizontal thin sections yielded the following results.

At 11 cm an equidimensional grain mosaic was identified as recrystallized snow ice. The layer at 131 cm contained very coarse frazil and possibly fragments of congelation ice. At 214 cm very coarse frazil enclosed some fragments of congelation ice. At 300 cm there was a mixture of congelation and frazil ice similar in appearance to the ice at 131 cm. In this instance the fragments of congelation ice contained numerous brine pockets. This section at 300 cm was located just above a layer of congelation ice measuring 30 cm thick. The section at 450 cm showed coarse-grained frazil with some crystals identified as congelation ice on the basis of brine pockets. This floe displayed a relatively uniform salinity profile that averaged 2.5‰. A small increase in fluoresence (ranging in value from 225 to 145) began with the congelation/ frazil ice transition at around 85 cm and continued to 129 cm. Measurements of $\delta^{18}O$ yielded a value of –2.67‰ for frazil at 110–116 cm, consistent with
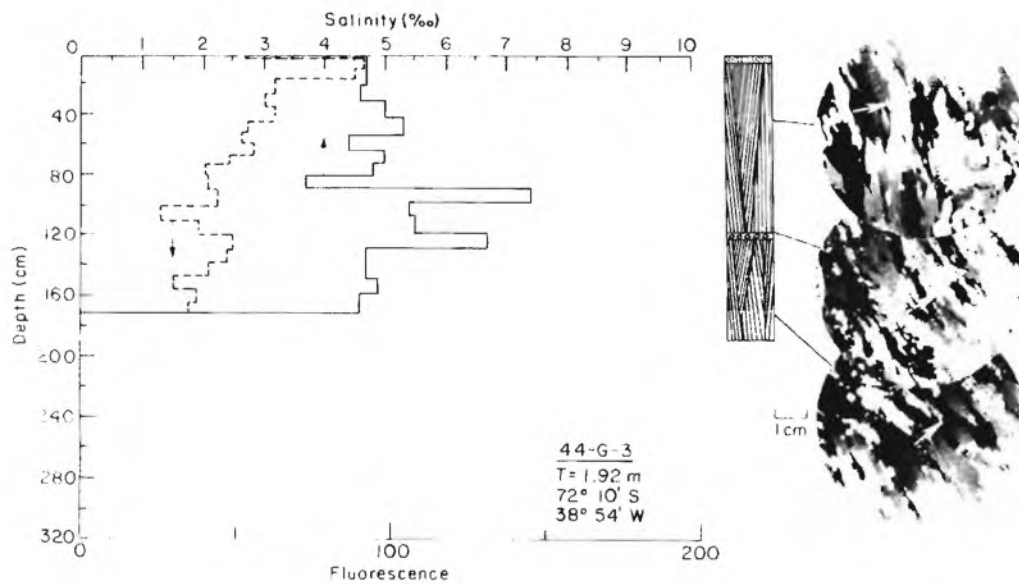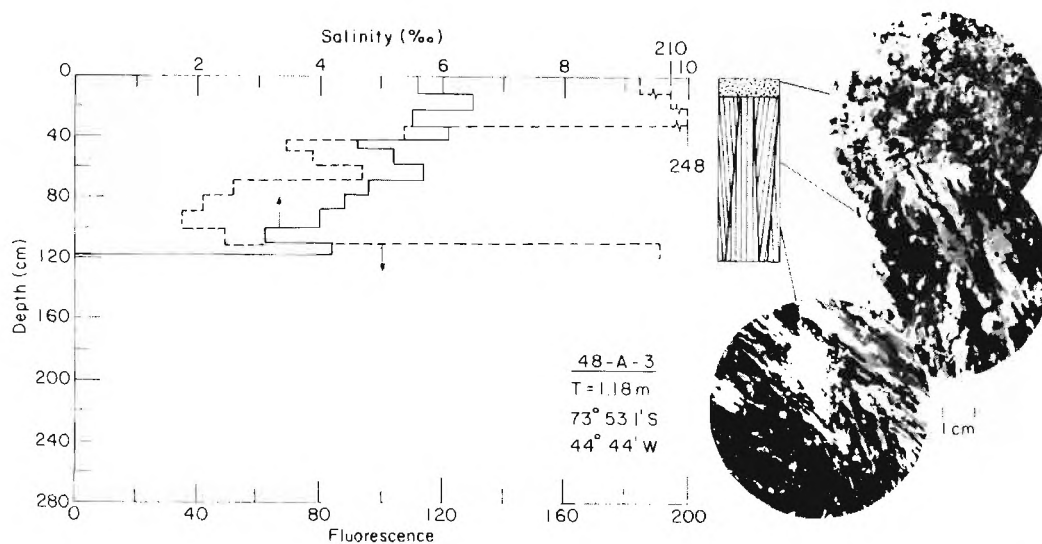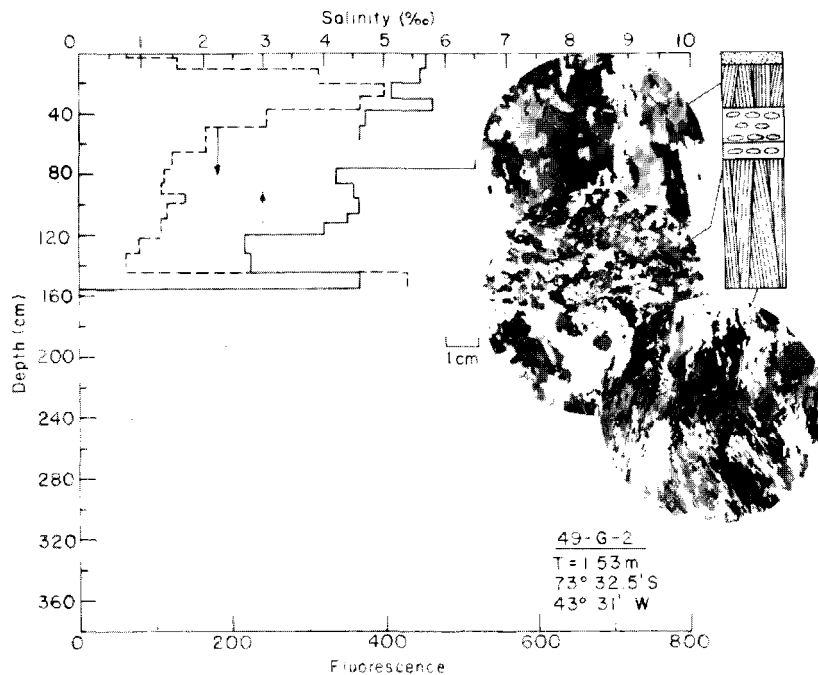
18

Figure 17. Salinity and fluorescence profiles, vertical structure section and horizontal thin sections of ice floe 42-G-1.

freezing from seawater containing a small input of freshwater possibly derived from snow on top of the tilted block. Two analyses of frazil deeper in the floe both confirm crystallization from normal seawater.

Site 43-A-2 (Fig. 18)

The exact age and origin of this 2.4-m-thick floe are difficult to assess. However, a maximum salinity of only 5‰ and a bulk salinity of 3.2‰ indicate that this was a multi-year floe. It contained just two thin layers of congelation ice, totaling 6% of the floe thickness, and 91% frazil ice of variable grain size, including a layer from near the bottom where grain diameters generally exceeded 4 mm. As indicated in Table 2, $\delta^{18}O$ values of three samples of frazil ice are completely compatible with crystallization from normal seawater. The peak fluorescence of 623 occurred across the transition from congelation to frazil ice at around 80 cm, with a second peak of 390 at the bottom of the floe.

Site 43-G-3 (Fig. 19)

This is a second core from the same floe as site 43-G-2 (Fig. A14). The structural and salinity characteristics of this core were very similar to those in 43-G-2, but the ice at 43-G-3 was appreciably thicker (1.91 m). The ratio of congelation to frazil ice at this location was 60:33, with snow ice (7%) accounting for the remaining ice in the floe. Horizontal thin sections all featured granular ice with the sections from 45 cm and 145 cm showing coarse-grained frazil at major congelation/frazil transitions. However, vertical sectioning of the entire core established that congelation ice was the principal component. The salinity varied from 2.6 to 6.5‰ and averaged 4.2‰. In this part of the floe, unlike at site 43-G-2, fluorescence and salinity maxima tend to be associated. A peak fluorescence of 880 was recorded in the bottom of the first thick layer of congelation ice (35–40 cm deep); other peaks also were confined to congelation ice.

19

Figure 18. Salinity and fluorescence profiles, vertical structure section and horizontal thin sections of ice floe 43-A-2.
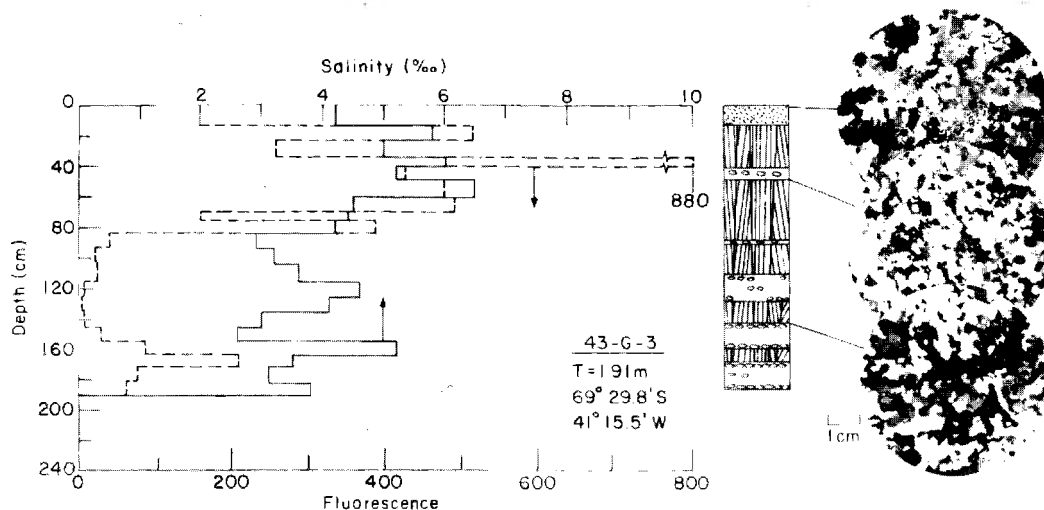
Figure 19. Salinity and fluorescence profiles, vertical structure section and horizontal thin sections of ice floe 43-G-3.

Site 44-G-3 (Fig. 20)

This 1.92-m-thick floe was located in a region of recently disintegrated sheet ice that produced floes approximately 30 m long. Identified as first-year ice with an average salinity of 5.1‰, this floe was composed almost entirely of congelation ice (94%). The crystals exhibited a well-developed brine lamella and ice plate structure, with plate spacings averaging 0.8 mm and a strong alignment of the c-axes. The constancy of this alignment indicates that freezing occurred either under fast-ice conditions or in an immobilized part of the winter pack. Fluorescence was high in the top 20 cm, but absolute levels were low at all depths.
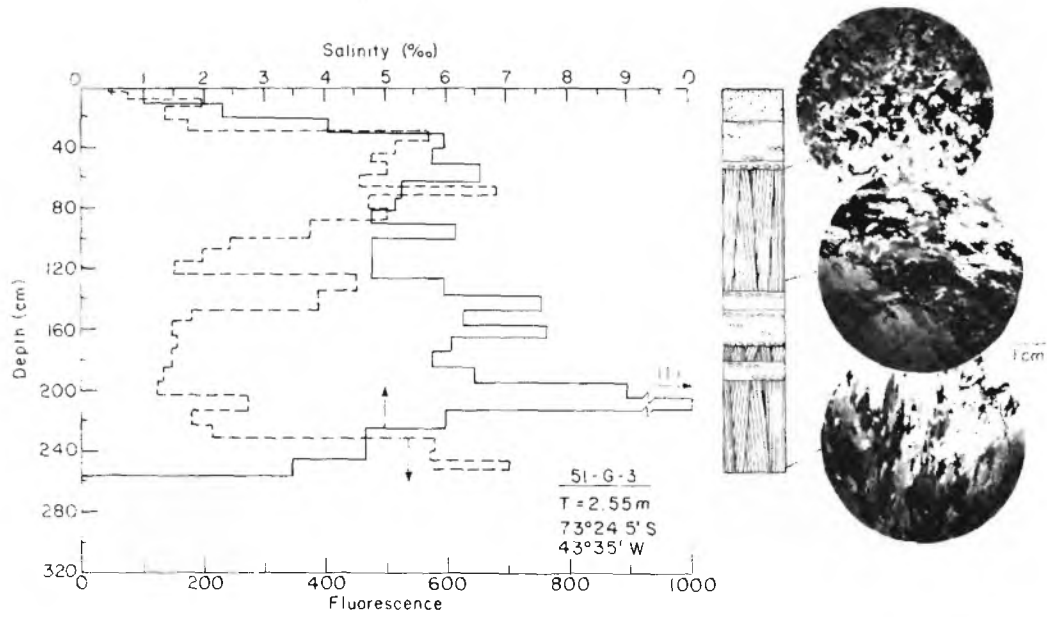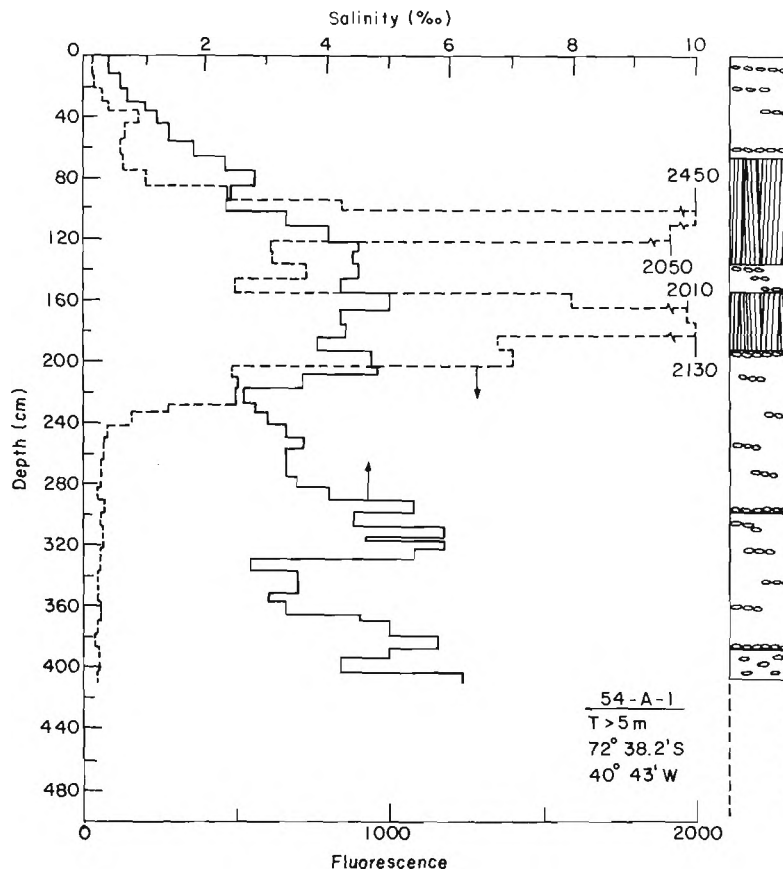
20

Figure 20. Salinity and fluorescence profiles, vertical structure section and horizontal thin sections of ice floe 44-G-3.

Figure 21. Salinity and fluorescence profiles, vertical structure section and horizontal thin sections of ice floe 48-A-3.

Site 48-A-3 (Fig. 21)

This was a first-year floe (1.18 m thick) that was very similar structurally to floe 48-A-2 (Fig. A21) located in the same vicinity. Except for a 14-cm-thick layer of mixed snow and frazil ice, the floe was composed entirely of congelation ice with moderately aligned c-axes, especially near the bottom. The salinity tended to decrease with increasing depth. The bulk salinity measured 5.0‰. The fluorescence peaks were at the top and bottom of the floe.
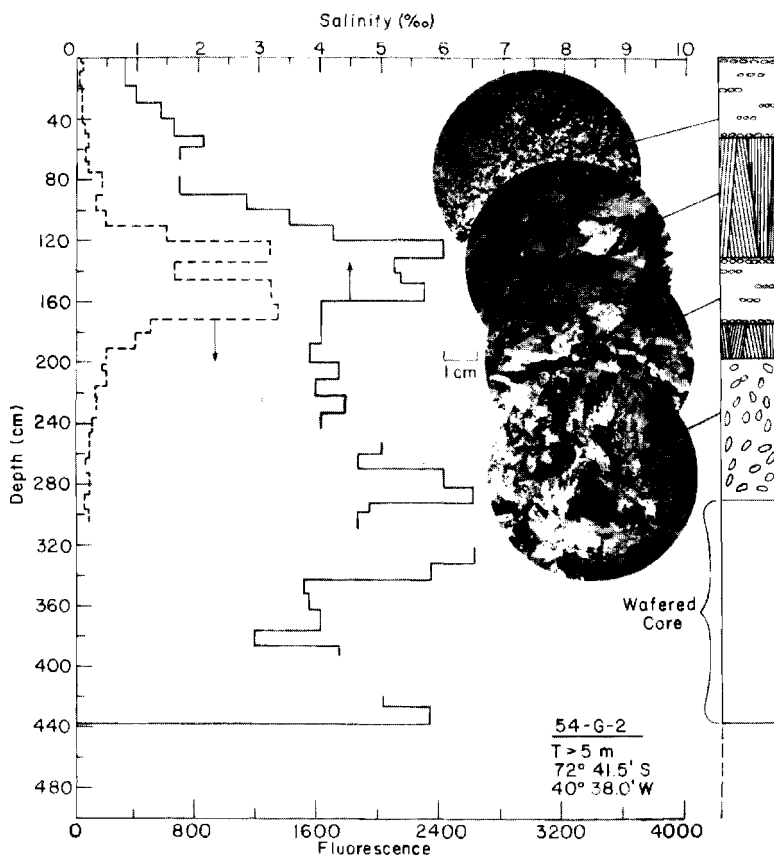
21

Figure 22. Salinity and fluorescence profiles, vertical structure section and horizontal thin sections of ice floe 49-G-2.

Site 49-G-2 (Fig. 22)

This first-year 1.53-m-thick floe was composed principally of congelation ice (72%), with the frazil ice (23%) confined to a zone between 36 and 70 cm. The average salinity was 4.7‰. Evidence for extensive channeling of brine was observed at 30–40 cm. The thin section from 71 cm clearly intersected two ice types, since its texture is transitional between fine-grained frazil and coarser-grained congelation ice. The bottom section comprised fibrous-textured crystals with randomly aligned c-axes. Two fluorescence peaks were measured, one at the bottom of the first layer of congelation ice (20–40 cm) and the second in ice from the bottom of the floe.

A second core, designated 49-G-1, was taken from the same floe and used solely to measure salinities on samples of a full-sized core. The mean salinity of this 1.43-m-thick core measured 4.7‰, identical with that obtained at 49-G-2 located just 3 m away.

Site 51-G-3 (Fig. 23)

This floe was thicker (2.55 m) than all the other first-year floes investigated, but it was clearly identified as first-year ice because of its crystal structure and salinity profile. A peak salinity of

11‰ was recorded at 204-212 cm; the average salinity measured 5.7‰. A peak fluorescence of 704 was recorded in the bottom ice, but overall the fluorescence profile showed little correlation with the salinity profile. Structurally this floe consisted of 8% snow ice overlying alternating layers of frazil (33%) and congelation ice (59%). The congelation ice was characterized by abundant banding, with 22 bands between 90 and 123 cm and occasional banding both above and below this zone.

Examinations of crystalline texture and fabrics in five thin sections yielded the following results. The ice at 51 cm was from a zone of fairly coarse-grained frazil and contained crystals up to 5 mm in diameter. At 123 cm the ice was composed entirely of fibrous-textured congelation ice with plate spacings averaging 0.6–0.7 mm. The c-axes were moderately aligned, deviating by no more than 25° on either side of the average alignment vector. The section at 172 cm showed principally congelation ice; occasional inclusions of small grain clusters were of frazil origin. Plate spacings averaged 0.8 mm in congelation crystals, which in this section were not azimuthally oriented. At 212 cm the ice was composed entirely of congelation crystals with c-axes aligned within a 35–40° range. Plate widths averaged 0.8 mm. Again, the section at 254 cm
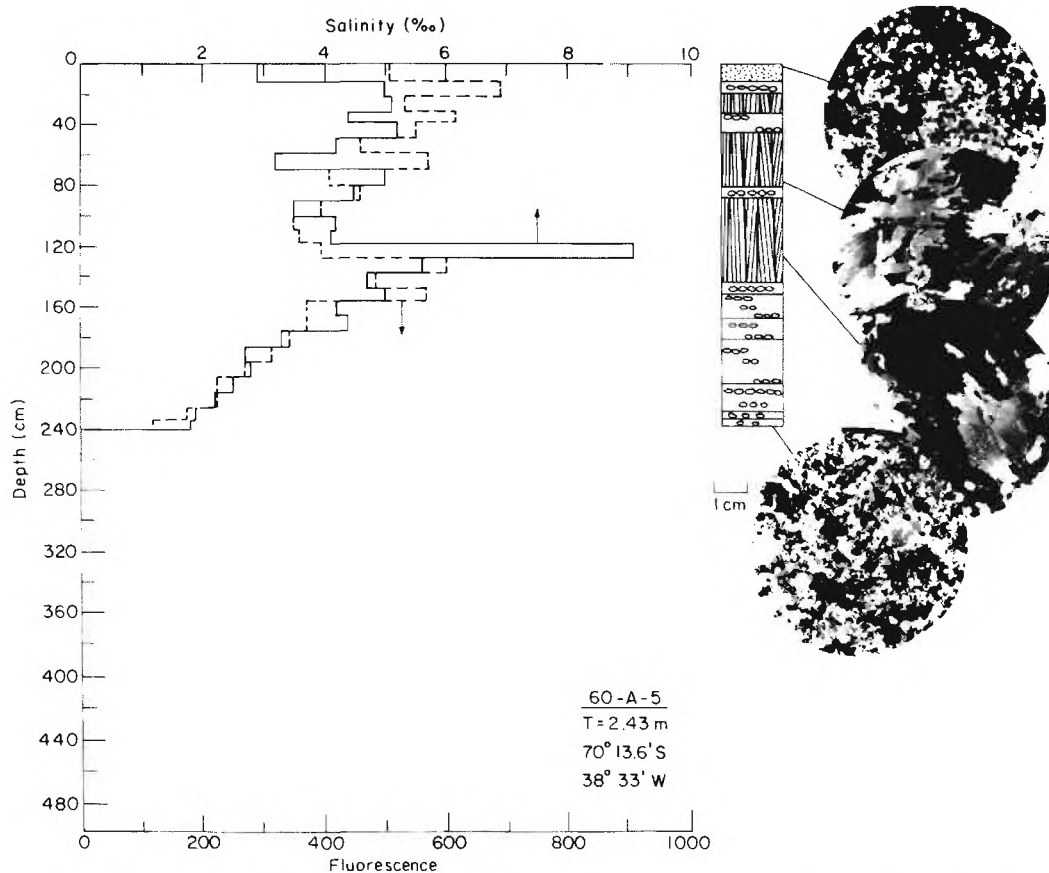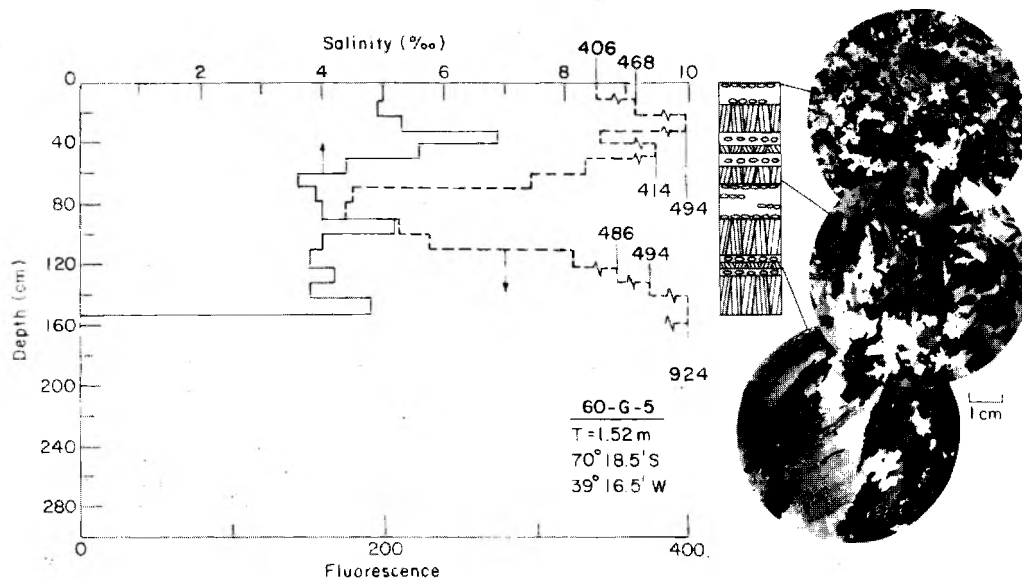
22

Figure 23. Salinity and fluorescence profiles, vertical structure section and horizontal thin sections of ice floe 51-G-3.

Figure 24. Salinity and fluorescence profiles and vertical structure section of ice floe 54-A-1.

consisted solely of congelation ice in which crystals were very strongly aligned in the same direction as crystals in the section from 212 cm. The existence of aligned c-axes in the two major zones of congelation ice indicates that both zones originated either in fast ice or under stationary conditions in the winter pack ice. Unfortunately, cores from the two zones could not be oriented with respect to one another, so we couldn't tell if both zones exhibited identical c-axis alignments.

Site 54-A-1 (Fig. 24)

This was a multi-year floe exceeding 5 m in thickness, as determined by drilling, though only 4.1 m of core was actually recovered for analysis. The recovered core consisted of 73% frazil and 27% congelation ice, with the latter confined to two layers in the top half of the core. No horizontal thin sections were prepared, so observations of the structural characteristics of this floe were limited to vertical sections. The salinity profile showed appreciable desalination of the ice in the top meter, with the average salinity less than 1.6‰ in this section of the floe. In the younger ice below 200 cm, the average salinity exceeded 4‰. The maximum salinity, 6.2‰, was recorded at the bottom of the core. The mean salinity for the 410 cm of recovered core measured 3.5‰. Structurally the first year's growth, probably of fast ice origin, apparently terminated at the bottom of the second layer of congelation ice, with all subsequent ice growth occurring as frazil. Fluorescence peaks ranging from 2050 to 2450 were all restricted to the congelation ice. An abrupt decline to less than 100 characterized the frazil ice from below 240 cm. As shown in Table 2, $\delta^{18}0$ analyses of frazil ice from three levels in 54-A-1 are all consistent with crystallization in normal seawater.

Site 54-G-2 (Fig. 25)

This floe contained multi-year ice measuring more than 5 m thick, as determined by drilling.

Figure 25. Salinity and fluorescence profiles, vertical structure section and horizontal thin sections of ice floe 54-G-2.

24

Excellent cores were obtained to a depth of 3.1 m, but all deeper ice consisted of wafered platy crystals that were loosely consolidated and difficult to extract as continuous cores. The latter cores may represent underwater ice as described by Russian observers at Antarctic coastal locations (for example, Serikov 1963).

Structurally the ice at site 54-G-2 consisted of alternating layers of frazil and congelation ice in approximately equal proportions in the top 200 cm; beneath that was a zone, nearly 100 cm thick, composed of a mixture of coarse-grained frazil and plate-like crystals of congelation ice exhibiting vertical c-axes. This zone appeared structurally transitional between the congelation layer directly above and the wafery, plate-like crystals below 290 cm. Ice from the top meter of the floe contained numerous brine drainage channels, consistent with the desalination indicated by the salinity profile. The bottom of the second layer of congelation ice probably marks the termination of first-year ice growth. A moderate to strong alignment of c-axes in the two congelation ice layers is interpreted as indicating growth under either fast-ice conditions or in the immobile part of the winter pack. Widespread banding was also observed in the top congelation ice layer. Most salinity values below 120 cm exceed 3.8‰, which is the average salinity of the floe due to the desalination in the top 120 cm. Fluorescence peaks of 1260 and 1320 were confined to the frazil ice layer at 1.2–1.7 m, and the fluorescence was positively correlated with salinity in this floe to a depth of about 260 cm. The unique structure of this core coincides almost exactly with that of core 54-A-1, obtained from a floe about 5 km away. We suspect these two floes broke off from the same piece of fast ice and then diverged slightly as the pack drifted.

Site 60-A-5 (Fig. 26)

It is difficult to determine the age of this floe but the relatively high salinities in the top half of the floe indicate that it is first-year ice, albeit thick (2.43 m). Structurally, however, the transition from congelation to frazil ice at about 140 cm might signal the onset of growth of second-year
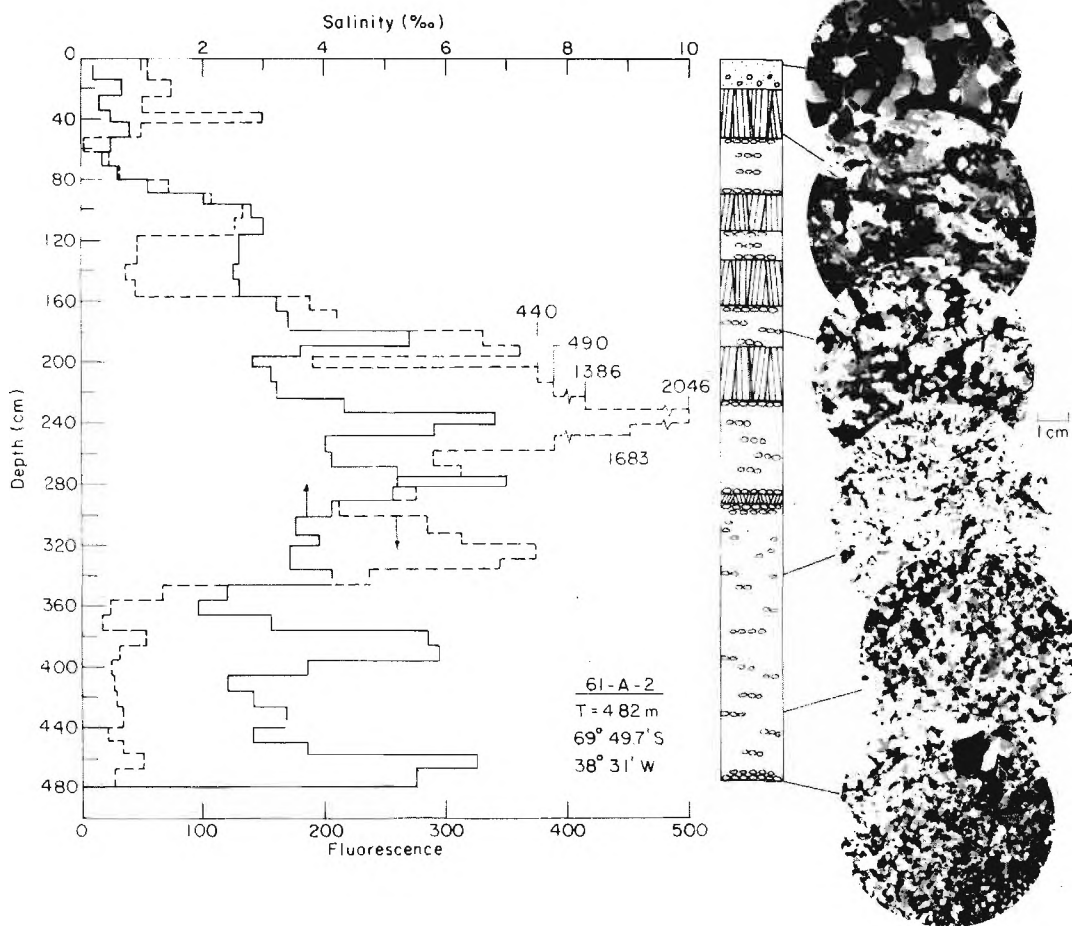

Figure 26. Salinity and fluorescence profiles, vertical structure section and horizontal thin sections of ice floe 60-A-5.

ice. The average salinity measured 4.1‰. An unusually rapid decrease in salinity was recorded between 140 and 240 cm. This was closely paralleled by changes in fluorescence. Four samples of frazil were analyzed for $\delta^{18}O$ at locations indicated in Table 2. These data are consistent with crystallization from ordinary seawater.

Site 60-G-5 (Fig. 27)

This core, from a first-year floe 1.52 m thick, consisted of congelation ice (60%) and frazil (40%) in alternating layers. The bottom layer of congelation ice was composed of large crystals showing moderate to strong c-axis alignment. The average salinity was 4.6‰. The fluorescence profile was characterized by several peaks of 400-500

in the top 50 cm and in cores from near the bottom; the maximum value of 924 was at the bottom. Measurements of $\delta^{18}O$ levels in frazil from 8-12 cm and 69-75 cm were +0.21‰ and +0.06‰, respectively, indicating crystallization of the frazil from seawater containing a small input of freshwater.

Site 61-A-1 (Fig. 28)

This 1.32-m-thick first-year floe was composed of alternating layers of frazil (totalling 50% of the ice thickness) and congelation ice (45%), overlain by a mixed layer of snow and frazil ice (5%). The salinity averaged 4.8‰. This floe was characterized by very high relative values of fluorescence, including a peak of 6595 in the congelation ice
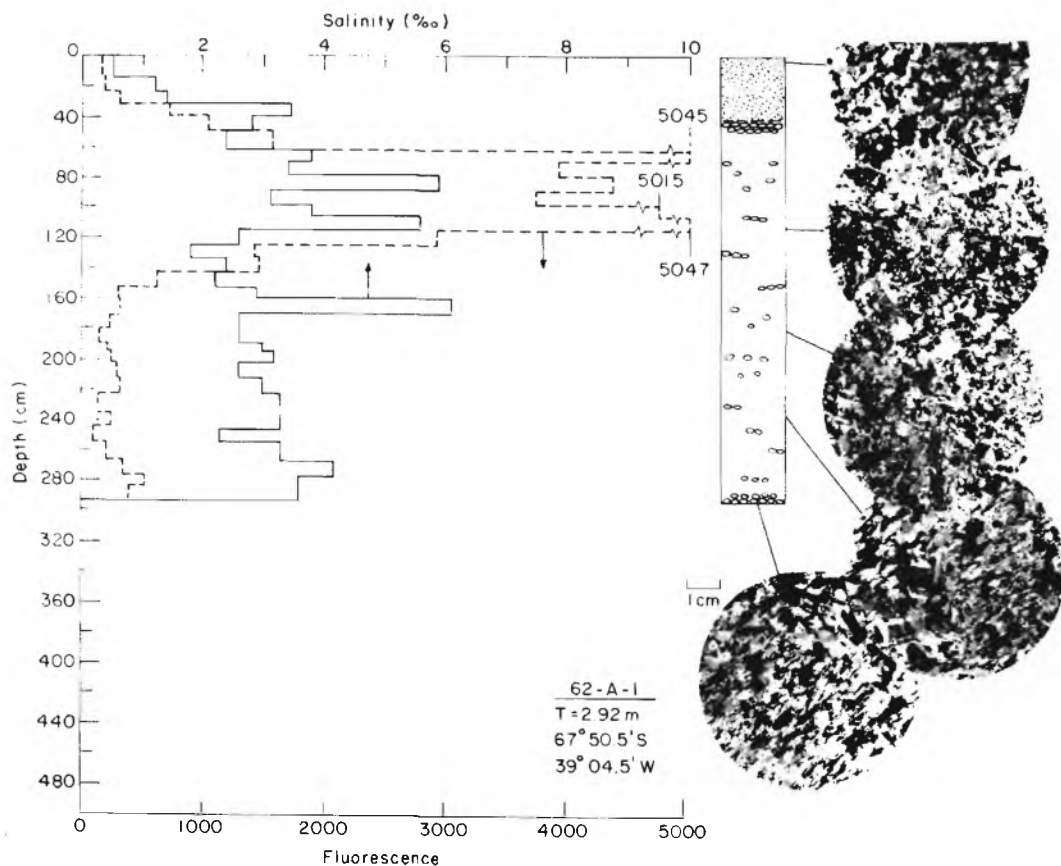
Figure 27. Salinity and fluorescence profiles, vertical structure section and horizontal thin sections of ice floe 60-G-5.
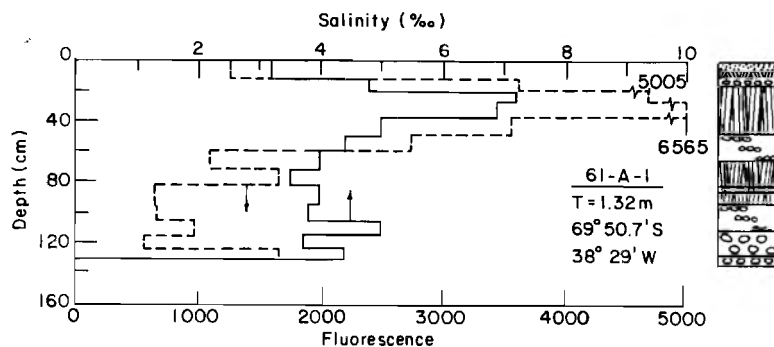
Figure 28. Salinity and fluorescence profiles and vertical structure section of ice floe 61-A-1.

near the top of the floe. In this instance the salinity and fluorescence profiles showed a strong positive correlation.

Site 61-A-2 (Fig. 29)

This was a multi-year floe, 4.82 m thick, consisting of alternating layers of frazil and congelation ice in the top 230 cm, underlain by 250 cm of frazil ice containing just one thin layer of congelation ice at 290 cm. Whereas the frazil in the top 230 cm occurred in a variety of grain sizes, varying from 1 to 6 mm or more, the thick layer of frazil in the bottom half of the floe was composed of crystals of relatively uniform size (3–4 mm). Frazil ice accounted for 69% of the total ice thickness. The top 4% of the floe was composed of a mixture of snow and frazil ice including about 10 cm of coarse-grained recrystallized snow. The age of this floe is difficult to determine from its structure. We might speculate that the end of the first-year's growth was the bottom of the congelation ice layer at 230 cm, with all subsequent growth occurring within the frazil regime. From the top of the floe to a depth of 80cm, the salinities did not exceed 1‰. The salinity was highly variable in the deeper ice, with values ranging from 2 to 7‰. The average for the entire floe was 3.2‰. Peak fluorescence values fluctuated in approximate accord with salinity values, including a maximum fluorescence of 2046 in the frazil ice just below the frazil/congelation transition at 230 cm. Minimal fluorescence was recorded in ice below 360 cm.

Site 61-G-1 (Fig. 30)

Classified as multi-year ice, this 3.01-m-thick floe was composed of uniform-sized granular frazil ice to a depth of 220 cm, underlain by a puz-

Figure 29. Salinity and fluorescence profiles, vertical structure section and horizontal thin sections of ice floe 61-A-2.

27
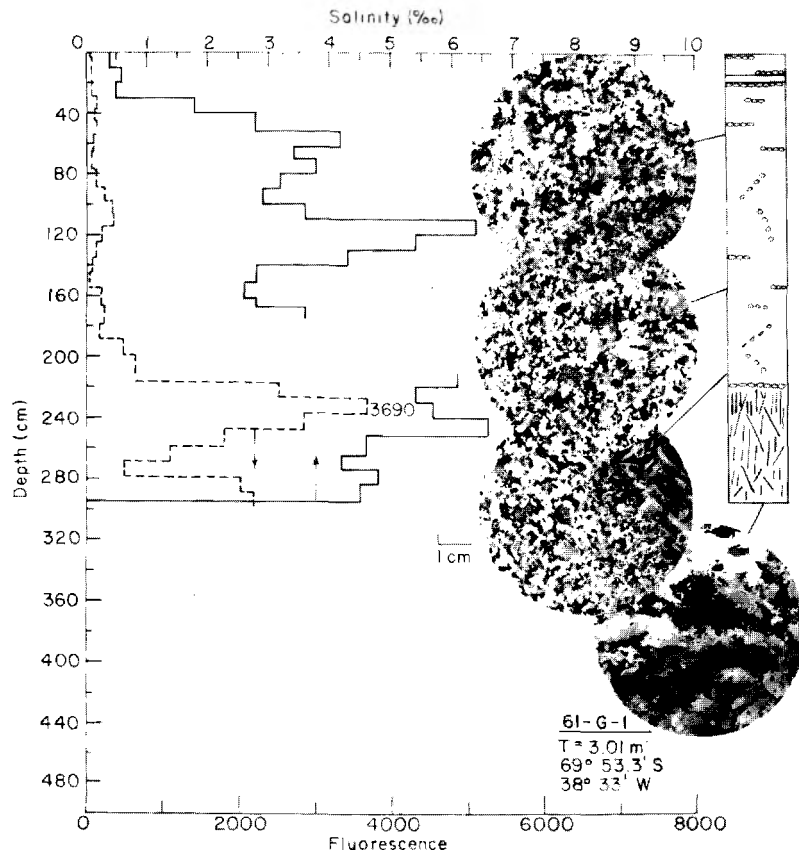
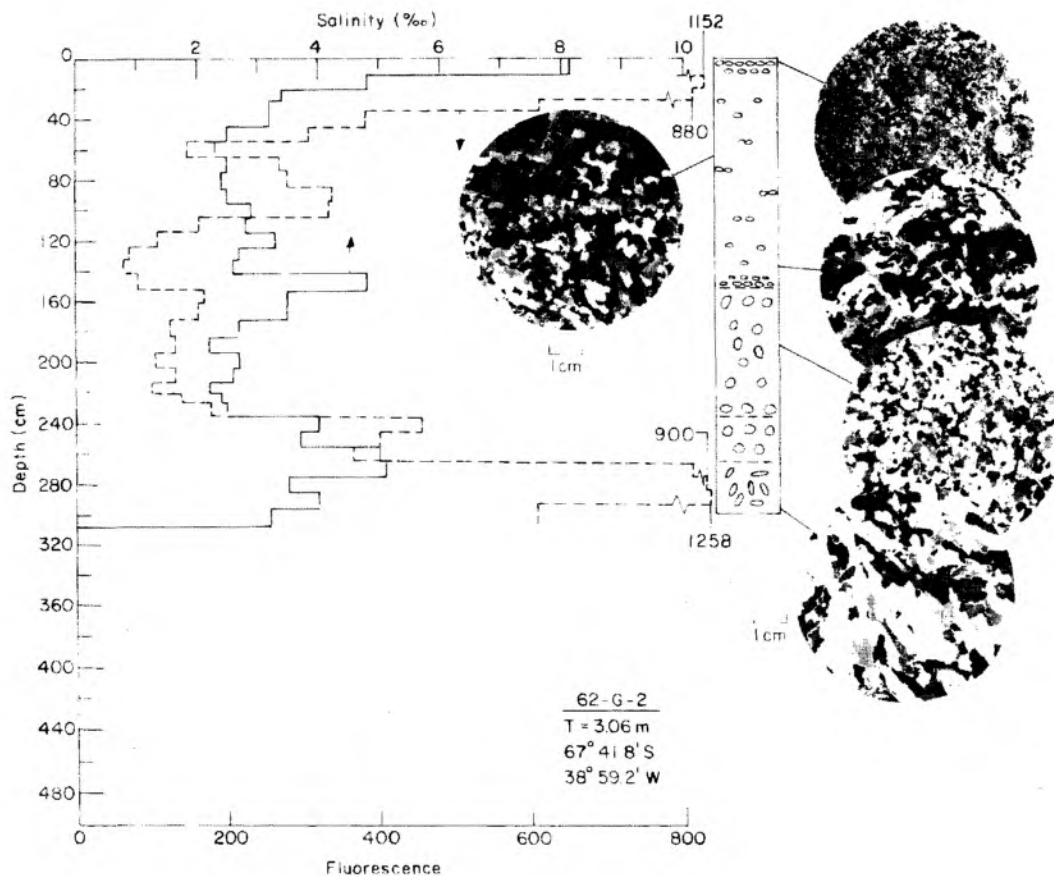*Figure 30. Salinity and fluorescence profiles, vertical structure section and horizontal thin sections of ice floe 61-G-1.*

zling ice type consisting substantially of large ice plates, that were not demonstrably of congelation columnar ice origin. This ice may have been skeleton layer ice, similar to the sub-ice platelet layer reported forming beneath landfast sea ice in McMurdo Sound (Gow et al. 1982, Paige 1966), with properties midway between those of congelation ice and frazil. The floe was substantially desalinated in the top 30 cm; the average salinity was 3.7‰. Relatively high fluorescence values in the bottom platy crystal zone, including a peak of 3690 at 230 cm, coincided with algae-rich bands. Samples from four levels in the floe were analyzed for $\delta^{18}0$. As shown in Table 2, only the topmost sample ($\delta^{18}0 = -0.97$‰) indicated that some input of freshwater, probably snow, had occurred prior to freezing. The deeper samples all yielded $\delta^{18}0$ values consistent with freezing from normal seawater.

Site 62-A-1 (Fig. 31)

This 2.92-m-thick floe was identified as of multi-year origin on the basis of its salinity profile and crystalline texture. Apart from a 40-cm-thick layer of frazil ice possibly mixed with snow in the top 10 cm, this floe was composed entirely of frazil ice of variable grain size and texture including bands of oriented crystals of the kind displayed in the thin section from the bottom of the floe. The average salinity was 3.1‰; the peak salinity measured 6.1‰. Fluorescence maxima, in excess of 5000, were recorded in a zone between 50 and 120 cm in which salinities were also elevated. The same zone also displayed evidence of extensive brine channeling, suggesting that high brine and fluorescence levels may be closely linked to mobilization of the brine. Measurements of $\delta^{18}0$ at five levels (Table 2) all yielded values consistent with frazil formation in normal seawater.

28

Figure 31. Salinity and fluorescence profiles, vertical structure section and horizontal thin sections of ice floe 62-A-1.

Site 62-G-2 (Fig. 32)

The age of this 3.06-m-thick floe was difficult to ascertain. On the basis of its thickness we have concluded that it was of multi-year origin. The elevated salinity at the top of the floe was attributed to flooding and was apparently not an indication of very thick first-year ice. However, the floe is unusual in that it consisted entirely of frazil ice, which could have accumulated in a single season; more interestingly the frazil occurred in a variety of grain sizes and textures, as demonstrated in the thin sections (Fig. 32). Except for the fine-grained frazil ice at the top of the floe, all the sections displayed coarse-grained textures, with grains up to

10 mm or more in their longest dimensions. The coarse crystals of the bottom ice, which occasionally showed dimensional orientation, may indicate a growth regime transitional to skeleton ice or congelation ice formation. The range of textures in this floe suggests that several separate regimes of frazil ice growth had contributed to its structure. An average salinity of 3.3‰ is in accord with multi-year ice of about 3 m thickness. Fluorescence peaks of 1152 and 1258 occurred at the top and bottom of the floe, respectively. Generally the fluctuations in salinity and fluorescence were as strongly correlated in this floe as they were in any other floe we examined.

29

Figure 32. Salinity and fluorescence profiles, vertical structure section and horizontal thin sections of ice floe 62-G-2.

CONCLUSIONS

Observations of the internal structure of 62 ice floes in the Weddell Sea, Antarctica, have revealed the existence of granular ice, principally frazil, in amounts not previously observed in the Arctic or the Antarctic. In many of the Weddell Sea floes, especially multi-year floes, frazil was the dominant component of the ice, averaging 72% of the ice thickness of 13 multi-year floes and 37% of 49 first-year floes we examined. The overall average composition was 54% frazil ice, 39% congelation ice and 7% admixtures of the two, together with snow ice restricted to the tops of floes. Such widespread occurrence of frazil has resulted in exceptional thicknesses of ice, with up to 5 m growth in less than two years. Frazil ice also occurred in a variety of textures and in relationships with congelation ice, including frequent sandwiching of frazil between layers of congelation ice, that indicate that mechanisms other than surface turbulence ef-

fects, including rafting events, have contributed to frazil ice production in the Weddell Sea. These other mechanisms are believed to include thermohaline convection, related to surface freezing and the formation of descending brine plumes, and adiabatic expansion of seawater ascending from beneath the Filchner and Ronne ice shelves, which form the rear boundary of the Weddell Sea embayment. Oxygen isotope analyses of frazil from 13 floes (7 first-year and 6 multi-year) show that it is predominantly of normal seawater origin and is not associated with melt, such as freshwater from bottom melting of ice shelves. The abundance of frazil in Weddell Sea floes contrasts dramatically with its strictly limited occurrence in Fram Strait, the principal outflow region of sea ice from the Arctic basin. Results obtained by Tucker et al. (1985) during MIZEX-84 indicate that, on average, undeformed floes in Fram Strait contained less than 15% granular ice (including snow ice as well as frazil). Amounts in excess of 15% were in-

30

variably confined to areas of ridged ice, where the granular ice was usually located in the voids between tilted blocks of congelation ice.

In the Weddell Sea floes, congelation ice was most prevalent in first-year ice, averaging 58% of the ice thickness of 49 floes. It was structurally similar to Arctic congelation ice, and its c-axes often had a preferred alignment. These alignments are probably related to the orienting effect of currents on crystal growth at the ice/water interface. This is likely to have happened during shelffast ice growth or under tight winter pack conditions.

Large plate crystals, several centimeters long, were observed forming at the bottom of the thickest floes. They appear to form by direct freezing to the underside of existing ice. This plate ice is structurally very similar, if not identical, to the sub-ice platelet layer observed at the base of sea ice sheets at coastal locations in Antarctica.

Thickness and salinity measurements of the 66 floes we examined in the Weddell Sea did not reveal ice demonstrably older than two years.

The Weddell Sea pack ice was appreciably more saline than sea ice of comparable age and thickness in the Arctic. For example, the average salinity of 61 profiles from 49 warm first-year floes measured 4.5‰ compared to values of around 3‰ reported for warm Arctic ice of comparable thickness. Similarly measurements of 14 warm multi-year floes yielded an average salinity of 3.5‰, which also exceeds that of warm Arctic first-year ice and is appreciably higher than the 2–2.5‰ value reported for Arctic floes of comparable age and thickness (3–5 m). Enhanced salinity of Weddell Sea floes is attributed to the lack of top surface summer melt, allowing floes to retain brine that would otherwise be flushed out by downward percolation of surface meltwater, the primary cause of brine loss and desalination of Arctic summer ice.

Fluorescence proved useful as an index of combined living and dead material in the ice. However, extensive measurements of 68 profiles failed to establish any consistent relationship between fluorescence and salinity, as had been suggested by earlier work in the Weddell Sea. However, measurements did reveal a variety of habitats, consisting of surface, near-surface, interior and bottom populations in Weddell Sea pack ice, in striking contrast to the fast ice in McMurdo Sound, where biology is dominated by late-season bottom communities.

LITERATURE CITED

Ackley, S.F. (1979a) Drifting buoy measurements in Weddell Sea pack ice. *Antarctic Journal of the United States,* 16(5): 106–108.

Ackley, S.F. (1979b) Mass balance aspects of Weddell Sea pack ice. *Journal of Glaciology,* 24(90): 391–405.

Ackley, S.F. (1981) Sea–ice atmosphere interactions in the Weddell Sea using drifting buoys. In *Proceedings of Symposium, Sea Level, Ice and Climatic Change, Canberra 1979.* International Association of Scientific Hydrology, Publication 131, pp. 177–191.

Ackley, S.F., S. Taguchi and K.R. Buck (1978) Primary productivity in sea ice of the Weddell Sea region. USA Cold Regions Research and Engineering Laboratory, CRREL Report 78-19.

Ackley, S.F., A.J. Gow, K.R. Buck and K.M. Golden (1980) Sea ice studies in the Weddell Sea aboard USCGS *Polar Sea. Antarctic Journal of the United States,* 15(5): 84–86.

Andreas, E.L. and S.F. Ackley (1982) On the differences in ablation seasons of Arctic and Antarctic sea ice. *Journal of Atmospheric Sciences,* 39(3): 440-447.

Bennington, K.O. (1963) Some crystal growth features of sea ice. *Journal of Glaciology,* 4(36): 669–688.

Clarke, D.B. and S.F. Ackley (1984) Sea ice structure and biological activity in the Antarctic marginal ice zone. *Journal of Geophysical Research,* 89(C2): 2087–2095.

Cox, G.F.N. and W.F. Weeks (1973) Salinity variations in sea ice. USA Cold Regions Research and Engineering Laboratory, Research Report 310.

Friedman, I., B. Schoen and J. Harris (1961) The deuterium concentration in arctic sea ice. *Journal of Geophysical Research,* 66(6): 1861–1864.

Garrison, D.L. and K.R. Buck (1984) Sea-ice algal communities in the Weddell Sea: Species composition in ice and plankton assemblages. In *Marine Biology of Polar Regions and Effects on Marine Organisms.* New York: John Wiley and Sons, pp. 103–122.

Gow, A.J. and S. Epstein (1972) On the use of stable isotopes to trace the origins of ice in a floating ice tongue. *Journal of Geophysical Research,* 77(33): 6552–6557.

Gow, A.J. and W.B. Tucker (1987) Physical properties of sea ice discharged from Fram Strait. *Science,* 236: 436–439.

Gow, A.J. and W.F. Weeks (1977) The internal structure of fast ice near Narwhal Island, Beaufort Sea, Alaska. USA Cold Regions Research and Engineering Laboratory, CRREL Report 77-29.

Gow, A.J., W.F. Weeks, G. Hendrickson and R. Rowland (1965) New light on the mode of uplift of the fish and fossiliferous moraines of the McMurdo Ice Shelf, Antarctica. *Journal of Glaciology,* 5(42): 813–828.

Gow, A.J., W.F. Weeks, J.W. Govoni and S.F. Ackley (1981) Physical and structural characteristics of sea ice in McMurdo Sound. *Antarctic Journal of the United States,* 16(5): 94–95.

Gow, A.J., S.F. Ackley, W.F. Weeks and J.W. Govoni (1982) Physical and structural characteristics of Antarctic sea ice. *Annals of Glaciology,* 3: 113–117.

Langhorne, P. (1983) Laboratory experiment on crystal orientations of NaCl ice. *Annals of Glaciology,* 4: 163–169.

Langhorne, P. and W.H. Robinson (1986) Alignment of crystals in sea ice due to fluid motion. *Cold Regions Science and Technology,* 12(2): 197–214.

Lyons, J.B., S.M. Savin and A.J. Tamburi (1971) Basement ice, Ward Hunt Ice Shelf, Ellesmere Island, Canada. *Journal of Glaciology,* 10(58): 93–100.

Martin, S. (1979) A field study of brine drainage and oil entrapment in sea ice. *Journal of Glaciology,* 22(88): 473–502.

Osterkamp, T.E. and J.P. Gosink (1984) Observations and analyses of sediment-laden sea ice. In *The Alaskan Beaufort Sea: Ecosystems and Environments.* New York: Academic Press, pp. 73–93.

Paige, R.A. (1966) Crystallographic studies of sea ice in McMurdo Sound, Antarctica. Naval Civil Engineering Laboratory, Technical Report R494.

Serikov, M.I. (1963) Structure of Antarctic sea ice. *Information Bulletin of the Soviet Antarctic Expedition,* 4(5): 265–266.

Tucker, W.B., A.J. Gow and W.F. Weeks (1985) Physical properties of sea ice in the Greenland Sea. In *Proceedings, 8th International Conference on Port and Ocean Engineering under Arctic Conditions (POAC-85), Narssarssuaq, Greenland, September 7-14, 1985.* Vol. 1, pp. 177–188.

Untersteiner, N. (1968) Natural desalination and equilibrium salinity profile of perennial sea ice. *Journal of Geophysical Research,* 73(4): 1251–1257.

Untersteiner, N. and F. Badgley (1958) Preliminary results of thermal budget studies on arctic pack ice during summer and autumn. In *Arctic Sea Ice.* U.S. National Academy of Sciences, National Research Council Publication 598, pp. 85–89.

Weeks, W.F. and A.J. Gow (1978) Preferred crystal orientations in the fast ice along the margins of the Arctic Ocean. *Journal of Geophysical Research,* 83(C10): 5105–5121.

Weeks, W.F. and A.J. Gow (1980) Crystal alignments in the fast ice of Arctic Alaska. *Journal of Geophysical Research,* 85(C2): 1137–1146.

Weeks, W.F. and S.F. Ackley (1982) The growth, structure, and properties of sea ice. USA Cold Regions Research and Engineering Laboratory, Monograph 82-1.

World Meteorological Organization (1956) *Abridged Ice Nomenclature.* Executive Committee Report, vol. 8, pp. 107–116.

APPENDIX A: FLOE DESCRIPTIONS

The representation scheme for the structure sections is the same as in Figure 16.
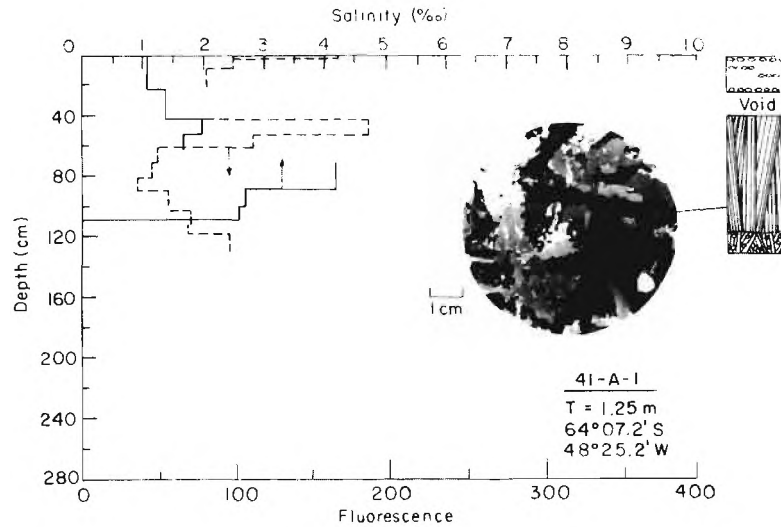
Figure A1. Site 41-A-1.

This first-year floe was characterized by a large void at 25–40 cm. Excluding this void the floe was composed of 66% congelation ice, 21% frazil and 13% of mixed frazil and congelation ice located at the bottom of the floe. The salinity averaged a low 2.0‰. Ice directly beneath the void showed a relatively significant increase in fluorescence to 186 possibly related to an influx of seawater in the vicinity of the void.
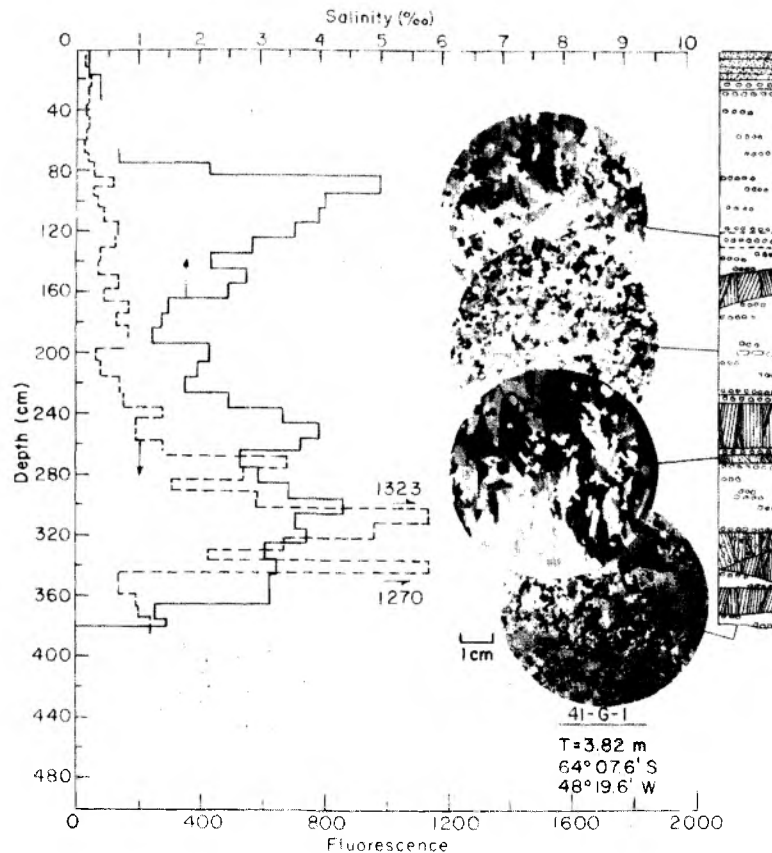
Figure A2. Site 41-G-1.

This multi-year floe contained 25% congelation ice interlayered with frazil ice that made up 70% of the total ice thickness (382 cm). The maximum salinity of 5.0‰ was measured in frazil ice from 80–90 cm, but above this level the salinity did not exceed 1‰ in any of the samples; the average salinity was 2.5‰. Petrographic examinations of thin sections from several levels yielded the following results. The ice at 120 cm had a mosaic-type grain texture composed mainly of frazil grains generally less than 5 mm in diameter, but it also included some larger crystals exhibiting a brine pocket structure more typical of congelation ice. Frazil ice at 195 cm was composed of grains generally smaller than 3 mm. This ice also contained bubbles (possibly air) and brine inclusions. At 264 cm the ice was composed mainly of congelation crystals larger than 10 mm in cross-sectional diameter. Most crystals displayed a well-developed ice plate and brine lamella structure, but the crystals themselves show no azimuthal alignment of their c-axes. The relatively bubbly, fine-grained ice at 381 cm was identified as frazil, but it contained a few large crystals exhibiting a brine pocket structure similar to that in the ice at 120 cm. Fluorescence increased perceptibly at about 270 cm, attaining peak values of 1323 in the frazil ice at 302–311 cm and 1270 in congelation ice at 336–343 cm. Stable isotope ($\delta^{18}O$) analyses of samples from the three major frazil layers in 41-G-1 (Table 2) yielded values consistent with crystallization of frazil from normal seawater.

34
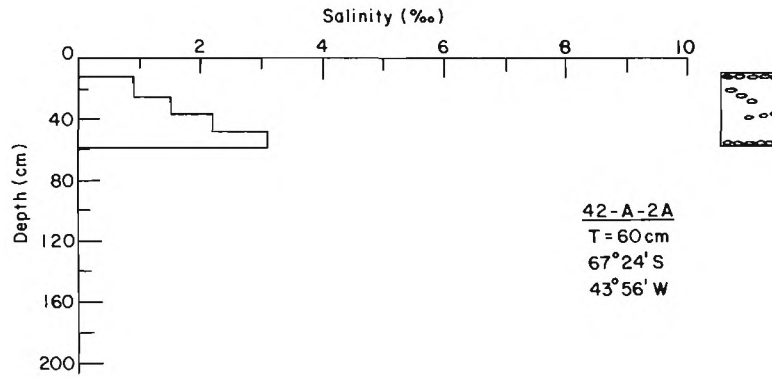
Figure A3. Site 42-A-2A

This 60-cm-thick first-year floe was composed entirely of fine-grained ice identified as frazil. This floe was further characterized by a progressive increase in salinity, which averaged $1.9^o/_{oo}$.
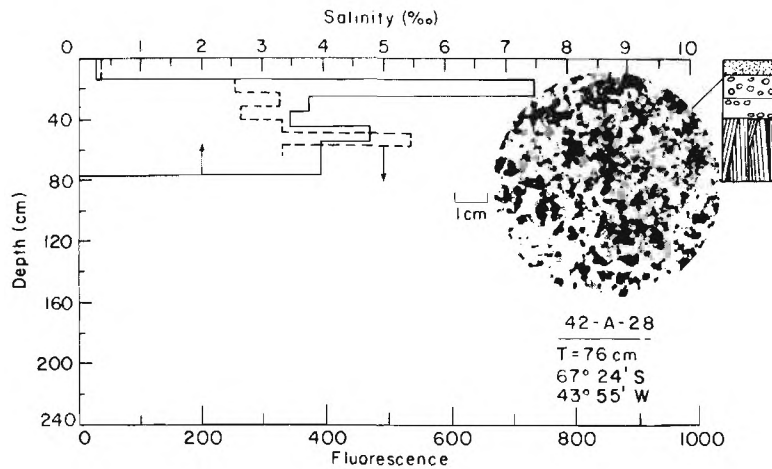
Figure A4. Site 42-A-2B.

This profile was obtained from the same floe as 42-A-2A, but the bottom half of this part of the floe was composed of congelation ice. Samples of this core also proved much saltier, averaging $4.0^o/_{oo}$, compared to less than $2^o/_{oo}$ at site 42-A-2A. The peak fluorescence of 546 was recorded in the congelation ice at 60-68 cm.
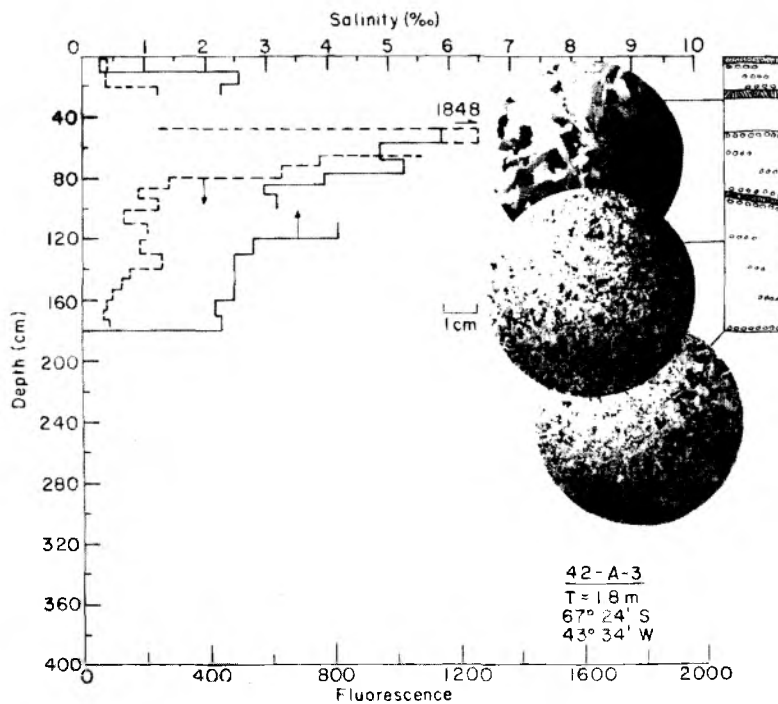
Figure A5. Site 42-A-3.

This 1.8-m-thick first-year floe contained 92% frazil ice and 6% congelation ice, confined to just two layers at ≈ 30 and 100 cm, respectively. The bulk salinity was 3.2‰, with a maximum salinity of 5.9‰ coinciding with the fluorescence maximum of 1848 at 47–57 cm. Horizontal thin section studies yielded the following data. At 28 cm, congelation ice included long-bladed crystals at the transition with the frazil ice. At 118 cm fine-grained frazil exhibited two distinct grain size modes, 1–2 mm and less than 0.5 mm. Fine-grained frazil at 179 cm also exhibited a bimodal size distribution, with the larger grains measuring 2 mm and more in diameter and the smaller grains seldom exceeding 0.3 mm.

36
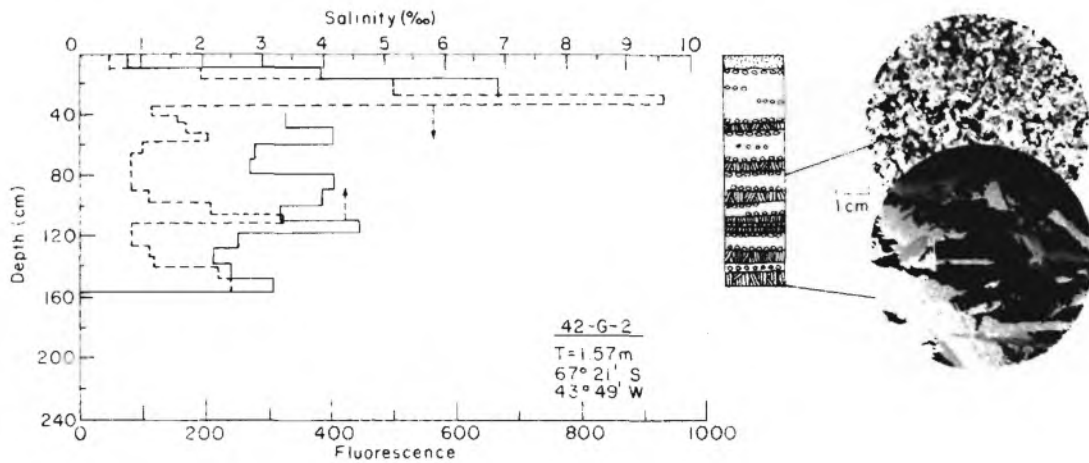
Figure A6. Site 42-G-2.

This 1.57-m-thick first-year floe was composed of a mixture of frazil and congelation ice layers but dominated by frazil ice in a ratio of about 2:1. Seven layers of congelation ice were interspersed with frazil ice; this structure may be related to multiple rafting events. The average salinity of the floe was 3.4‰, with a maximum value of 6.9‰ occurring just above a fluorescence peak of 968 in the frazil ice at 27–34 cm.
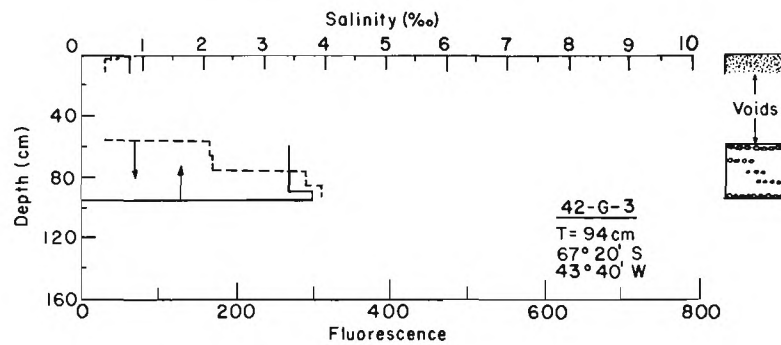
Figure A7. Site 42-G-3.

This was a relatively thin (94-cm) floe from which incomplete core was obtained because of voids in the ice. The cores consisted of snow ice at the top and frazil ice at the bottom. Surface flooding of the floe resulted in the formation of pools of frozen saltwater containing abundant algae. Melted samples from one pool yielded an average salinity of 20‰. In this floe the maximum salinity coincided with the fluorescence peak at the bottom of the floe.

37
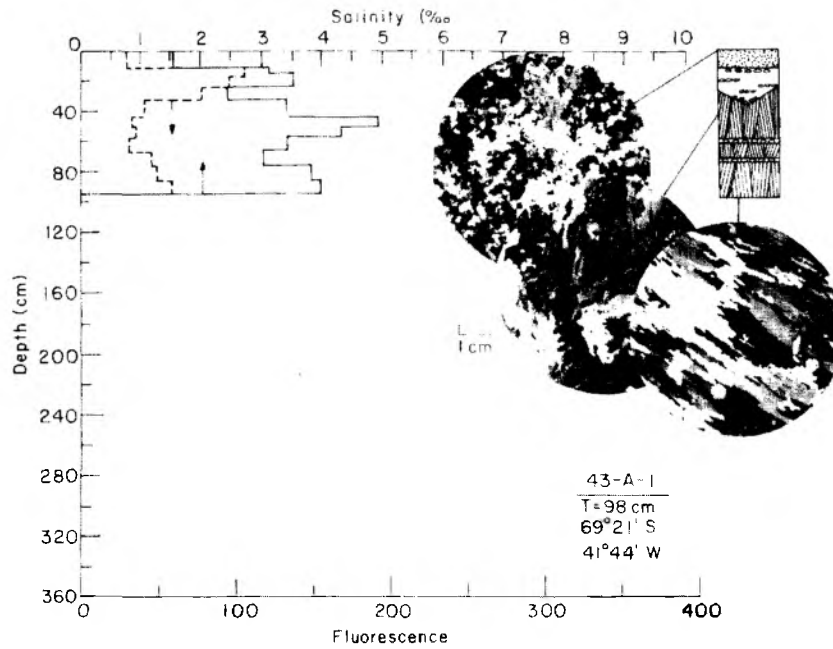
Figure A8. Site 43-A-1.

This floe consisted of thin (98-cm) first-year ice containing 69% congelation ice overlain by snow ice (9%) and frazil ice (22%). The c-axes in the thin section of congelation ice from the bottom of the floe were very strongly aligned. The average salinity was 3.4‰, with a maximum value of 4.9‰. Fluorescence was unremarkable, with a maximum of 108 at 12–15 cm.
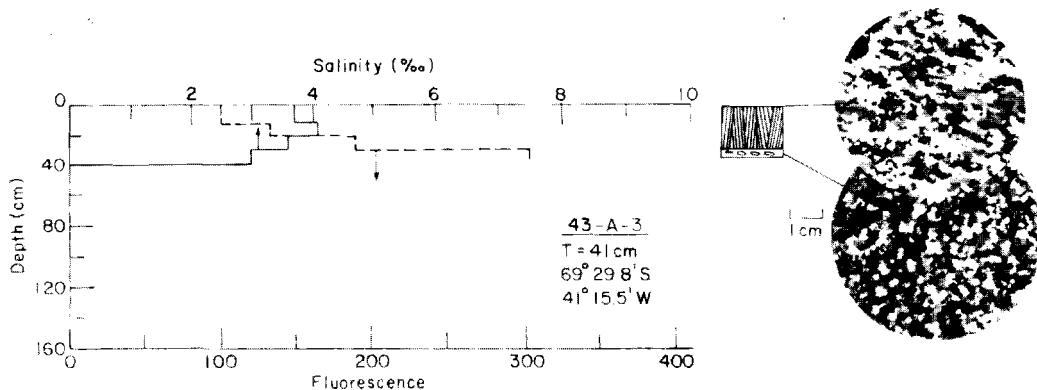
Figure A9. Site 43-A-3.

This 41-cm-thick first-year floe was composed of fine-grained congelation ice (82%) underlain by a thin layer of moderately coarse-grained frazil ice exhibiting a fluorescence peak of 304. The average salinity was 3.6‰.

38
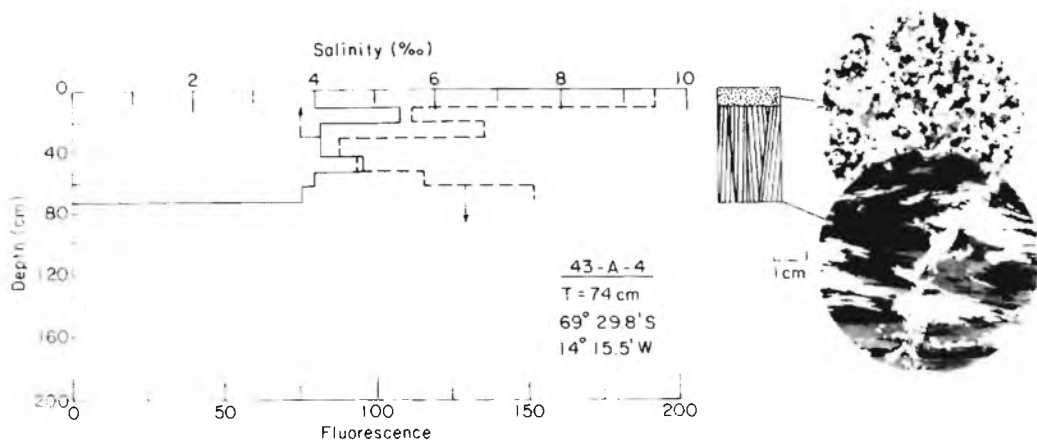
Figure A10. Site 43-A-4.

This 74-cm-long core was obtained from the same floe as 43-A-3, but it lacked the bottom layer of frazil ice and was overlain by a substantial thickness (18%) of bubbly snow ice. The congelation ice was much coarser grained than at site 42-A-3, and the thin section from the bottom displayed signs of c-axis alignment of the crystals. The bulk salinity of 4.3‰ was significantly higher than that at site 43-A-3. The fluorescence was highest in the snow ice (192) but not remarkably so.
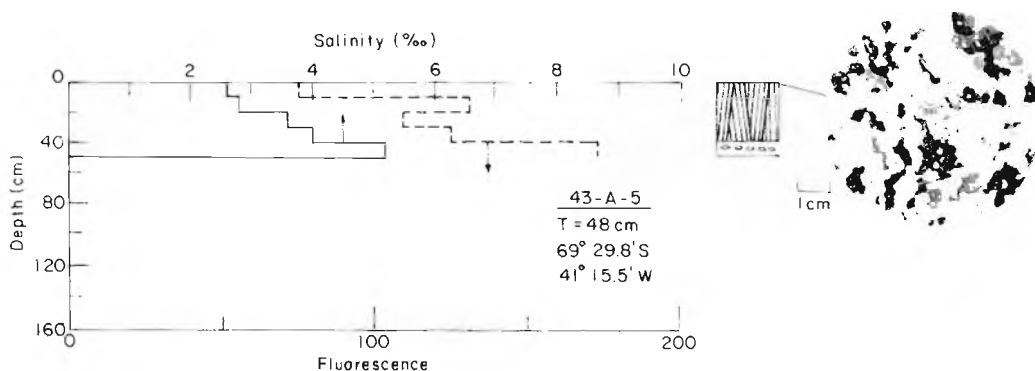
Figure A11. Site 43-A-5.

This sample was also from the same floe as profiles 43-A-3 and 43-A-4, and in terms of its crystalline texture, salinity and fluorescence, this ice is essentially the same as that observed at Site 43-A-3.
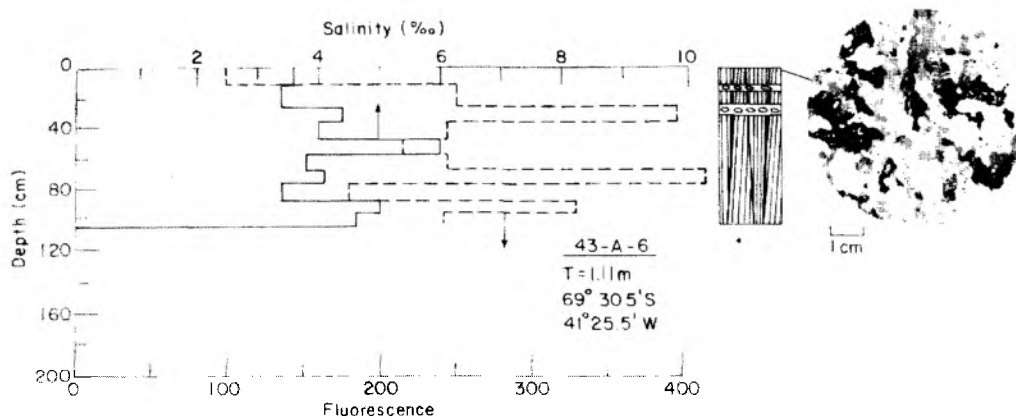
Figure A12. Site 43-A-6.

This first-year ice was 1.11 m thick and was composed principally of congelation ice (85%), with a maximum salinity of 6.0‰ and an average salinity of 4.2‰. Fluorescence maxima of 415 and 396 were observed in congelation and frazil ice, respectively, but were not related in any obvious way to salinity variations.
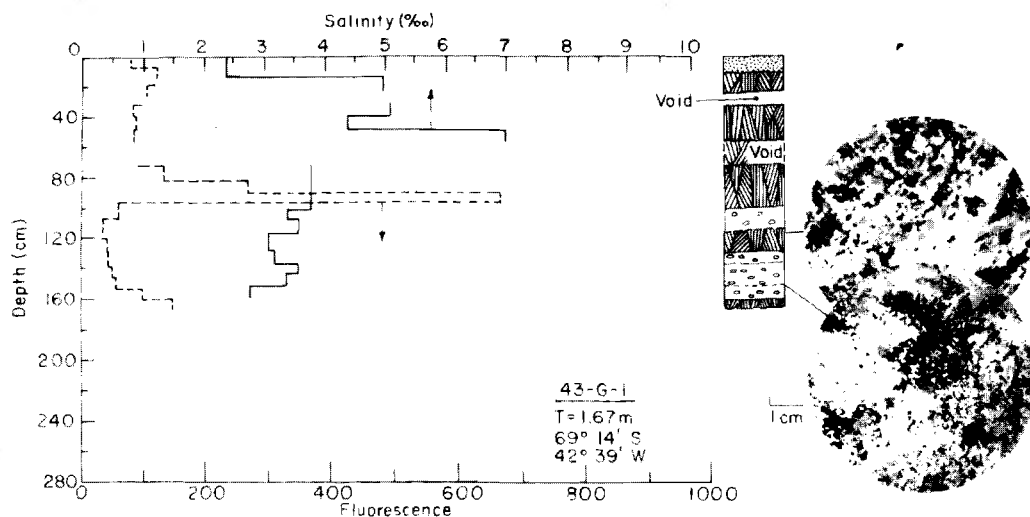
Figure A13. Site 43-G-1.

This first-year floe was 1.67 m thick and was composed of 7% snow ice, 32% frazil ice and 61% congelation ice. A large void, possibly related to brine drainage, was observed in congelation ice at a depth of 25-31 cm. The frazil ice in the bottom half of the floe was generally fine-grained. The alternating structure of frazil and congelation ice in this floe may indicate an origin by multiple rafting. The maximum salinity was 7.0‰, and the bulk salinity was 3.9‰. The peak fluorescence of 693 was in the congelation ice at 90-96 cm, but fluorescence showed no correlation with salinity.

40
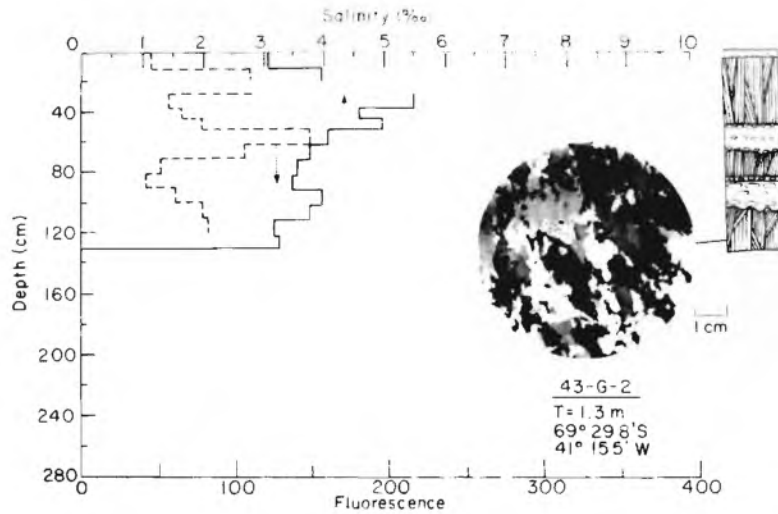
Figure A14. Site 43-G-2.

This first-year floe, measuring 1.3 m at this location, consisted mainly of congelation ice (69%) interspersed with frazil ice (28%) of variable grain size. In this floe and at Site 43-G-3 (a second core from the same floe) alternating frazil and congelation ice may be related to multiple rafting events. The average salinity of the floe at this site was 4.0‰. Fluorescence appeared unremarkable, with a peak value of 152 at 51-61 cm.
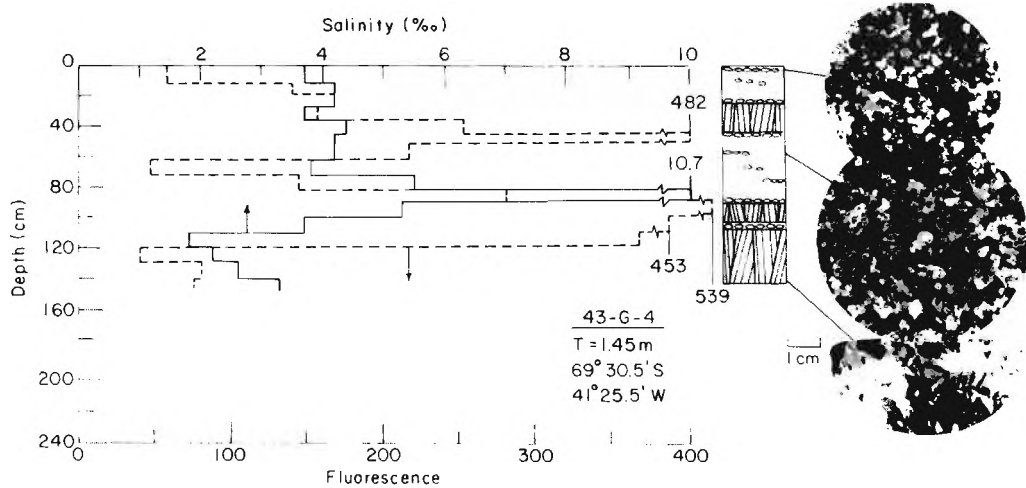
Figure A15. Site 43-G-4.

This first-year floe (1.45 m thick) was composed of approximately equal proportions of frazil ice (dominating the top half of the floe) and congelation ice (dominating the lower half). The maximum salinity of 10.7‰ was at 80-85 cm in the frazil ice located directly on top of congelation ice in which a peak fluorescence of 539 was measured. Several other peaks associated with frazil/congelation ice transitions were also recorded, but they were not related in any systematic way with salinity variations. The average salinity of the floe was 4.2‰. Values of +1.03‰ and +1.24‰ for $\delta^{18}O$ in frazil from 56-60 and 85-90 cm, respectively, indicate crystallization from seawater containing minor amounts of freshwater.
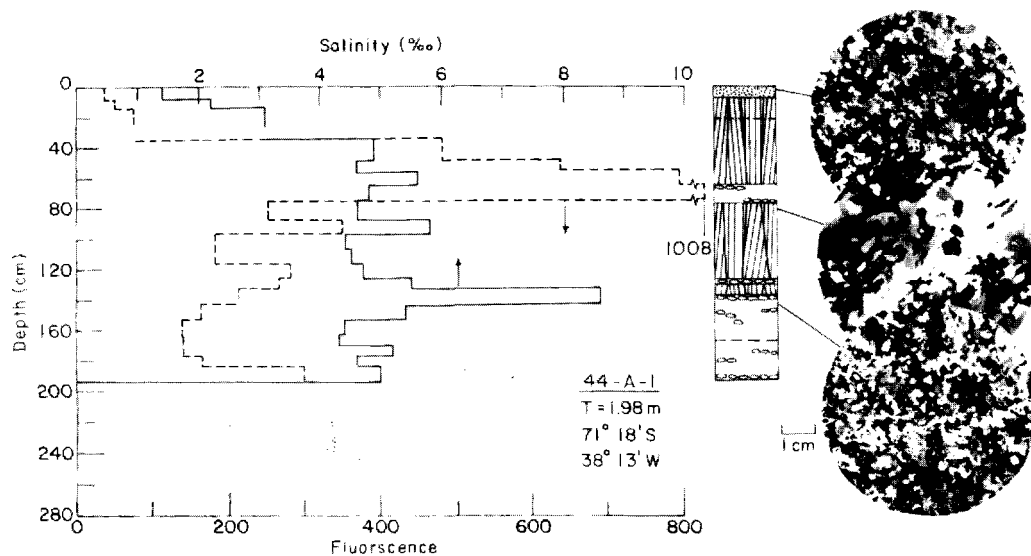
Figure A16. Site 44-A-1.

This first-year floe measured 1.98 m thick and was composed of 4% snow ice, 39% frazil ice (most of which was located at the bottom of the profile) and 57% congelation ice. The average salinity was 4.7‰, and a peak salinity of 8.6‰ was recorded in a sample that spanned ice across the congelation/frazil transition at approximately 140 cm. The peak fluorescence of 1008 was at 75–80 cm in a thin frazil layer directly beneath a thick layer of congelation ice in which fluorescence values were also high for about 30 cm above the transition. A $\delta^{18}O$ analysis of frazil from 67–72 cm is compatible with crystallization from normal seawater. However, a $\delta^{18}O$ value of $+0.80$‰ at 143–148 cm indicates some freshwater addition to the seawater prior to freezing.
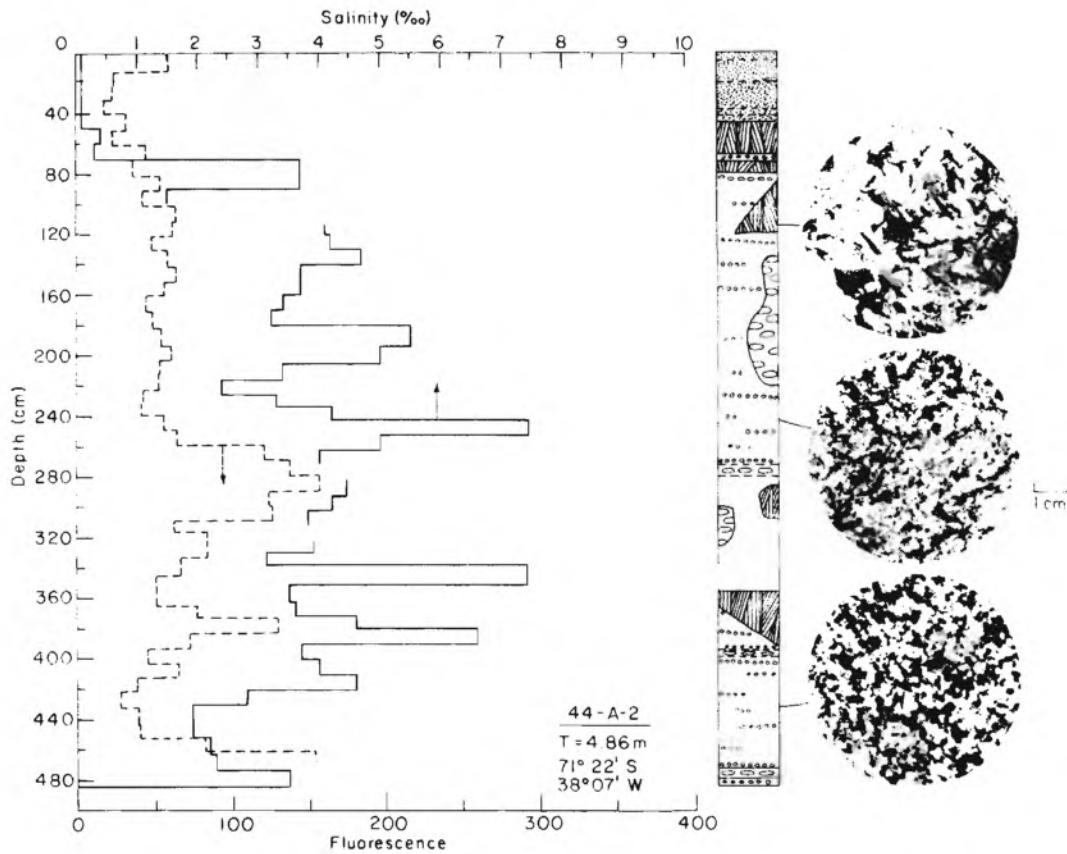
Figure A17. Site 44-A-2.

This 4.86-m-thick multi-year floe was composed principally of frazil ice (75%) overlain by several layers of snow ice representing nearly 10% of the total ice thickness. The fragmented appearance of some of the congelation ice suggests that it was incorporated as blocks during consolidation of the frazil ice. Some frazil ice also appears to have originated by a similar mechanism, particularly the coarse-grained frazil. This floe is also characterized by a highly variable salinity profile, with a maximum of 7.4‰ and an average of 3.4‰. Fluorescence was minimal, with no value exceeding 200 at any depth in the floe. Structurally, this floe was very similar to 42-G-1.
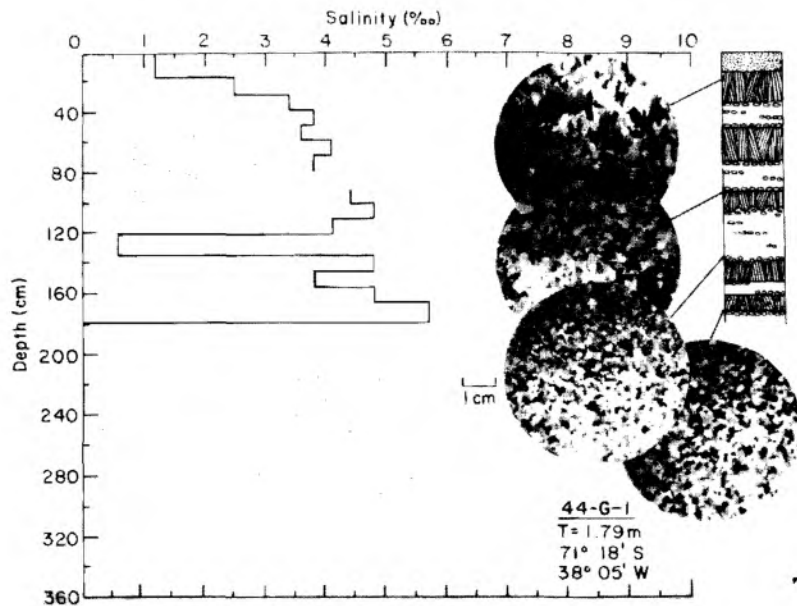
Figure A18. Site 44-G-1.

This is an excellent example of first-year ice in which layers of congelation and frazil ice, possibly related to multiple rafting events, are interspersed at regular intervals throughout the 1.79-m-thick floe. This floe also demonstrates the tendency for cores to break naturally at structural transitions. Horizontal thin sections at 89, 133 and 176 cm all exhibited frazil ice textures, which, by themselves, would have yielded a very misleading estimate of the proportions of ice types in the floe; vertical sectioning showed the floe to be composed of 7% snow ice, 45% frazil ice and 48% congelation ice. The salinity profile slowly increased with depth. A notable exception was the unusually low salinity of 0.7‰ measured in the frazil ice at 120–135 cm; the average salinity was 3.5‰.
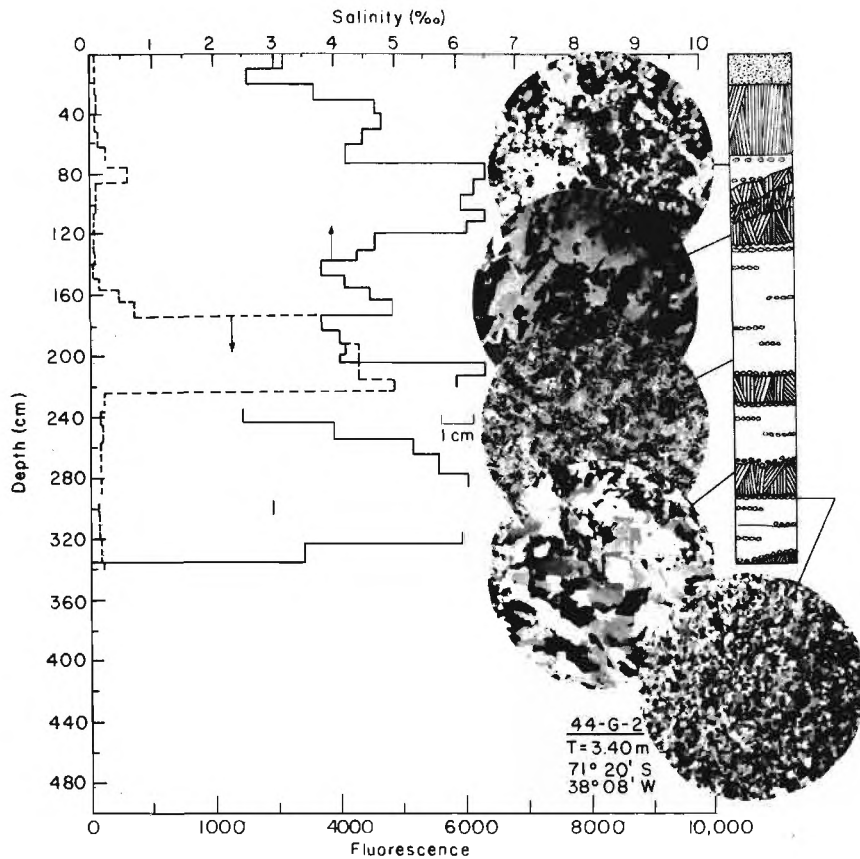
Figure A19. Site 44-G-2.

This multi-year floe, 3.40 m thick, consisted of 56% frazil ice and 36% congelation ice overlain by 8% snow ice and a relatively thick (25 cm) blanket of snow. The frazil ice was characterized by highly variable grain size in the different layers within this floe. The congelation ice textures were similar at all depths, and there was no indication of any significant alignment of the crystallographic c-axes. Tilted layers of congelation ice in the upper section of the profile suggest that rafting or overriding of ice had occurred during the early stage of growth of the ice sheet. For a multi-year floe, the ice was appreciably more saline than most, averaging 4.7‰. Very high fluorescence levels, ranging from 3737 to 4949, were recorded between 175 and 225 cm, mainly in frazil ice, though the peak value occurred in the top of the congelation ice immediately underlying the frazil ice. Elsewhere in the core, levels of fluorescence were low, and there was no systematic variation with salinity.

45
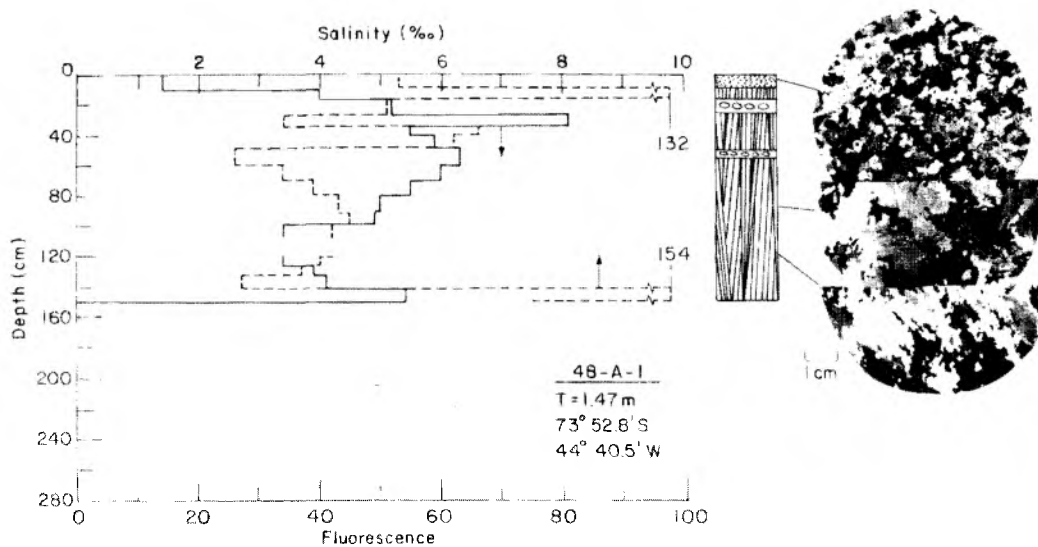
Figure A20. Site 48-A-1.

This 1.47-m-thick first-year floe was composed principally of congelation ice (83%). Frazil ice was restricted to two layers in the upper half of the floe. The bottom half of the core was used for salinity and fluorescence measurements before vertical sectioning could be performed. However, observations on several horizontal sections indicate that congelation ice was the predominant ice type in this floe, and composition percentages were calculated on this assumption. The average salinity was 5.0‰, with a maximum value of 8.1‰ at 30–35 cm. Two fluorescence peaks were measured near the top and at the bottom of the floe.
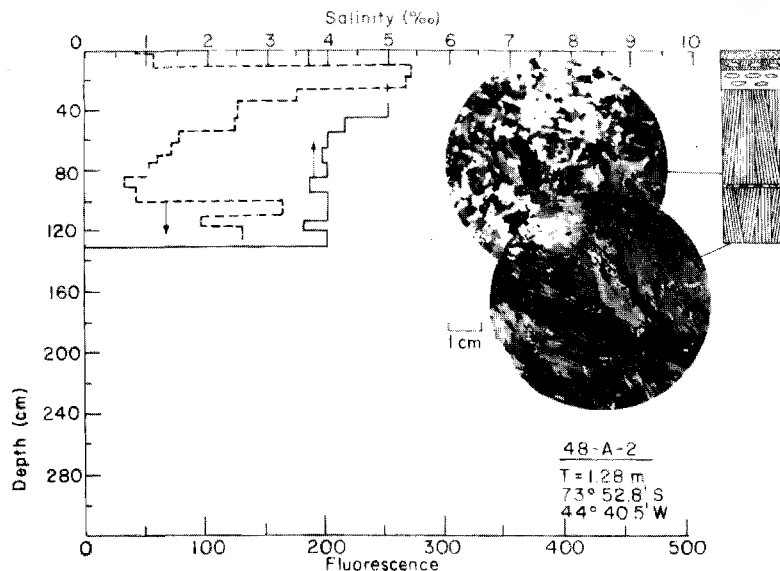
Figure A21. Site 48-A-2.

This relatively thin (1.28-m-thick) first-year floe consisted mainly of congelation ice (80%). The average salinity was 4.3‰. A peak fluorescence of 270 occurred entirely in the layer of coarse-grained frazil overlying the congelation zone.
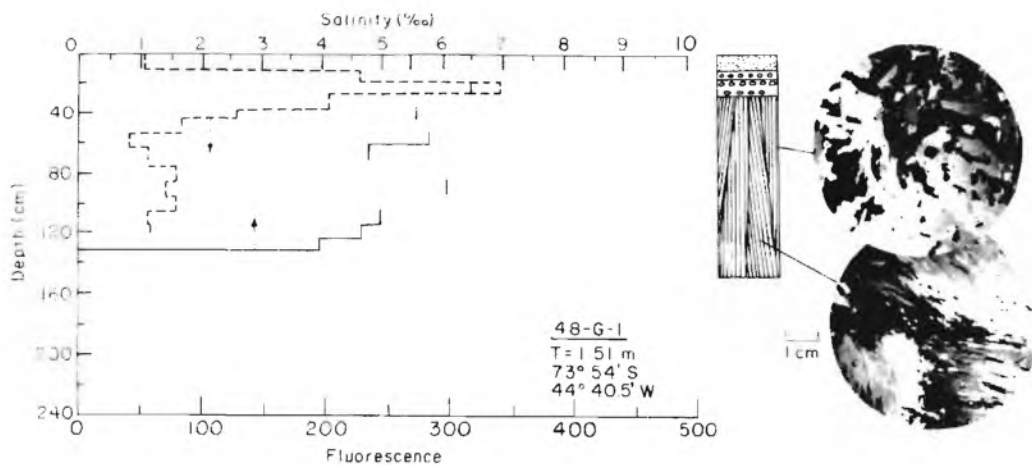
Figure A22. Site 48-G-1.

This was a first-year profile (1.51 m thick) in which congelation ice (81%) was the dominant ice type. The bottom 30 cm was retained for salinity measurements and was not vertically sectioned. However, measurements on horizontal thin sections showed that the bottom ice was composed entirely of congelation crystals. At the top of the core was mixed snow and frazil ice underlain by a frazil ice layer. The plate widths in the congelation ice averaged 0.8 mm, but observations of several thin sections showed no significant alignment of crystallographic c-axes. The fluorescence peak (340) coincided with the frazil ice layer. Salinities varied between 4 and 6‰ in the congelation ice, and the average salinity of the floe at this location was 5.3‰.
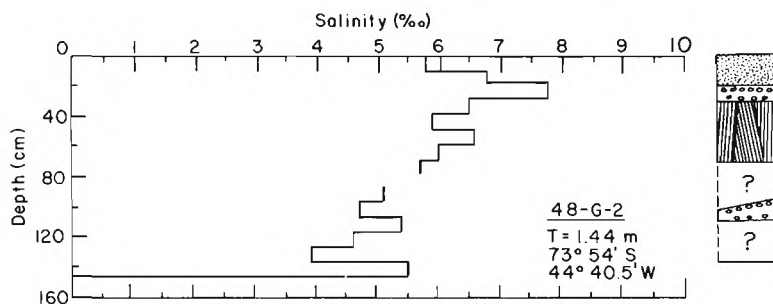
Figure A23. Site 48-G-2.

This profile was obtained from the same floe as 48-G-1; the two cores were drilled less than 2 m apart. Structurally the two cores were very similar in their upper sections. This core was drilled primarily for large-sample salinity measurement, and only the top 74 cm was vertically sectioned, together with one smaller section from near 100 cm, which revealed frazil ice in this part of the profile. The mean salinity was 5.7‰, compared with 5.3‰ for the adjacent profile. The two salinity profiles matched quite closely.

47
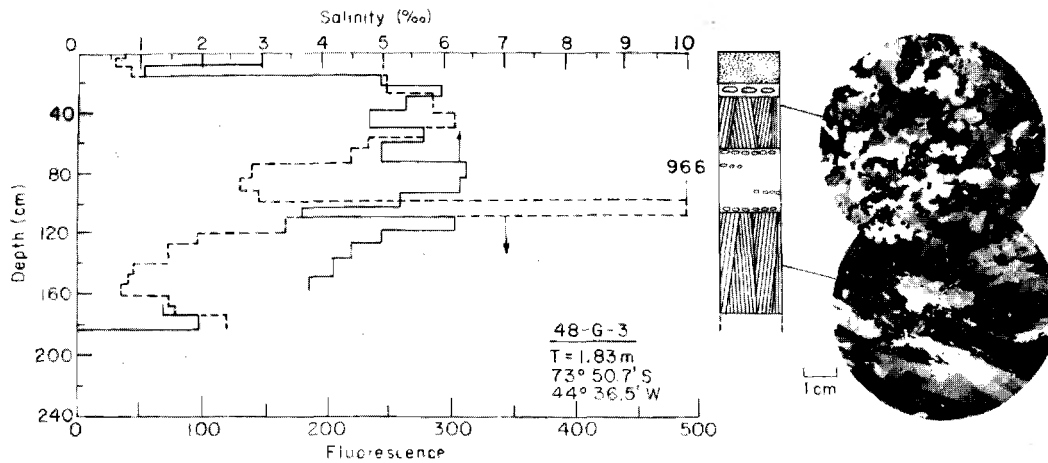
Figure A24. Site 48-G-3.

This moderately thick (1.83 m) first-year floe was composed of 62% congelation ice, 27% frazil ice and an unusually thick layer (11%) of mixed snow and frazil ice at the top of the profile. The bottom 20 cm was not sectioned vertically, but it was assumed to be congelation ice. Salinity varied from 1.1 to 6.3‰, with an average value of 4.5‰. Fluorescence varied greatly throughout the floe, with the peak value of 966 in the frazil ice in contact with congelation ice at 110 cm. Congelation ice in the bottom half of the floe was composed primarily of large, bladed crystals.
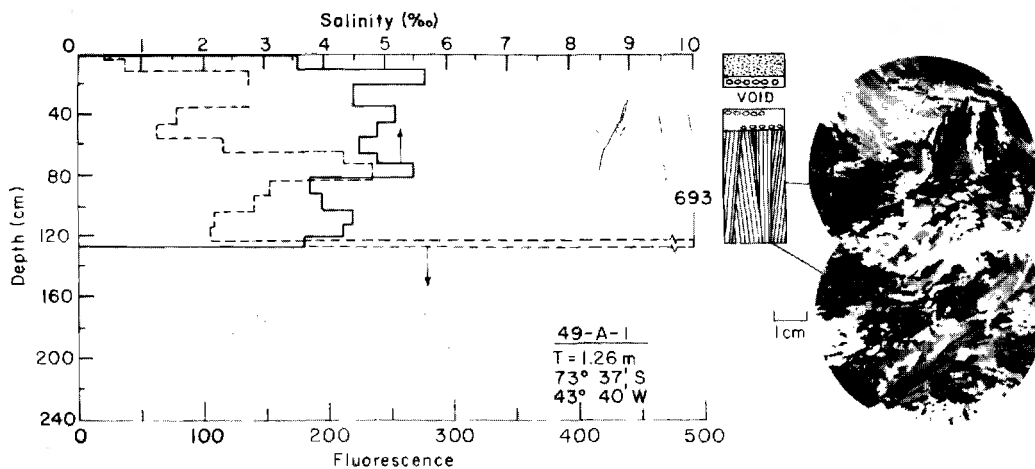
Figure A25. Site 49-A-1.

This first-year floe, 1.26 m thick, was characterized by a void at 22–38 cm. Except for the void, this floe was composed approximately of 66% congelation ice overlain by 14% snow ice and 20% frazil ice. The average salinity was 4.5‰. A peak fluorescence of 693 was measured at the bottom of the floe.
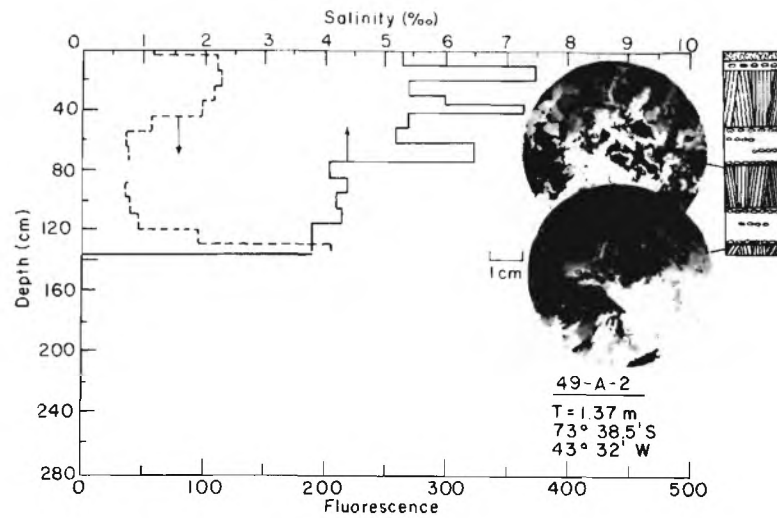
Figure A26. Site 49-A-2.

This first-year 1.37-m-thick floe consisted of congelation ice (55%) interlayered with frazil ice (36%) and overlain by snow ice (9%). There were several salinity peaks in the upper half of the floe; the average salinity was 5.2‰. The maximum fluorescence was in the bottom ice. A $\delta^{18}O$ value for a sample of frazil from 107–114 cm was $+1.86‰$, indicative of crystallization from normal seawater.
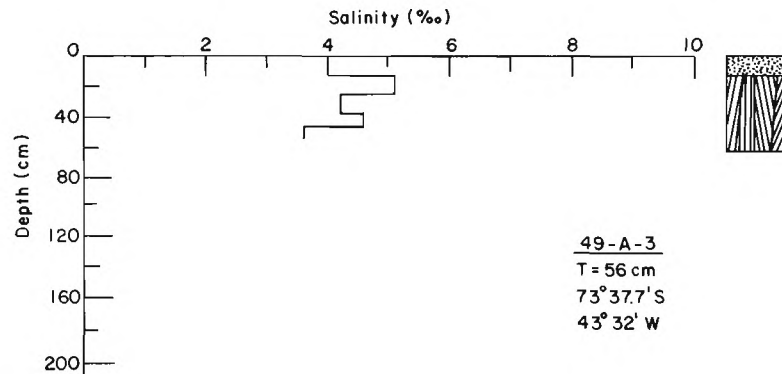
Figure A27. Site 49-A-3.

This 0.56-m first-year ice had a mean salinity of 4.3‰ and was composed mainly of congelation ice (77%) overlain by a mixture of snow and frazil ice.
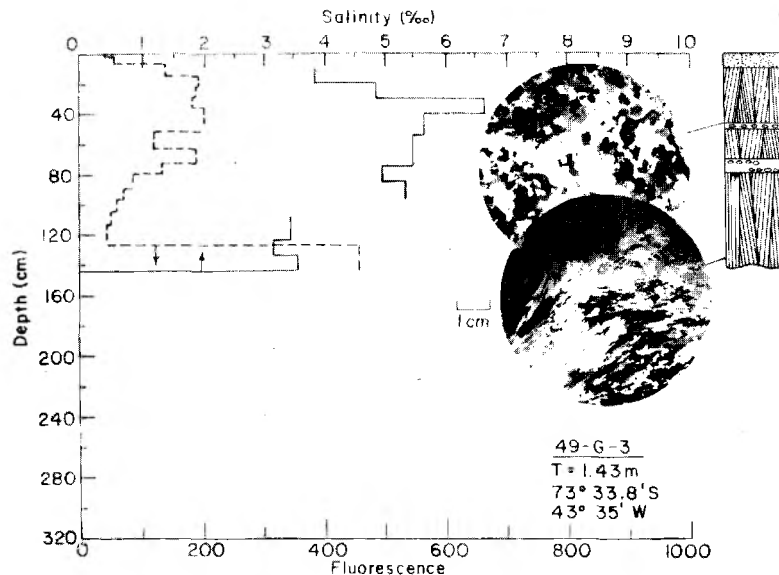
Figure A28. Site 49-G-3.

This first-year ice (1.43 m thick) was dominated by congelation ice (80%) and contained less than 10% frazil ice, confined to two layers near the middle of the section. The thin section from 50 cm included some frazil, but it was composed mainly of fine-grained congelation ice. The section from 135 cm consisted entirely of fibrous-textured congelation ice with moderately aligned c-axes. Some crystals had linear dimensions of several centimeters, and all had brine pockets, with plate spacings averaging 0.7 mm. Much of the core from this location was prominently banded, especially in the zone from 55–92 cm, but the banding was restricted in all cases to the congelation ice. A fluorescence peak of 456 was recorded in ice from near the bottom of the floe. The average salinity was 4.8‰.
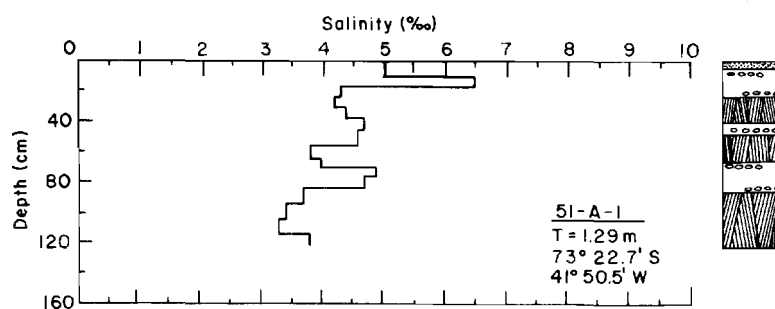
Figure A29. Site 51-A-1.

This first-year floe (1.29 m thick) contained frazil ice (36%) interlayered with congelation ice (61%), possible related to multiple rafting events. A maximum salinity of 6.5‰ was recorded in the frazil ice near the top of the floe; the average salinity was 4.4‰.
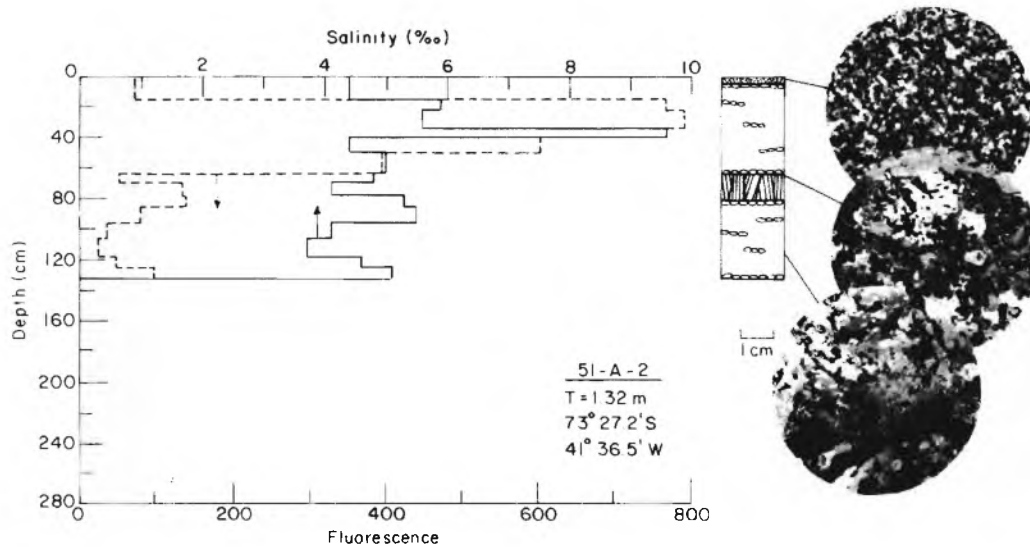
Figure A30. Site 51-A-2.

This 1.32-m-thick first-year ice was composed mainly of frazil ice (83%). Congelation ice (14%) was confined to the middle of the floe. Frazil zones often contained large crystals exhibiting congelation ice characteristics such as brine pockets. The maximum salinity of 9.6‰ was recorded in the frazil ice associated with peak fluorescences of 770–792. The average salinity of the floe was 5.2‰.
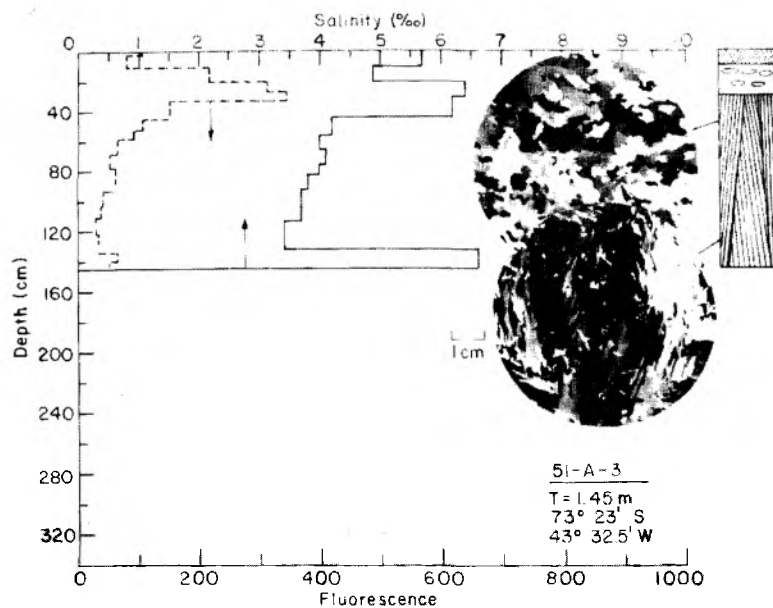
Figure A31. Site 51-A-3.

This first-year, 1.45-m-thick floe was composed predominantly of congelation ice (79%) overlain by moderate- to coarse-grained frazil ice (14%) and mixed snow and frazil ice (7%) in the surface layer. The congelation ice, which contained many semi-transparent bands in the lower half of the floe, had an overall texture that can be best described as fibrous. The plate widths in this ice averaged 0.6 mm, and individual crystals showed a moderately strong alignment of their c-axes, indicating that growth probably occurred either as fast ice or under relatively stationary conditions in the pack ice. The average salinity of the floe was 4.6‰. A peak fluorescence of 344, which also coincided with a peak in salinity (6.2–6.4‰), was recorded in the frazil ice directly above the congelation ice layer.
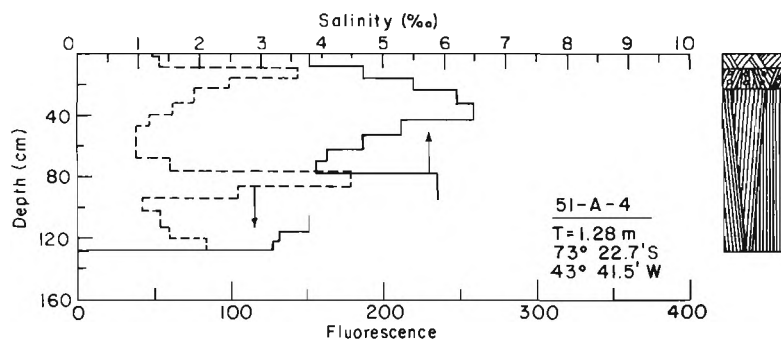
Figure A32. Site 51-A-4.

This first-year 1.28-m-thick floe consisted of 87% congelation ice and 13% mixed congelation and frazil ice. Rhythmic banding occurred throughout the congelation ice. The average salinity of the floe was 4.8‰, and the peak fluorescence of 180 occurred at 77–87 cm in ice with locally high salinity (5.9‰).
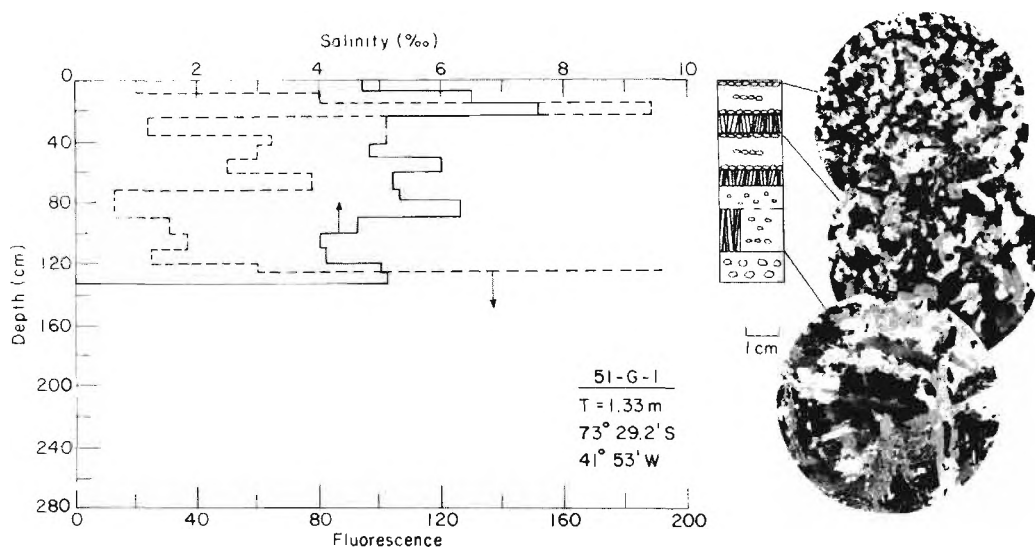
Figure A33. Site 51-G-1.

This first-year 1.33-m-thick ice floe was composed of alternating layers of frazil (72%) and congelation ice (28%) possibly linked to rafting. The average salinity of 5.3‰ was moderately high. The size of frazil grains varied greatly from layer to layer and within layers. The thin section from 118 cm shows large vertically oriented plate-like crystals of congelation ice in sharp contact with fine-grained frazil. This mixed crystal zone extends from 82 to 118 cm. There were two fluorescence peaks, one in frazil in contact with the congelation ice at 24 cm and the second in frazil from near the bottom of the floe.
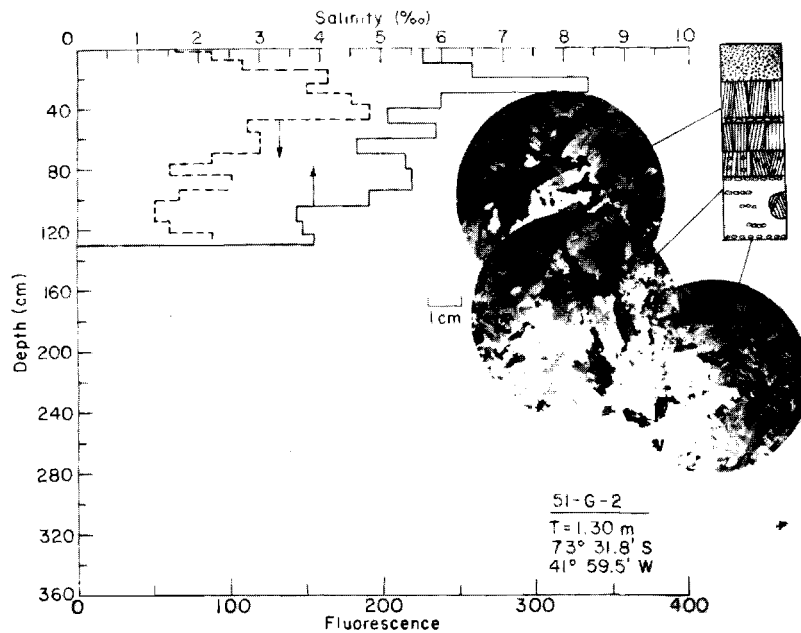
Figure A34. Site 51-G-2.

This first-year 1.30-m-thick floe consisted of 18% snow ice overlying a mixture of frazil and congelation ice in equal proportions (41%). The bottom third of the floe was composed mainly of frazil ice. Relatively large plate spacings of 0.9–1.0 mm were observed in the congelation ice at 38–41 cm. The maximum salinity of 8.4‰ was recorded in the congelation ice directly below the snow ice layer; the average salinity was 5.3‰. The fluorescence did not exceed 200.
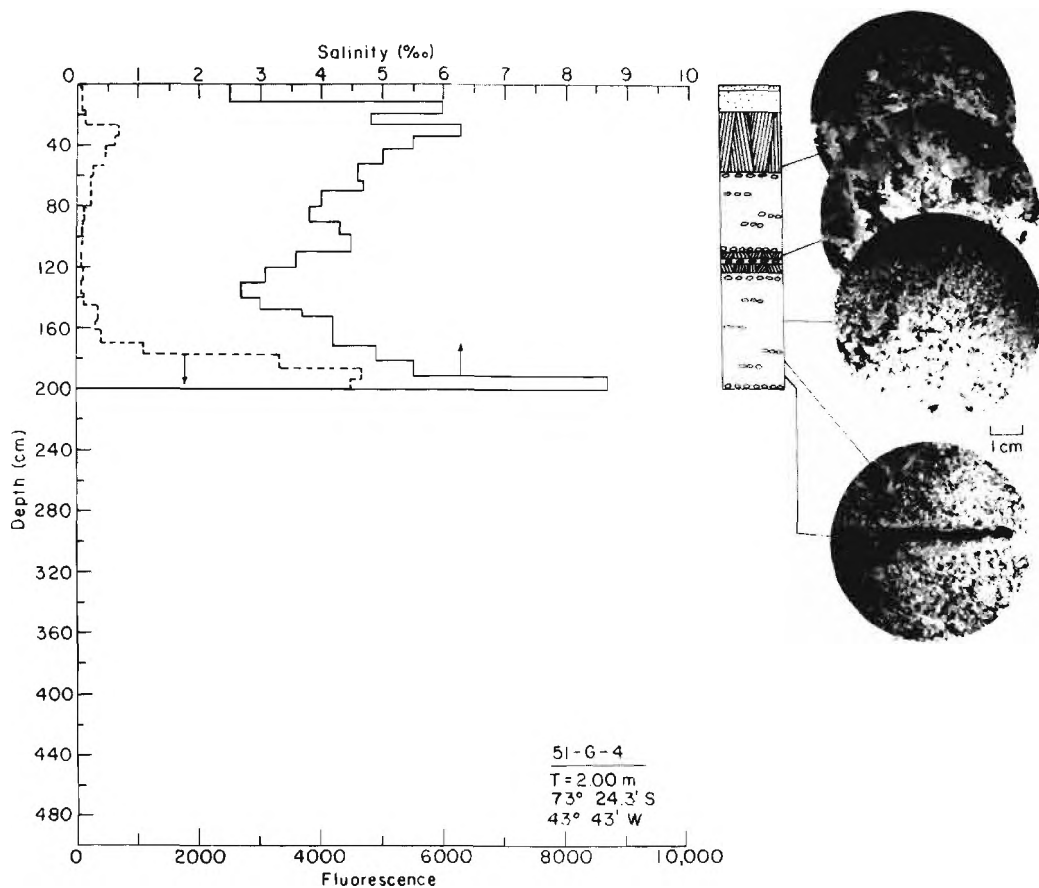
Figure A35. Site 51-G-4.

This first-year floe, 2.00 m thick, was composed of 65% frazil ice, 25% congelation ice and 10% mixed snow and frazil ice at the top of the floe. The average salinity was 4.5‰; the maximum salinity of 8.9‰, recorded in a sample from the bottom of the floe, also co-incided with a fluorescence peak that exceeded 4400. The sharp increase in fluorescence beginning at 170 cm corresponded with the appearance of algae bands in the ice.
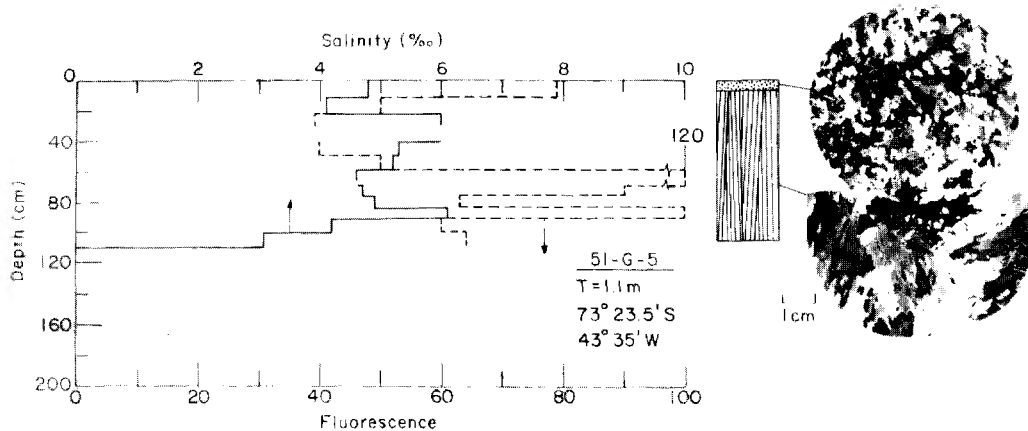
Figure A36. Site 51-G-5.

This relatively thin (1.10 m) first-year floe was composed of 94% congelation ice overlain by a layer of mixed snow and frazil ice (6%). The average salinity was 4.8‰. The fluorescence did not exceed 120.
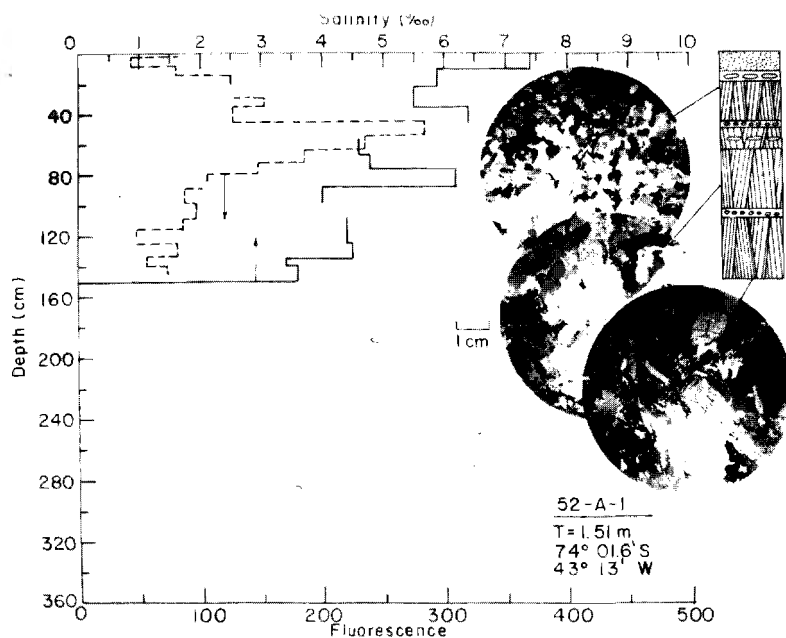
Figure A37. Site 52-A-1.

This first-year ice, 1.51 m thick, consisted predominantly of congelation ice (69%) interspersed with thin layers of frazil ice (22%). A salinity maximum of 7.4‰ was recorded in the mixed snow and frazil ice from the top of the floe; the average salinity was 5.0‰. In congelation ice the plate widths averaged 0.7–0.8 mm. No alignment of crystals was evident.
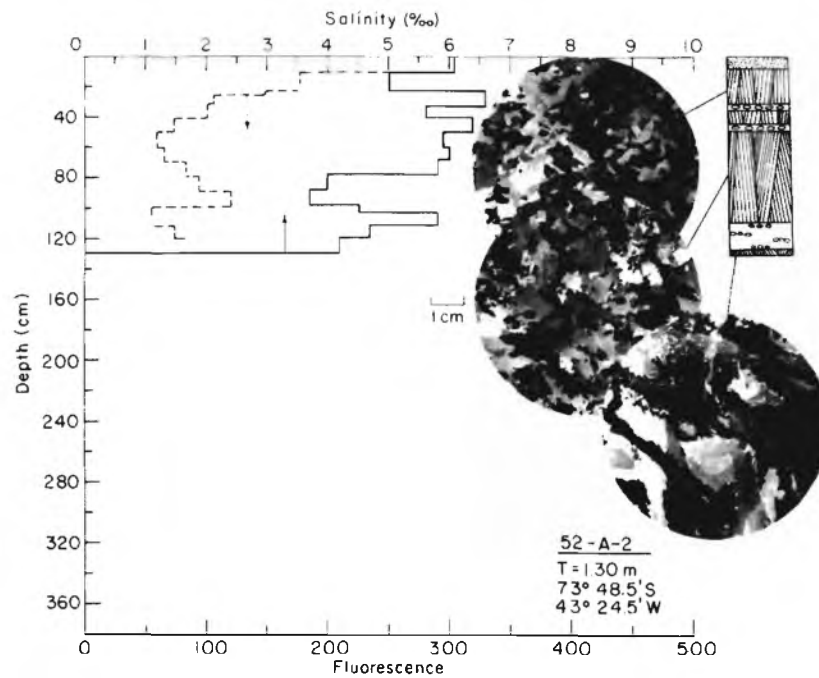
Figure A38. Site 52-A-2.

This floe (1.30 m thick) was very similar to floe 52-A-1 in its salinity profile and structure. The floe salinity averaged 5.3‰, and structurally it was dominated by congelation ice (74%). The peak fluorescence of 288 was recorded in snow and frazil ice from the top of the floe.
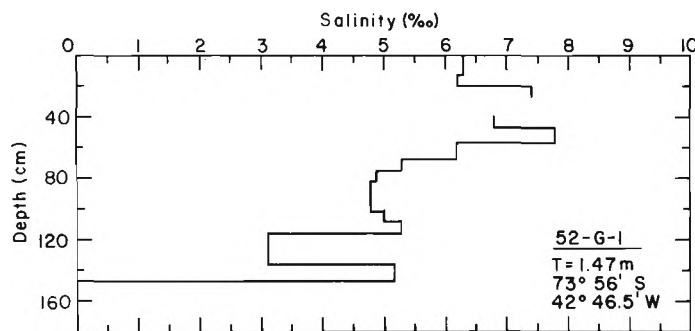
Figure A39. Site 52-G-1.

This is one of three cores drilled less than 4 m apart in a very large first-year floe about 20 km in diameter. This core was used entirely for salinity measurements, which yielded a maxmimum value of 7.8‰ and an average of 5.5‰.
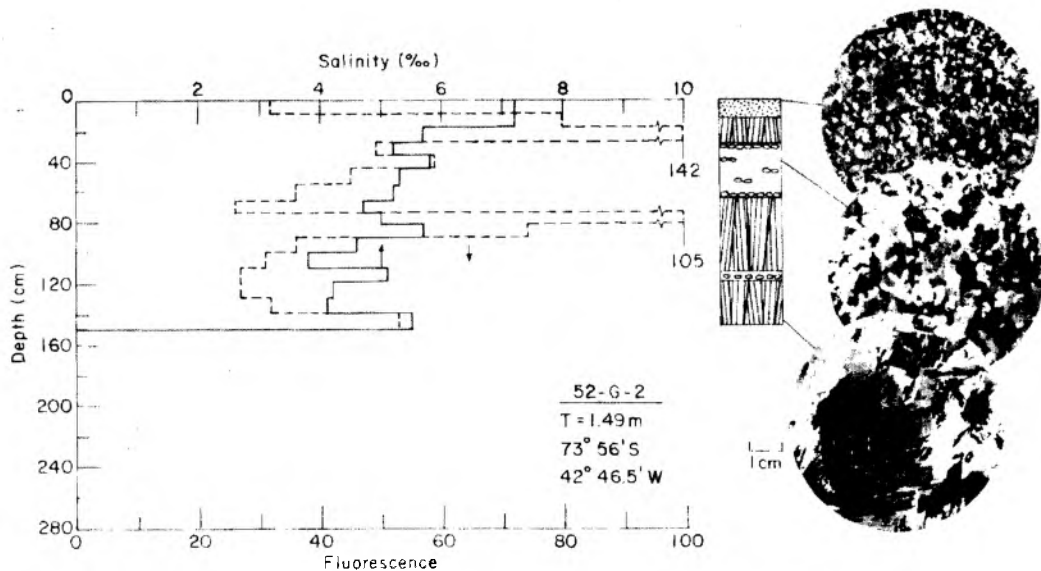
Figure A40. Site 52-G-2.

This core was from the same site as 52-G-1. Its salinity profile was similar to that at 52-G-1. The average salinity was 5.3‰. Structurally the ice consisted of 62% congelation ice and 30% frazil ice overlain by 8% snow and frazil ice. The fluorescence did not exceed 142, and there was no obvious correlation with salinity.
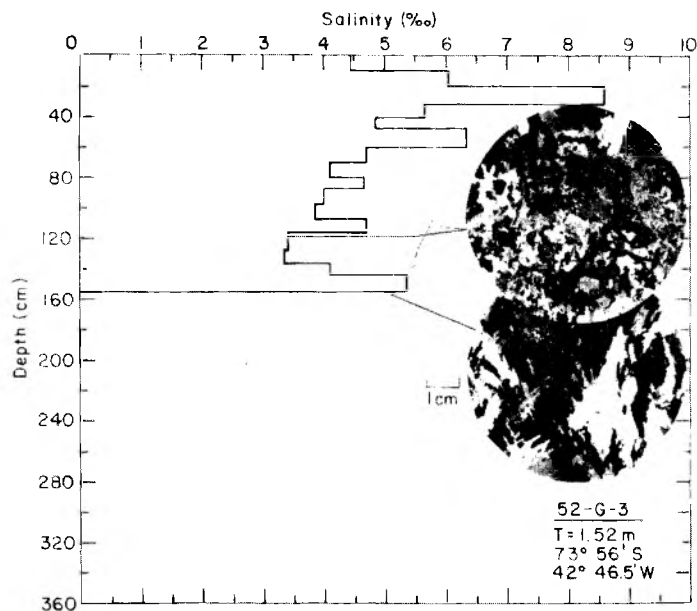
Figure A41. Site 52-G-3.

This was the third of three cores drilled within 4 m of one another. This core was not sectioned vertically, but based on observations of horizontal thin sections, the bottom ice at this location is structurally identical with that from site 52-G-2. Details of the overall salinity profile are similar to those from sites 52-G-1 and 52-G-2, but the average salinity was slightly lower, 4.9‰.
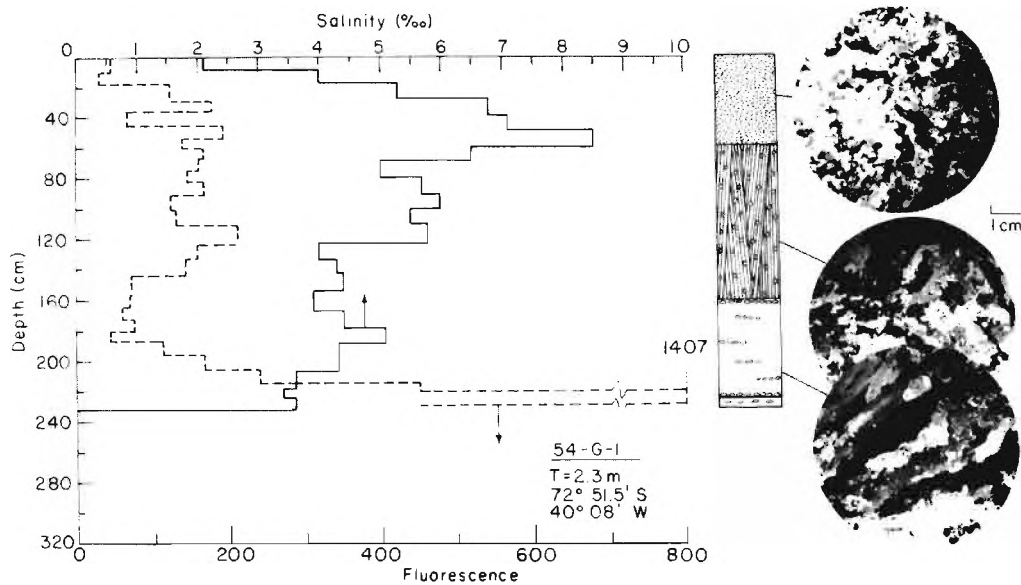
Figure A42. Site 54-G-1.

This thick (2.3 m) first-year floe contained a thicker-than-usual layer of mixed snow and frazil ice, representing 26% of the floe thickness. Congelation ice (45%) containing some frazil crystals appeared to be limited to a single layer beneath the surface layer. The bottom layer of this core was composed mainly of frazil ice, but it included some very large plate-like crystals of ice with plate widths of about 0.8 mm. The top and middle portions of the congelation ice also displayed evidence of widespread drainage of brine. The average floe salinity was 4.8‰; a peak value of 8.5‰ was recorded in the transition ice directly above the top of the congelation ice layer. The maximum fluroescence of 1407 was recorded in a sample from the bottom of the floe. Fluorescence showed no obvious correlation with salinity.
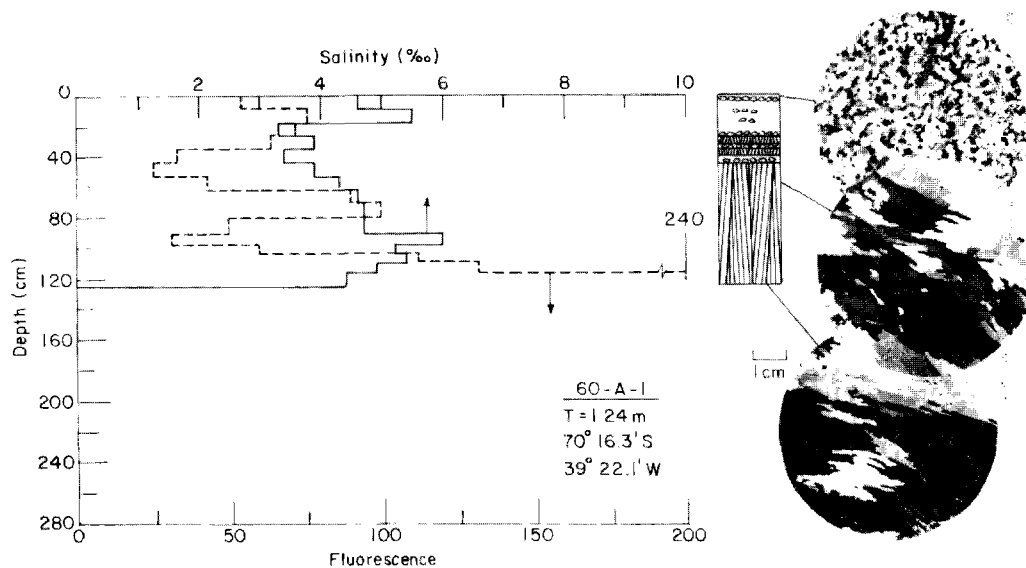
Figure A43. Site 60-A-1.

This first-year floe, 1.24 m thick, consisted of 31% frazil ice and 69% congelation ice. The bottom 60% of the floe is composed of large crystals of congelation ice with very strongly aligned c-axes, indicative of extended growth under stationary pack or fast ice conditions. The average salinity was 4.6‰. The peak fluorescence of 240 was recorded in ice from the bottom of the floe.
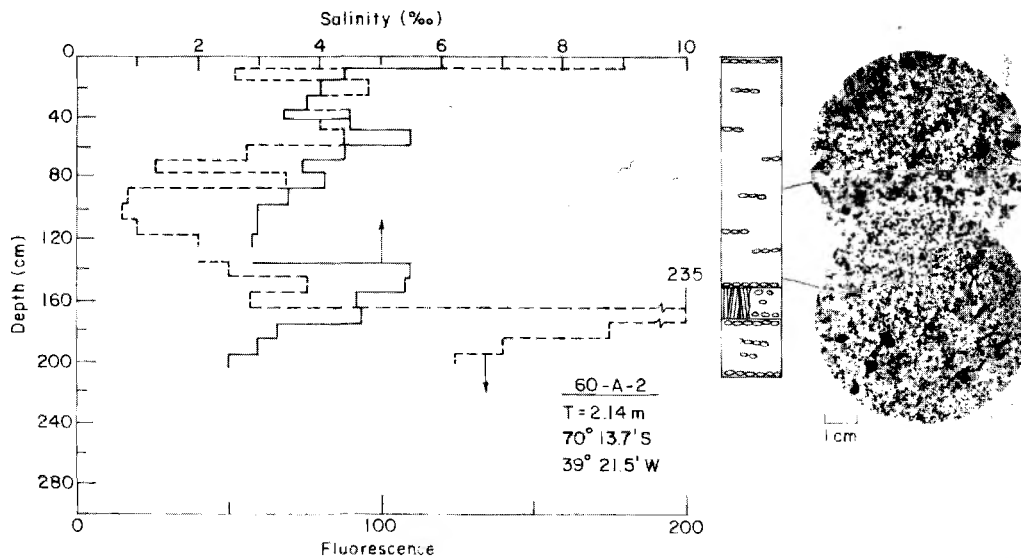
Figure A44. Site 60-A-2.

This first-year ice, 2.14 m thick, consisted of 96% frazil ice of remarkably uniform grain size (2–3 mm in diameter). The 4% of congelation ice is intimately mixed with frazil ice at 150–170 cm. This zone also yielded the maximum fluorescence of 235; a second peak was in ice from the top 10 cm of the floe. The average salinity was 4.1‰. A single $\delta^{18}O$ measurement at 30–35 cm gave a value of $+1.69‰$; proof that the frazil had crystallized in normal seawater.

60
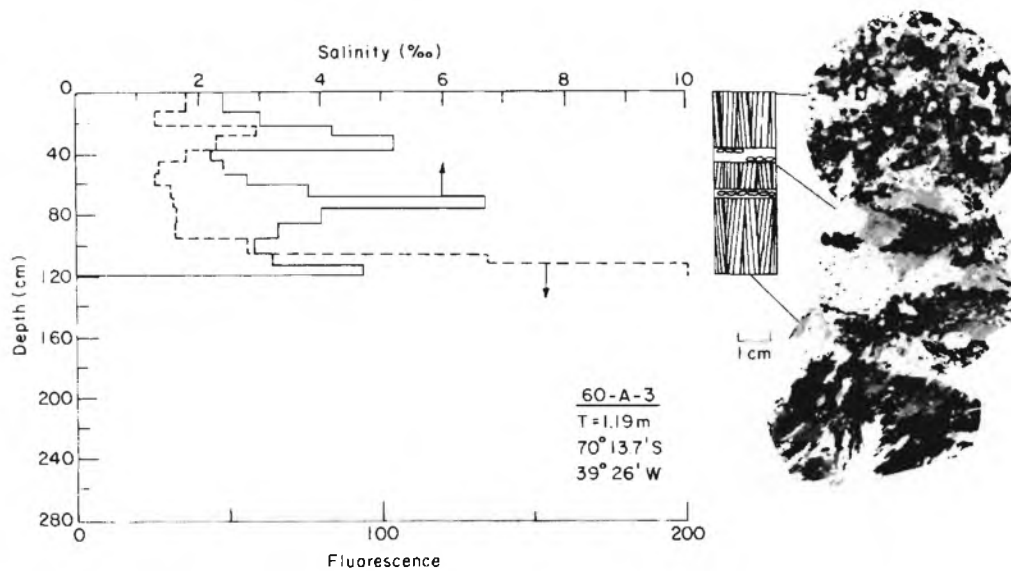
Figure A45. Site 60-A-3.

This first-year floe (1.19 m thick) was composed predominantly of congelation ice (86%) and two thin layers of frazil ice (14%). This floe is unusual because the transition to congelation ice occurred within a centimeter of the top of the ice sheet. The average salinity was 3.6‰. The peak fluorescence (200) was at the bottom of the floe.
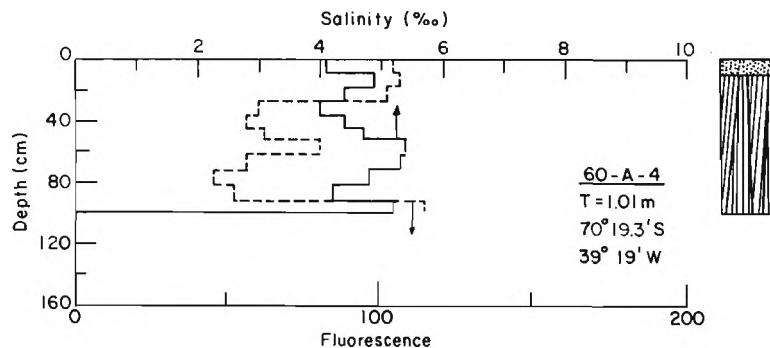
Figure A46. Site 60-A-4.

This 1.01-m-thick, first-year ice consisted predominantly of congelation ice (90%). The average floe salinity was 4.7‰. Fluorescence peaks were measured at the top and bottom of the floe.

61
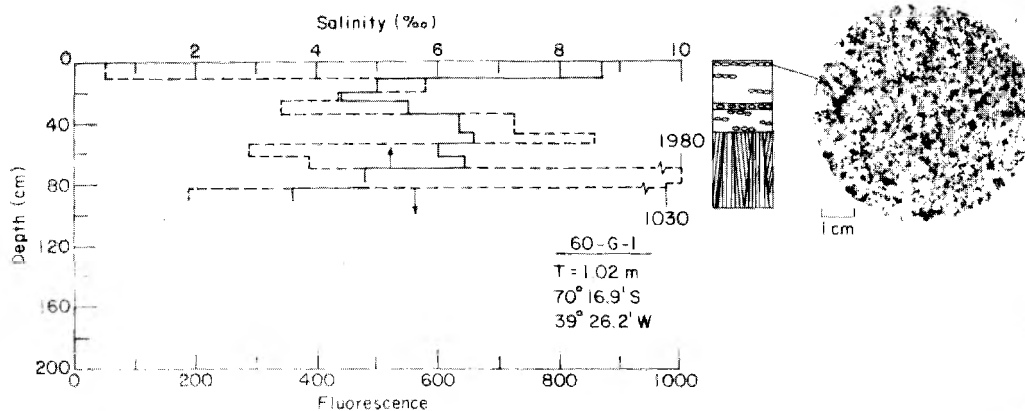
Figure A47. Site 60-G-1.

This 1.02-m-thick, first-year floe consisted of frazil ice overlying congelation ice, each in approximately equal proportions. The average salinity was 5.7‰. The fluorescence peak near the bottom of the floe coincided closely with the occurrence of abundant brown algae in the ice. Two samples of frazil from 11–17 cm and 34–39 cm yielded $\delta^{18}O$ values of +0.51 and +1.01‰, respectively, indicating very slight mixing with snow during the early stages of formation of this ice.
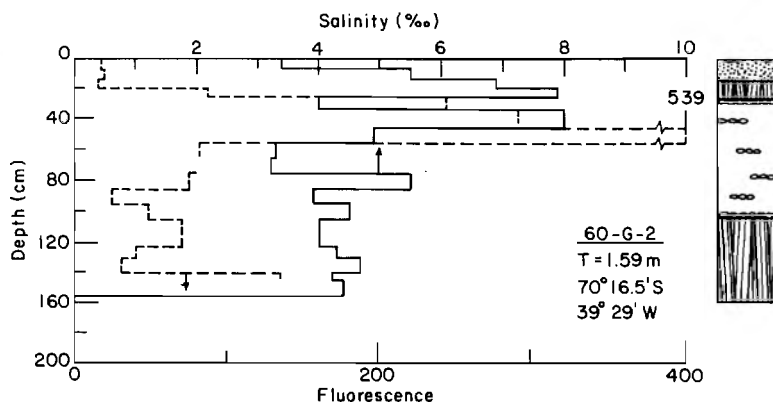
Figure A48. Site 60-G-2.

This first-year ice, measuring 1.59 m thick, consisted of 9% snow and frazil ice and 49% frazil ice located between two layers of congelation ice totaling 42% of the floe thickness. The average salinity was 4.8‰. A maximum salinity of 8.0‰ was recorded in the frazil ice directly above the peak fluorescence of 539.
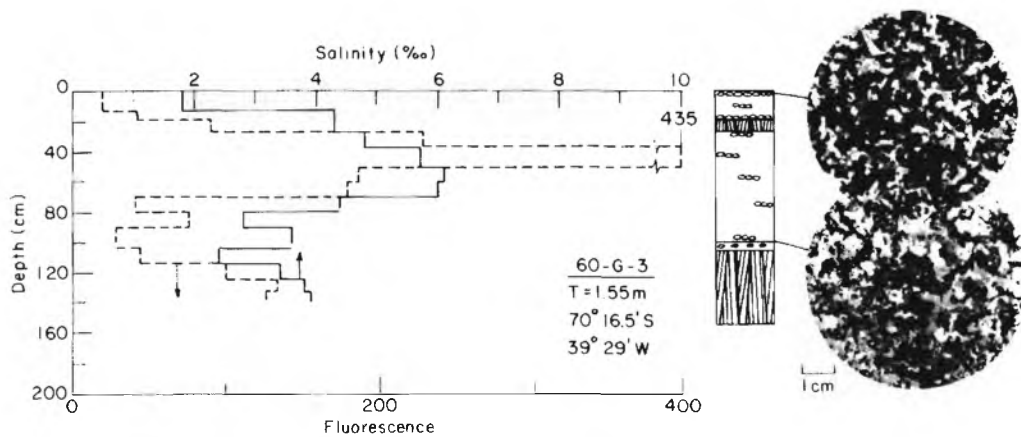
Figure A49. Site 60-G-3.

This first-year, 1.55-m-long core was from the same floe as 60-G-2. Its structural, salinity and fluorescence profiles are practically identical to those of the 60-G-2 core. The only major differences were the absence of snow ice and the increased percentage of frazil ice (63%). Also, fluorescence variations showed a stronger positive correlation with salinity than at site 60-G-2. However, the average salinity was somewhat lower, 4.1‰, compared to 4.8‰ at site 60-G-2.
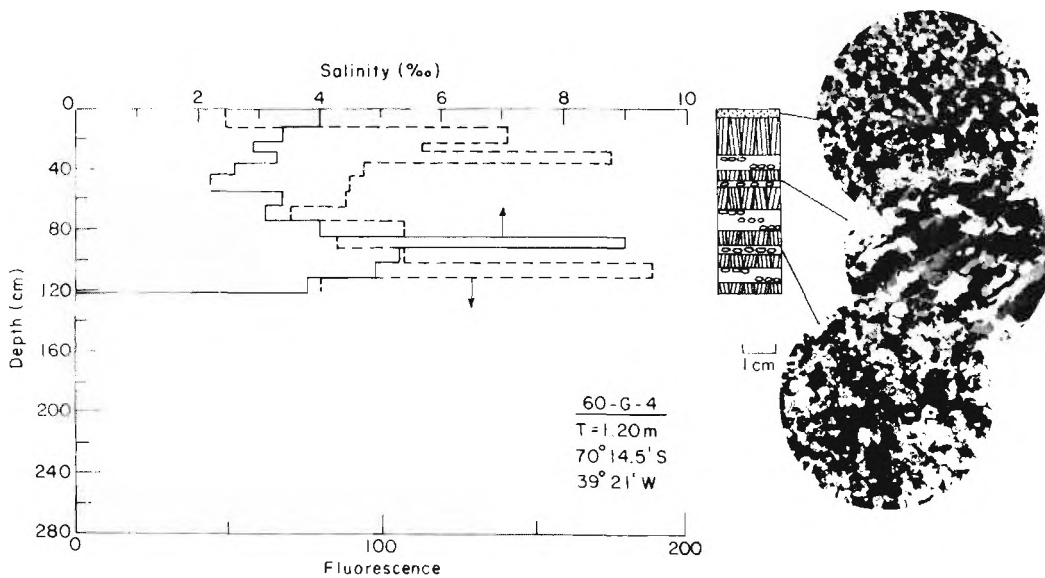

Figure A50. Site 60-G-4.

This first-year, 1.20-m-thick floe was composed of alternating layers of frazil ice and congelation ice, with the latter predominating (64%). Frazil ice was of uniform size throughout, averaging 2–3 mm. The average salinity was 4.0‰. Two fluorescence peaks occurred in the top and bottom frazil ice layers. The alternating layers of congelation and frazil ice in this core possibly indicate an origin by rafting.
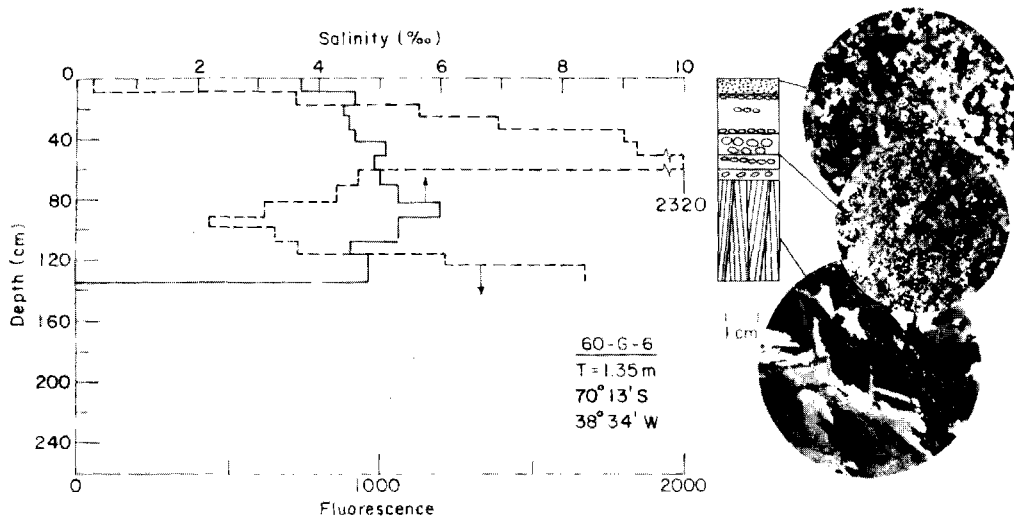
Figure A51. Site 60-G-6.

This first-year ice was 1.35 m thick and consisted, in order from the top, of 9% mixed snow and frazil ice, 40% frazil ice and 51% congelation ice. The bottom of the congelation layer was composed of very large crystals and also exhibited well-developed brine drainage channels. Several coarse-grained zones in which grain diameters exceed 5 mm were observed in the frazil ice. The peak fluorescence of 2320 was recorded in the bottom of the frazil layer. A second peak of 1679 was measured in congelation ice at the bottom of the floe. Salinities were remarkably uniform; the mean salinity was 4.9%.
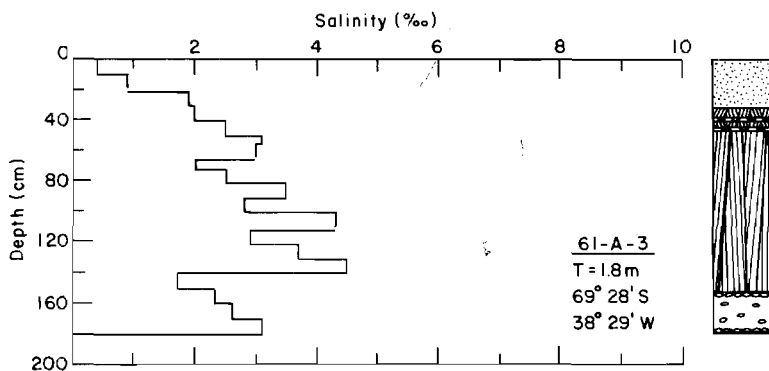
Figure A52. Site 61-A-3.

Tentatively identified as first-year ice, this floe measured 1.8 m thick and consisted of congelation ice (64%) overlain by mixed frazil and snow ice (18%) and underlain by frazil ice (18%). The floe had very low salinities, averaging only 2.6%, a value possibly more in keeping with thin multi-year ice.
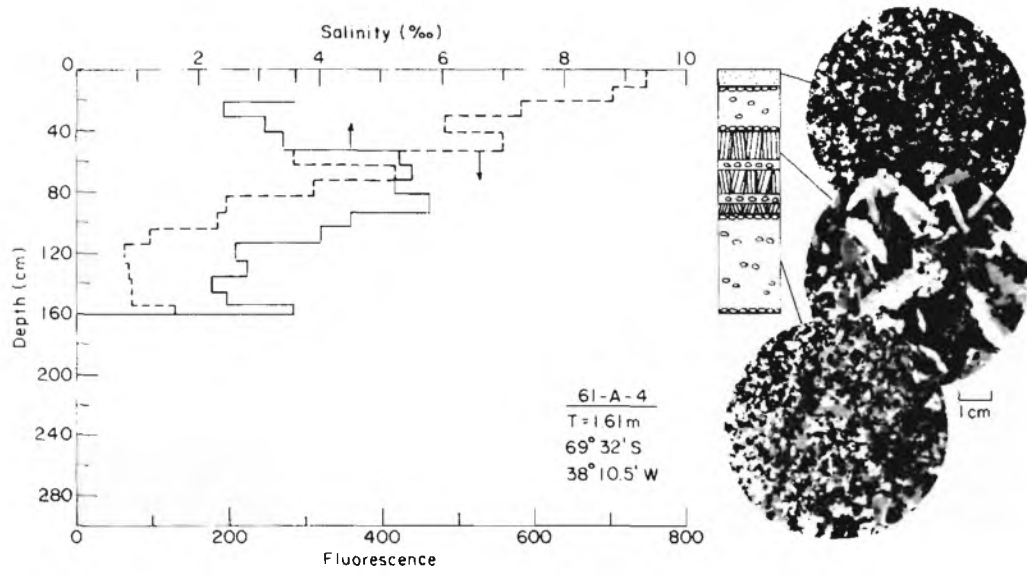
Figure A53. Site 61-A-4.

This first-year ice, measuring 1.61 m thick, was composed of alternating layers of frazil ice (68%) and congelation ice (25%). The c-axes of congelation ice crystals were not visibly aligned. The fluorescence peaked in the surface sample and decreased with depth; in the lower half the fluorescence correlated closely with salinity, which averaged 3.7‰.
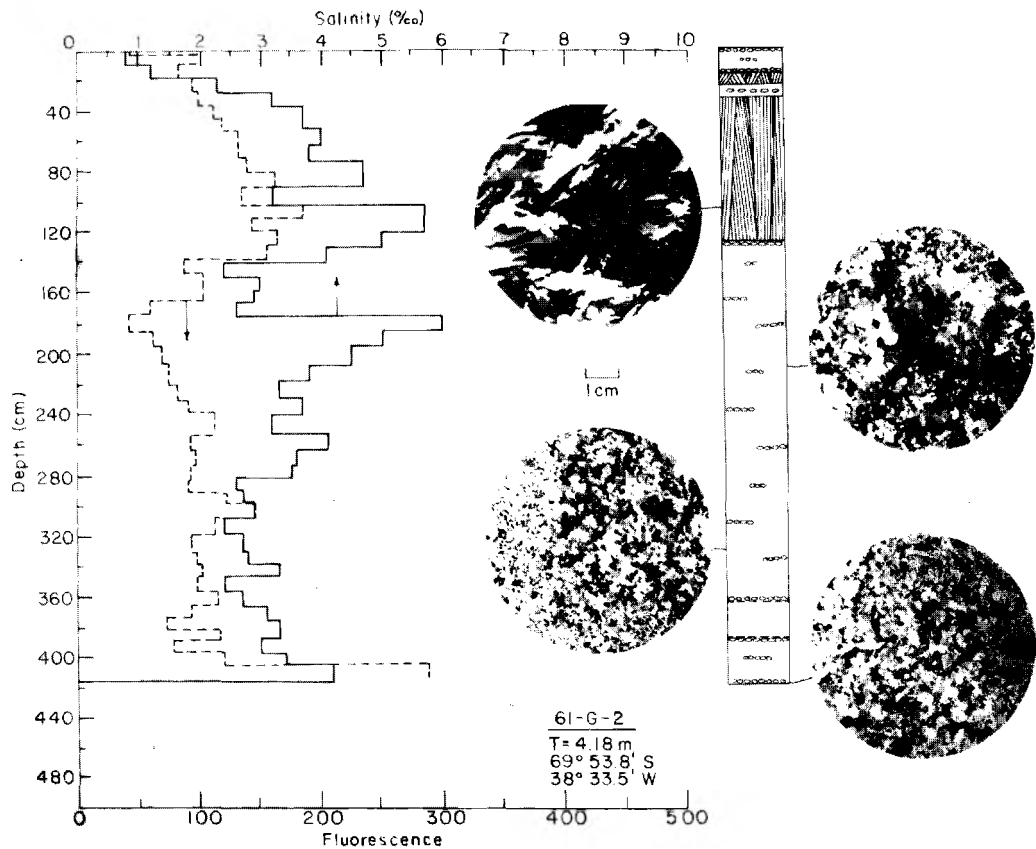
Figure A54. Site 61-G-2.

This multi-year floe, 4.18 m thick, consisted of 25% congelation ice that was limited to the top 1.3 m and was underlain by frazil ice representing 75% of the total ice thickness. The top of this floe was not as severely desalinated as is the case with most multi-year floes. The salinities never exceeded 6‰, and the average salinity was 3.5‰. The size of the grains in the frazil ice varied over a considerable range, as amply demonstrated in the thin sections. No significant peaks in the fluorescence were observed except for a minor peak of 282 at the bottom. The first-year growth apparently ended at the bottom of the congelation ice layer, and all subsequent growth occurred in the frazil regime.
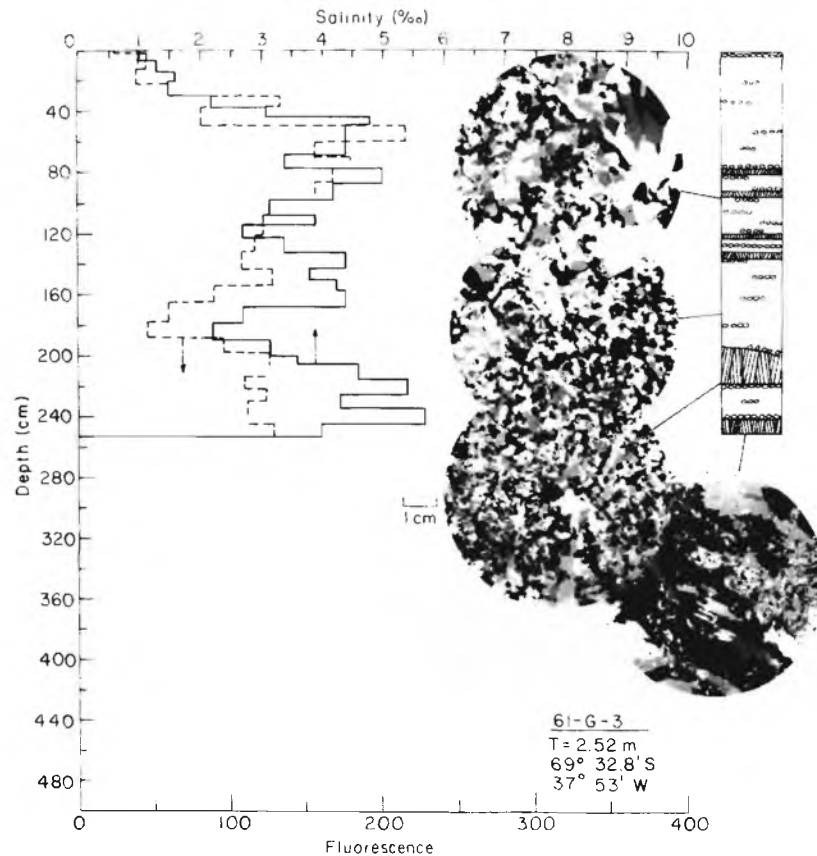
Figure A55. Site 61-G-3.

This floe is 2.52 m thick and probably of multi-year origin, based on the low salinity values in the top 40 cm. The mean salinity was 3.5‰, and the maximum salinity was 5.7‰. Structurally, this floe is characterized by interlayered frazil and congelation ice, possibly related to rafting. Frazil, with grains ranging in size from 1 to 3 mm, was the predominant ice type, however, representing 82% of the total thickness. Thin sections from 95 and 215 cm both exhibited transitional textures. In the section from 95 cm, elongated crystals of congelation ice displaying a characteristic brine lamella and ice plate structure could be easily distinguished from the nearly shapeless grains of frazil. Congelation ice from the bottom of the floe displayed moderately strong alignment of its crystals, indicative of growth under essentially stationary conditions in the pack. The fine-grained structure in the same section was composed mainly of refrozen material in brine drainage channels. The fluorescence generally fluctuated sympathetically with the salinity profile.
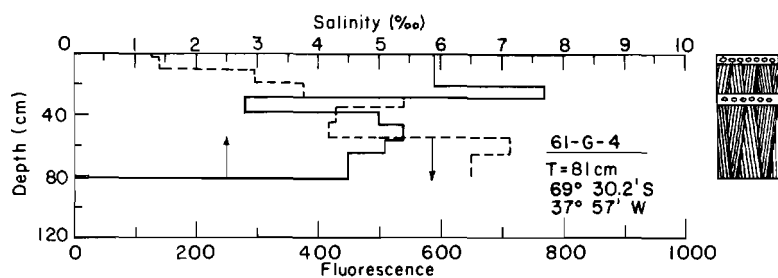
67

Figure A56. Site 61-G-4.

This first-year ice (0.81 m thick) consisted principally of congelation ice (85%) and two thin layers of frazil ice. The salinity averaged 5.2‰, and the maximum was 7.7‰. Brine channeling was prominent between 20 and 40 cm. The fluorescence increases with depth; peak values of 600–700 were recorded in bottom ice.
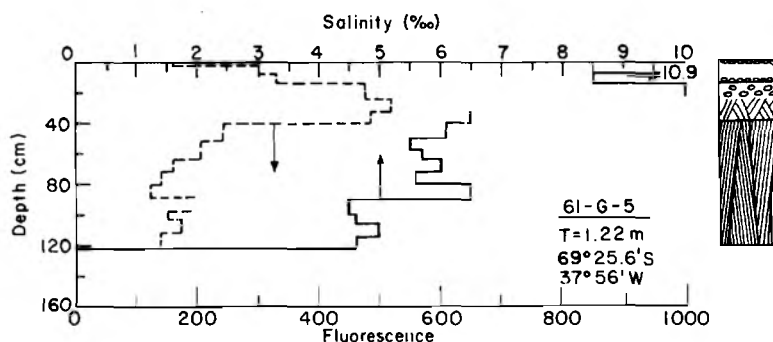

Figure A57. Site 61-G-5.

This 1.22-m-thick floe of first-year ice consisting of frazil ice (21%) overlying congelation ice (79%). The top of the congelation ice was characterized by very large crystals. This floe proved unusually saline; the average salinity was 6.4‰, with a maximum of 10.9‰ in the top 10 cm. The zone of peak fluorescence (520) coincided with the junction of the coarse-grained congelation ice layer and the frazil ice directly above it; algae bands were also observed in the frazil ice.
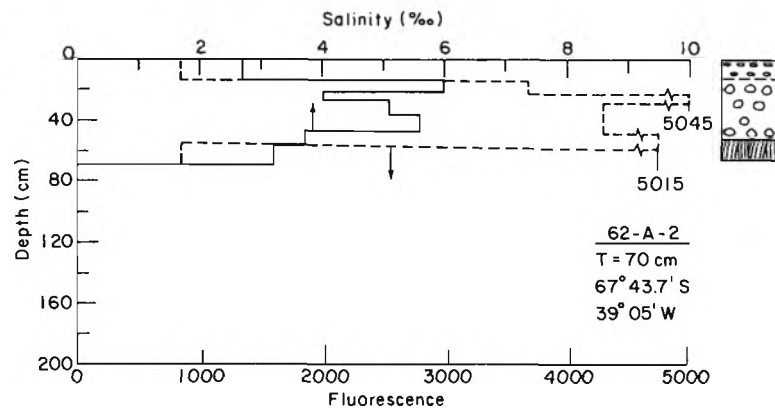
68

Figure A58. Site 62-A-2.

This 70-cm-thick, first-year floe consisted mainly of coarse-grained frazil ice, representing 79% of the total ice thickness, overlying a thin layer of congelation ice (21%) formed on the bottom of the floe. The average salinity of the floe was 4.3‰. A zone of high fluorescence was observed between 21 and 57 cm. This zone included two peaks exceeding 5000, with the second peak, at 47–57 cm, also occurring in conjunction with algae-rich ice containing numerous brine channels.
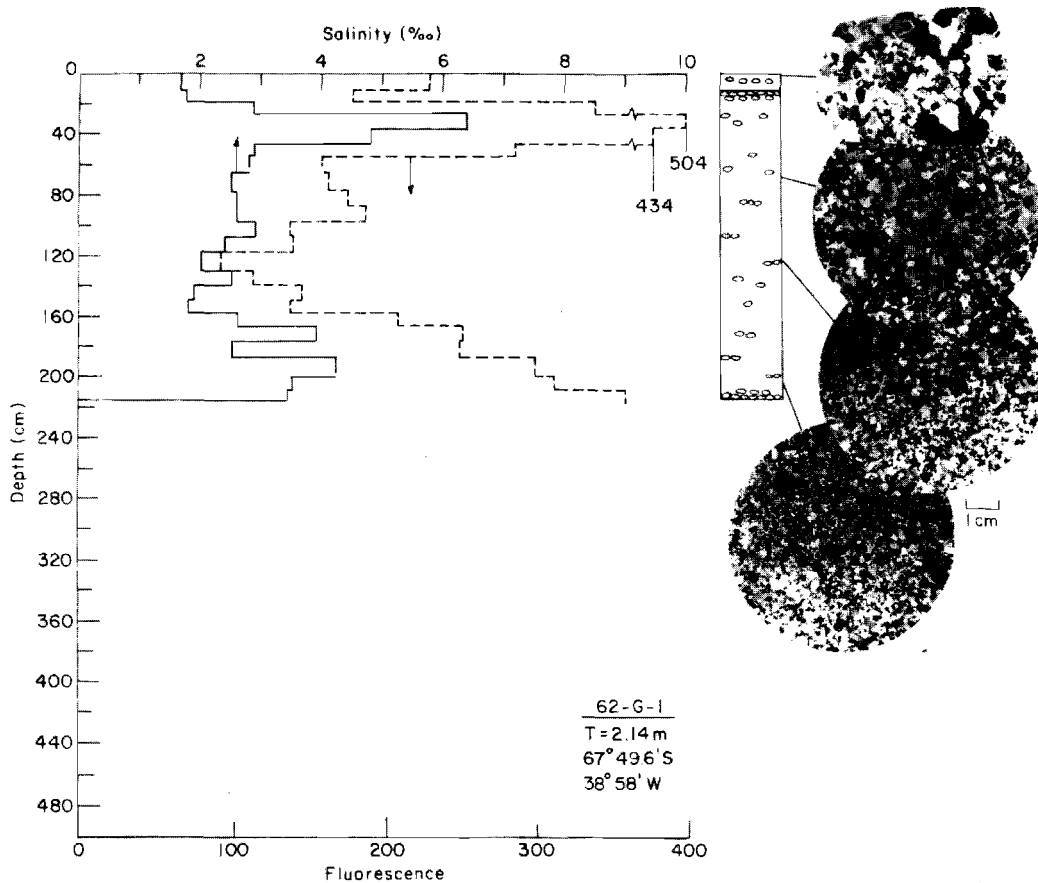
Figure A59. Site 62-G-1.

This first-year floe, 2.14 m thick, was composed completely of frazil ice. Apart from the top 10 cm, which contained many grains larger than 5 mm, the frazil ice in this floe displayed a fairly narrow range of grain sizes, averaging 2–3 mm in cross-sectional diameter. The average salinity was 2.9‰. The maximum salinity of 6.4‰ coincided with a fluorescence peak of 504 at 27–37 cm. In general the salinity and fluorescence profiles fluctuated in parallel.

A facsimile catalog card in Library of Congress MARC format is reproduced below.